

A Thesis Submitted for the Degree of PhD at the University of Warwick

Permanent WRAP URL:

<http://wrap.warwick.ac.uk/130204>

Copyright and reuse:

This thesis is made available online and is protected by original copyright.

Please scroll down to view the document itself.

Please refer to the repository record for this item for information to help you to cite it.

Our policy information is available from the repository home page.

For more information, please contact the WRAP Team at: wrap@warwick.ac.uk



University of Mons

Faculty of Science

Laboratory of polymeric and composite materials



University of Warwick

Department of Chemistry

Preparation of New (Co)polymers from an organo-based CO₂ valorization

Thesis presented by

Jin HUANG

Under the supervision of Olivier COULEMBIER and Andrew P. DOVE for the degree of Philosophical Doctor (Ph.D.) in Chemistry

Doctoral commission

Prof. Matthew GIBSON

Prof. Christophe DETREMBLEUR

Dr. Haritz SARDON

Prof. Roberto Lazzaroni (President)

Dr. Julien De WINTER (Secretary)

Dr. Olivier COULEMBIER (Promoter)

Prof. Andrew P DOVE (Co-promoter)

Prof. Vas STAVROS (Co-promoter)

Mons, March 2019

Acknowledgments

I still remember the day that Professor Philippe DUBOIS forwarded my application email to my great supervisor – Dr. Olivier COULEMBIER. Without his kind help, I would never join and work in Olivier's group. I appreciate Olivier's open mind to allow me choosing the topic of CO₂ valorization. During the study, he also provides me a free and open academic environment where I can do the research in many approaches. The active discussions, positive encouragement, and patient supervision from him will be the great properties in my life. I also would like to express my appreciation for Prof. Andrew P DOVE's supervision. His academic ambition and energetic guidance motivate me to seek the truth in chemistry. I do appreciate my both supervisors, Olivier and Andrew, who afford me patient guidance on my academic writing, although I put them out sometimes...

I do appreciate the moment that I work in Olivier's group. Thanks to the kind help from Sébastien MOINS and Laura WAUTERS to support my work for the chemical orders, SEC characterization, and glovebox issues and so on. Thanks to Prof. Jean-marie RAQUEZ, Dr. Julien De WINTER, Dr. Li-jiang SONG, Dr. Samira BENALI, Dr. Jérémy ODENT, Dr. Rosica MINCHEVA and Dr. Antoniya TONCHEVA, Mrs. Nathalie VANDEREST and Dr. Noémie HERGUÉ's support not only in academic field but also in normal life. Thanks to Sébastien DELPIERRE and Bertrand WILLOCQ, it is the great moment to talk with you, easy going and funny moment. Thanks to Alexandra BARONI, Ali KHALIL, Alexandre De NEEF, Romain LIENARD, Xavier CARETTE, Rana ELNAKEEB, Florence PILATE, Dalila SAAOUI Brian RAESKINET, Chiara MAGNANI, Meriam Ben ABDELJAWAD, Jean-Emile POTAUFEUX, Serena MURKANDASH.

I do appreciate the moment that I work in Andrew's group. Academic discussion with colleagues, regular group meeting and useful apparatus induction afford me a great environment to focus on science impressively. Thanks to Dr. Josh Worch, Dr. Mathieu J.-L. Tschan, Dr. Maria Chiara ARNO, Dr. Maria PEREZ-MADRIGAL, Dr. Andrew WEEMS, Paula Kishi KUROISHI, Gordon HERWIG, Connor STUBBS, Siobhan KILBRIDE, Zac COE, and Anissa KHALFA. Thanks to my lovely Chinese friends in the UK. Bo LI,

Zan HUA, Yu-jie XIE, Wei YU, and Bo DONG. It is my pleasure to stay with all of you and I pretty enjoy the moment for eating, traveling, and gaming.

I do appreciate the moment when I stay with my colleagues from SUSPOL project. Thanks to Prof. Daniel TATON who initiate such great project, Dr. Haritz SARDON, Dr. Mónica MORENO who manage the project in order, Prof. David MECERREYES, Prof. Lourdes IRUSTA, Prof. Rachel O'REILLY who provide helpful suggestions for my project. Thanks to Andere BASTERRETxea, Amaury BOSSION, Coralie JEHANNO, Panagiotis BEIXS, Noe Fanjul MOSTEIRIN, Sethum JIMAJA, Sophiem GARMENDIA, Beste ORHAN, and my lovely friend Leila MEZZASALMA. It is the appreciable moment to have talks and discussions with you.

Very importantly, I do appreciate the support from my family, my lovely wife, Ruo-chen SUN, my cute daughter, Zi HUANG, and my parents, Shu-fang, FENG and Yi-shu HUANG. They all encourage and spoil me for my decision of pursuing doctor degree. I would like to express my gratitude to my sister's family. Dr. Ming-hui HUANG, Dr. Michael HOUBEN, Nicolas HOUBEN, Doctor Rina JANSSEN, Jos WYSMANS and in memory of Leon HOUBEN...

I do appreciate the help from Prof. Robert Haener's kind help when I work in his group.

Thanks to the funding support from the European Commission on the programme of Maria Skłodowska-Curie actions research fellowship.

Finally, after a few years, I do give myself an answer although the journey is not pleasant. Stress, torture, and toughness stay with me which make me stronger.

在夜色下负重前行，我依然会仰望星空并期待黎明的来临.....

任何不能击败我的，终将令我更为强壮！

Jin HUANG
University of Mons
2019-01-29

Table of contents

| | |
|--|------------|
| Acknowledgments | I |
| General introduction | VII |
| List of Abbreviations | XII |
| Chapter I Update and challenges in CO₂-based polycarbonate synthesis | 1 |
| 1.1 Introduction | 3 |
| 1.2 Organometallic Catalysts | 6 |
| 1.2.1 Mechanism and kinetics of copolymerization..... | 6 |
| General mechanism..... | 6 |
| Kinetic perspective | 9 |
| 1.2.2 Main-group metal catalysts..... | 9 |
| Mg Catalysts | 10 |
| Al Catalysts | 11 |
| Zn Catalysts | 13 |
| 1.2.3 Transition metal catalysts | 18 |
| Co catalysts..... | 18 |
| Cr catalysts | 23 |
| Fe catalysts | 26 |
| Ni catalysts | 27 |
| Ti, Zr, Hf Catalysts..... | 28 |
| Lanthanide Catalysts | 33 |
| Cu Catalysts | 35 |
| 1.2.4 Novel Cyclic Carbonate Monomers derived from CO ₂ | 36 |
| 1.3 Organocatalysts | 38 |
| 1.4. Conclusion and Outlooks | 40 |
| References..... | 41 |
| Chapter II Organocatalyzed coupling of epoxide and CO₂ using a phosphazene superbase | 53 |
| 2.1 Introduction..... | 55 |
| 2.2 Results and Discussion | 60 |
| 2.2.1 Superbases efficiencies | 60 |
| 2.2.2 Modification of the experimental conditions. | 63 |
| • Temperature..... | 64 |
| • Reaction time | 65 |

| | |
|---|------------|
| • Effect of co-catalyst loading | 67 |
| 2.3 Conclusion | 74 |
| 2.4 References | 75 |
| <i>Chapter III Organocatalytic synthesis of poly (trimethylene carbonate) from CO₂ and oxetane</i> | 79 |
| 3.1 Introduction..... | 81 |
| 3.2 Results and Discussion | 84 |
| 3.2.1 Cocatalyst screening..... | 84 |
| 3.2.2 Reaction conditions modification..... | 90 |
| 3.3.3 MALDI-ToF spectrum analysis | 91 |
| 3.3.4 Attempts of increase molar mass..... | 92 |
| 3.3.5 Mechanism investigation | 95 |
| 3.3 Conclusions..... | 100 |
| 3.4 References | 101 |
| <i>Chapter IV From selective formation of trimethylene carbonate to its “on-demand” polymerization: Impact of the iodine/ionic liquid cooperative catalytic system</i> | 105 |
| 4.1 Introduction..... | 107 |
| 4.2 Results and discussion..... | 110 |
| 4.2.1 Temperature effect | 110 |
| 4.2.2 Cocatalyst screening..... | 114 |
| 4.2.3 Reaction conditions modification..... | 116 |
| 4.2.4 Solvent effect..... | 120 |
| 4.2.5 Copolymer synthesis | 124 |
| 4.2.6 Kinetics of coupling reaction | 128 |
| • Rate law of coupling reaction..... | 128 |
| • Activation energy | 132 |
| 4.3 Conclusion | 135 |
| 4.4 References | 136 |
| Conclusion and outlooks | 139 |
| <i>Chapter V Experimental Section</i> | 143 |
| 5.1 General comments..... | 144 |
| 5.1.1 Materials and methods | 144 |
| 5.1.2 Measurements | 145 |
| 5.2 General procedure for the synthesis of carbonates | 146 |

| | |
|---|------------|
| 5.2.1 General procedure for the synthesis of carbonates from CHO and CO ₂ as catalyzed by <i>trans</i> -CHD and <i>tert</i> -Bu-P ₄ | 146 |
| 5.2.2 General procedure for the synthesis of carbonates from CO ₂ and oxetane using iodine-based catalysis. | 147 |
| Publications | 149 |

Preparation of New (Co)polymers from an organo-based CO₂ valorization

Abstract: Phosphazene based organocatalysis was applied to prepare oligocarbonate from CO₂ and cyclohexane oxide under very mild conditions. Modification of experimental conditions such as temperature, reaction time and co-catalyst content, reveal that the oligocarbonate is a result of the polymerization of *in situ* generated cyclic carbonate. By changing the catalysis ratio, the product of oligo- and cyclic carbonates in selectivity is adjustable.

Iodine-based binary catalytic system has been applied to prepare poly(trimethylene carbonate) (PTMC) from CO₂ and oxetane in bulk. The results reveal that the nature of co-catalyst is prime important to the formations of products. A comparable high molar mass of PTMC was observed in presence of iodine and guanidine catalysis as characterized by size extrusion chromatography, while a unique selectivity of trimethylene carbonate (TMC) was found in the residue using iodine and phosphazene as catalysis. The mechanism of polymerization was proposed that PTMC was a result of the polymerization of *in situ* generated TMC.

The preparation of TMC from CO₂ and oxetane using iodine and ionic liquid catalytic system was studied. To enhance the selectivity and yield of TMC, temperature, co-catalyst, and solvent were investigated. Interestingly, the production of TMC and PTMC is controlled by temperature as catalyzed by iodine and ionic liquid. Importantly, the required energy to produce PTMC is only slightly higher than the one calculated by Darensbourg when applying the very efficient chromium salen catalytic complexes which provide useful information for the mechanism study with theoretical calculation.

General introduction

The increasing awareness of environmental protection and the depletion of fossil fuels has spurred the research for sustainable development. Over past decades, carbon dioxide (CO₂), a non-toxic, abundant C1 feedstock, received a great deal of attention of both academic and industrial communities for value-added chemical synthesis. Although the full oxidized state and centrosymmetric structure of the CO₂ molecule renders a relative inert activity, the development of catalysts promotes the synthesis of CO₂-based chemical products such as cyclic carbonates, urethane, carboxylic acid, methanol, and polycarbonates. The replacement of conventional plastic materials, alongside with the promise of carbon fixation, provides an opportunity to use CO₂ as a building block to polymer synthesis. As such, catalytic copolymerization of CO₂ with other monomers such as epoxides and oxetane is studied extensively in presence of metal-based catalysts. However, the metal pollution of such catalysis, associated with the drawbacks of uneconomic multi-step synthesis, sensitivity towards oxygen, and health impact limits its wide utilization, especially in the fields of biomaterials and microelectronics. To provide a green approach for the replacement of its metal-based counterpart, organocatalysis, with the advantages of low toxicity, low cost and high availability, turns to be an option for CO₂-based copolymerization recently.

As such, it motivates us to develop a green synthetic route to CO₂-based polycarbonate preparation. In this thesis, attempts of copolymerizing epoxide and oxetane with CO₂ were studied respectively with the aim of exploring a controllable approach to provide CO₂-based polycarbonate and its corresponding monomers.

Update and challenges in CO₂-based polycarbonate synthesis

Before presenting the research work of this thesis in detail, the recent progress of the catalytic synthesis of CO₂-based polycarbonate including metal-based catalysis, polymerizable monomers, and the novel multi-block copolymer is summarized in the first chapter (Chapter I) (Figure I) to give a brief insight into this field of research. Moreover, organocatalysis is introduced and discussed mainly in comparison to its metal-based counterpart.

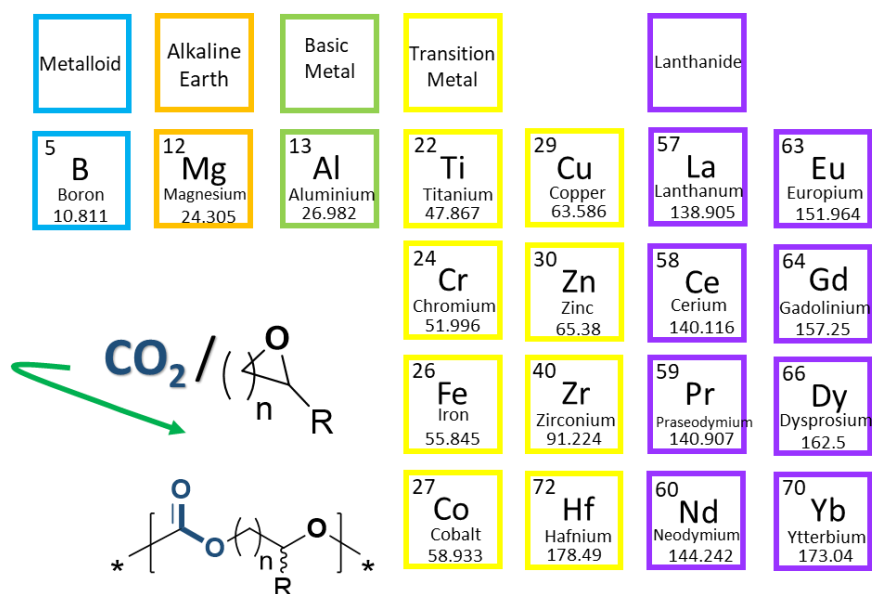


Figure I. Graphic abstract of Chapter I (update and challenge in CO₂-based polycarbonate synthesis).

Organocatalyzed coupling of epoxide and CO₂ using a phosphazene superbase

Encouraged by the importance of CO₂-based polycarbonate to replace conventional polymeric materials, alongside with the green chemistry development, the first doctoral project (Chapter II) focuses on the investigation of the coupling reaction of CO₂ with epoxide in presence of a phosphazene-based catalytic system. The chapter provides an overview of the development of coupling CO₂ with epoxide, which motivates us to develop a non-halogen catalytic system for CO₂ and epoxide coupling. After the investigation of the screening catalyst, phosphazene, in combination with *trans*-cyclohexane diol, was applied to the coupling reaction. The reaction conditions such as temperature, reaction time and catalyst loading were studied to increase the yield of polymerizable monomers and oligo-carbonate. The desired oligocarbonate ($M_n = 1,040 \text{ g}\cdot\text{mol}^{-1}$) was produced in presence of 8 equivalents *trans*-cyclohexane diol (related to phosphazene), which can be used as the agent for chain extension. Moreover, a plausible mechanism for such reaction was proposed.

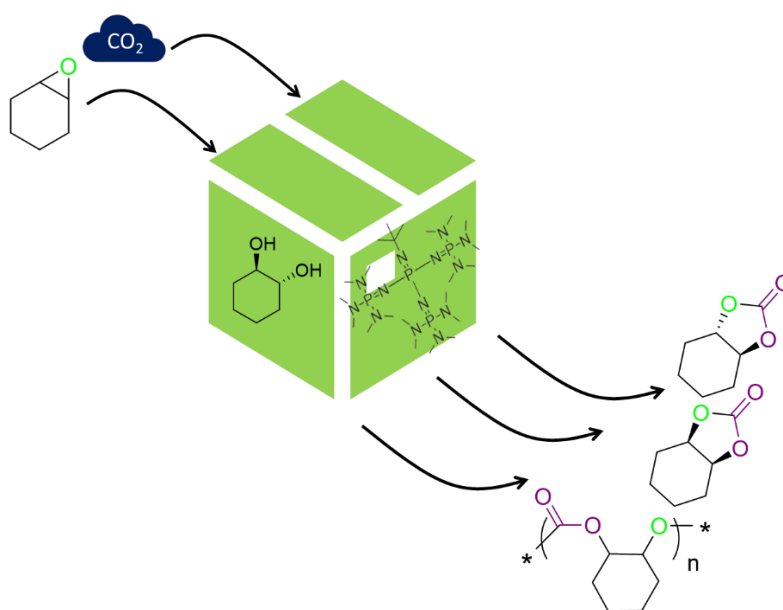


Figure II. Graphic abstract of Chapter II (Organocatalyzed coupling of epoxide and CO₂ using a phosphazene superbase)

Organocatalytic synthesis of poly (trimethylene carbonate) from CO₂ and oxetane

After the effort that was devoted to the preparation of polycarbonate from CO₂ and epoxide, the alternative oxygen-based heterocycle, oxetane, was selected for the copolymerization with CO₂. The second project (Chapter III) (Figure III) first introduces the progress of catalytic synthesis of poly (trimethylene carbonate) from CO₂ and oxetane. It also discusses the activation of oxetane and CO₂ by metal-based catalysts as well as the first example of oligo(trimethylene carbonate) synthesis using organocatalysts. This work, combined with past experience from our research group on the coupling of CO₂ and epoxide under very mild conditions using iodine-based catalytic binary system, encouraged us to study the copolymerization of CO₂ and oxetane. The research focused on the catalyst screening and modification of experimental conditions aiming to obtain the high molar mass copolymer. A poly (trimethylene carbonate) (PTMC) ($M_n = 4,000 \text{ g}\cdot\text{mol}^{-1}$) with high carbonate content (up to 95 mol%) was produced in presence of I₂ and guanidine superbases with a ratio of 1:1 under a 3 MPa CO₂, at 105 °C, for 7 days. Moreover, the plausible mechanism of such copolymerization was studied. The result suggests that the *in situ* generated TMC was polymerized following an active chain end mechanism.

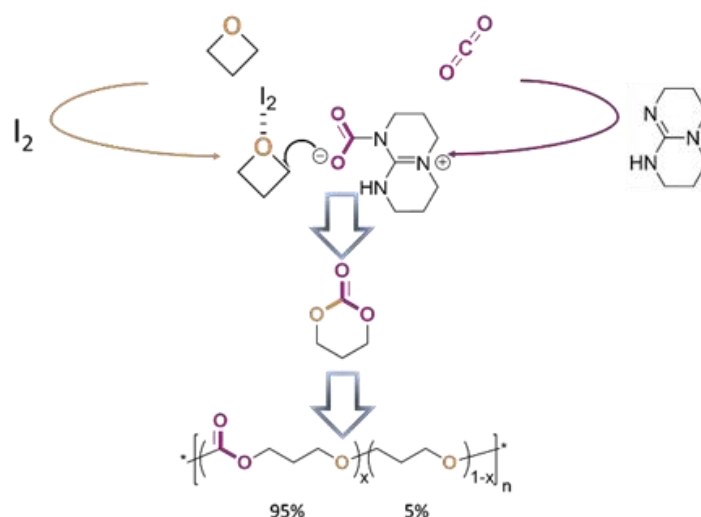


Figure III. Graphic abstract of Chapter III (Organocatalytic synthesis of poly (trimethylene carbonate) from CO₂ and oxetane)

***From selective formation of trimethylene carbonate to its “on-demand” polymerization:
Impact of the iodine/ionic liquid cooperative catalytic system***

As the unique selectivity of trimethylene carbonate (TMC) was observed in the initial reaction period (< 5 days) in presence of iodine and phosphazene as catalysis, the coupling of CO₂ and oxetane to prepare TMC with high yield using I₂-based catalytic system could be realized. To prepare the CO₂-based product (cyclic monomer and polymer formation) in a controllable manner, the third project (Chapter IV) (Figure IV) focuses on iodine and the ionic liquid binary system. The study of catalyst screening, temperature, and solvent effect provides the optimal conditions to obtain TMC and its polymer formation. Up to 93 mol% selectivity of TMC with 93 mol% conversion of oxetane was observed in presence of I₂ and tetrabutylammonium acetate as catalysis in dimethylformamide solution under a 3.0 MPa CO₂, at 55 °C, for 96 h. Moreover, the energy barriers of monomer (TMC) and polymer (PTMC) were calculated on the basis of kinetic study: 36.93 kJ·mol⁻¹ for TMC, and 49.94 kJ·mol⁻¹ for PTMC.

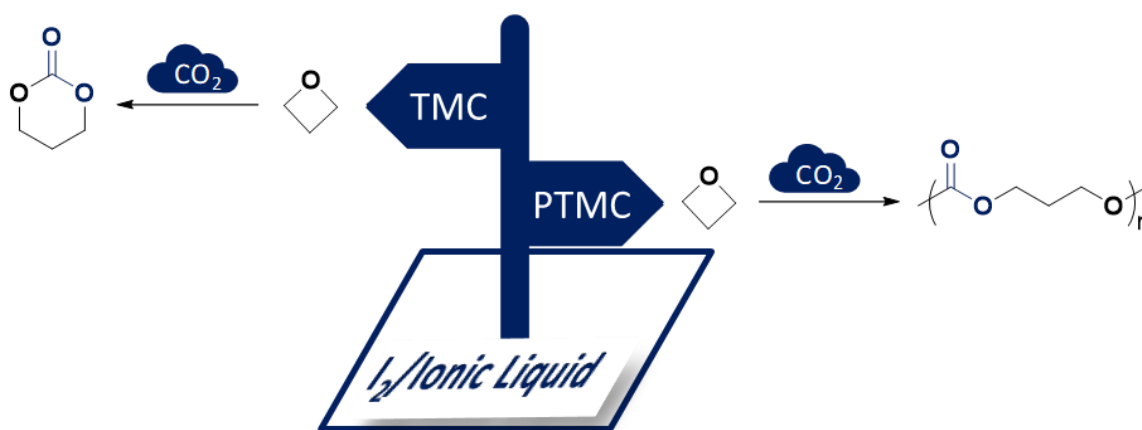


Figure IV. Graphic abstract of Chapter IV (From selective formation of trimethylene carbonate to its “on-demand” polymerization: Impact of the iodine/ionic liquid cooperative catalytic system)

List of Abbreviations

| | |
|-----------------|-------------------------------|
| CO ₂ | Carbon dioxide |
| CO | Carbon monoxide |
| ROcP | Ring-opening copolymerization |
| ROP | Ring-opening polymerization |
| HC | Heterocyclic molecules |
| EO | Ethylene oxide |
| EP | Epoxide |
| ES | Episulfide |
| AD | Aziridine |
| PO | Propylene oxide |
| CHO | Cyclohexane oxide |
| SO | Styrene oxide |
| LO | Limonene oxide |
| OO | Octene oxide |
| IO | Indene oxide |
| BO | Butene oxide |
| CPO | Cyclopentane oxide |
| CHDO | Cyclohexadiene oxide |
| DNO | 1,4-Dihydronaphthalene oxide |
| ECH | Epichlorohydrin |
| GPE | Glycidyl phenyl ether |
| VCHO | 4-Vinyl-1,2-cyclohexane oxide |
| TMO | Trimethylene oxide |
| FDCA | 2,5-Furandicarboxylic acid |
| PA | Phthalic anhydride |
| PCHC | Poly (cyclohexane carbonate) |
| PLO | Poly (limonene oxide) |
| EC | Ethylene carbonate |
| CHC | Cyclohexane carbonate |

| | |
|--------------------------------|--|
| OCC | Oligo-(cyclohexane carbonate) |
| <i>trans</i> -CHC | <i>trans</i> -Cyclohexane carbonate |
| <i>cis</i> -CHC | <i>cis</i> -Cyclohexane carbonate |
| <i>trans</i> -CHD | <i>trans</i> -Cyclohexane diol |
| <i>cis</i> -CHD | <i>cis</i> -Cyclohexane diol |
| TMC | Trimethylene carbonate |
| PTMC | Poly(trimethylene carbonate) |
| CL | ϵ -Caprolactone |
| β -BL | β -Butyrolactone |
| LA | Lactide |
| poly(β -BL) | Poly(β -butyrolactone) |
| SBs | Super bases |
| 5CCs | Five-membered cyclic carbonates |
| 6CCs | Six-membered cyclic carbonates |
| NHC | N-heterocyclic carbene |
| OiPr | Isopropoxide |
| bis-BZH | Benzotriazole phenolate |
| BZH | Tetra-benzotriazole phenolate |
| PPD | 1,3-Propanediol |
| DBU | 1,8-Diazabicyclo[5.4.0]undec-7-ene |
| DMAP | 4-Dimethylaminopyridine |
| <i>tert</i> -Bu-P ₄ | 1- <i>tert</i> -Butyl-4,4,4-tris(dimethylamino)-2,2-bis[tris(dimethylamino)-phosphoranylidenamino]-2 λ^5 ,4 λ^5 -catenadi(phosphazene) |
| TBD | 1,5,7-Triazabicyclo[4.4.0]dec-5-ene |
| MTBD | 7-methyl-1,5,7-triazabicyclo-[4.4.0]-dec-5-ene |
| GuD | Guanidines |
| E_r | Heterocyclic molecule ring strain energy |
| E_p | Activation energy barrier of polymerization |
| E_c | Activation energy barrier of cycloaddition |
| pK_a | Acid dissociation logarithmic constant |
| TOF | Turnover frequencies |

| | |
|------------------------|--|
| TON | Turnover numbers |
| ee | Enantiomeric excesses |
| ABP | Amine-bis(phenolato) |
| CeO ₂ | Cerium(IV) oxide |
| DMCA | Dihydroxy- <i>p</i> -tert-butylcalix[4]arene |
| Et ₄ NOAc | Tetraethyl acetate |
| ZnEt ₂ | Diethylzinc |
| Bu ₄ NX | Tetrabutylammonium halide |
| TBACl | Tetrabutylammonium chloride |
| TBAB | Tetrabutylammonium bromide |
| TBAI | Tetrabutylammonium iodide |
| TBAAc | Tetrabutylammonium acetate |
| TBABz | Tetrabutylammonium benzoate |
| TBAAi | Tetrabutylammonium azide |
| TETACl | Tetraethylammonium chloride |
| TMeACl | Tetramethylammounium chloride |
| BnOH | Benzyl alcohol |
| BuOH | 1,4-butanediol |
| OBn | Benzyl oxide |
| OAc | Acetate |
| N ₃ | Azide |
| OSi(OtBu) ₃ | Tri- <i>tert</i> -butyl silicate oxide |
| PPNCl | Bis(triphenylphosphine)iminium chloride |
| PPNN ₃ | Bis(triphenylphosphine)iminium azide |
| TiBA | Triisobutylaluminium |
| TMS | Trimethylsilane |
| TEB | Triethylene borane |
| O-M | Oxygen-metal bond |
| MPa | Megapascal |
| MHz | Megahertz |
| kJ·mol ⁻¹ | Kilojoule per mole |

| | |
|---------------------------------|--|
| $\text{kg}\cdot\text{mol}^{-1}$ | Kilogram per mole |
| $\text{mol}\cdot\text{L}^{-1}$ | Mole per liter |
| mg | Milligram |
| mL | Milliliter |
| $\text{nmol}\cdot\text{L}^{-1}$ | Nanomole per liter |
| nm | Nanometer |
| $\text{g}\cdot\text{mol}^{-1}$ | Gram per mole |
| m/z | Mass-to-charge ratio |
| h | Hour |
| $^{\circ}\text{C}$ | Celsius |
| K | Kelvin |
| M_n | Number average molecular weight |
| M_w | Weight average molecular weight |
| \mathcal{D}_M | Dispersity |
| T_g | Glass transition temperature |
| k_b | Rate constant of back-biting |
| k_p | Rate constant of copolymer chain propagation |
| k_{obs} | The observed rate constant |
| r | Initial rate |
| E_a | Activation energy |
| UV/Vis | Ultraviolet-visible |
| NMR | Nuclear magnetic resonance |
| FTIR | Fourier-transform infrared spectroscopy |
| SEC | Size-exclusion chromatography |
| MALDI | Matrix-assisted laser desorption/ionization |
| DTF | Density functional theory |
| THF | Tetrahydrofuran |
| CDCl_3 | Deuterated chloroform |
| CHCl_3 | Chloroform |
| CH_2Cl_2 | Dichloromethane |
| DMF | Dimethylformamide |

DMAc

Dimethylacetamide

NMP

N-methyl-2-pyrrolidone

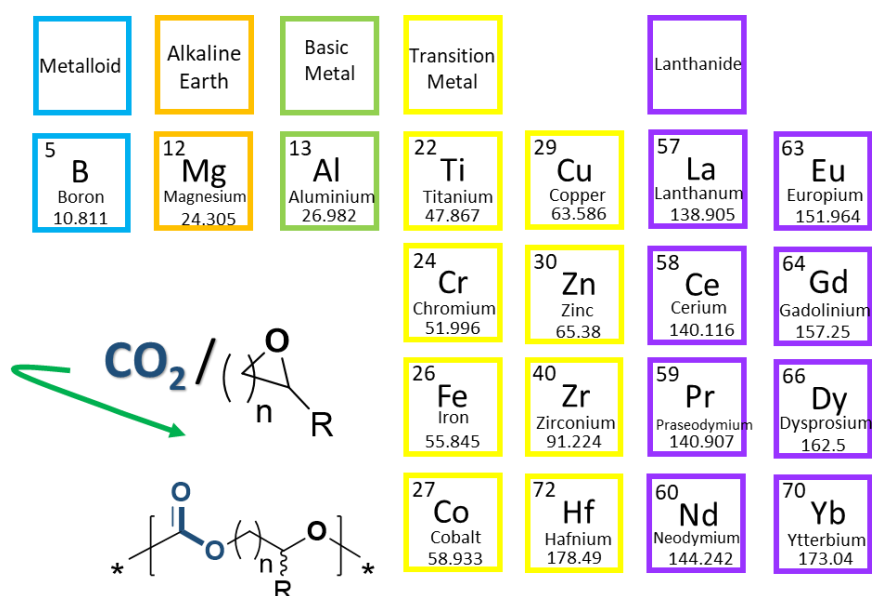
ACE

Active chain end

CTC

Charge transfer complexes

Update and challenges in CO₂-based polycarbonate synthesis



Keywords: Carbon dioxide, polycarbonate, catalytic copolymerization, cyclic carbonate

1.1 Introduction

Over the past century, plastics have revolutionized the industrial sector by allowing for the replacement of natural building blocks such as metal, wood and stone with cheaper, durable and adaptable synthetic materials.¹ Although the benefits in materials' evolution from plastic fabrication are numerous, the environmental stress of producing and disposing of such materials is acutely apparent. Currently, the majority of consumer plastics are manufactured from petroleum derived sources and the abuse of such fossil fuels is accelerating carbon dioxide (CO₂) emissions leading to a warmer, more unstable global environment.² Therefore utilisation of CO₂ has received a great deal of attention and made great advances in recent decades, albeit converting CO₂ as a synthon to high value-added organic products is not the most efficient approach to mitigate CO₂ levels.

As compared to the highly reactive carbon monoxide (CO), both fully oxidized state and centrosymmetric structure of the CO₂ render it relatively inert. The presence of the two electronegative oxygen atoms confers however to the carbon atom a somewhat electrophilic behaviour making it susceptible to undergo a nucleophilic attack.³ From a chemical perspective, CO₂ is a sustainable, biorenewable, non-toxic and non-flammable C1 feedstock that could be valorized in a variety of chemicals. Those last include small molecules such as carboxylic acids, cyclic carbonates, methanol, or longer hydrocarbon chains (C5-C11)^{4,5} but also polymeric structures.

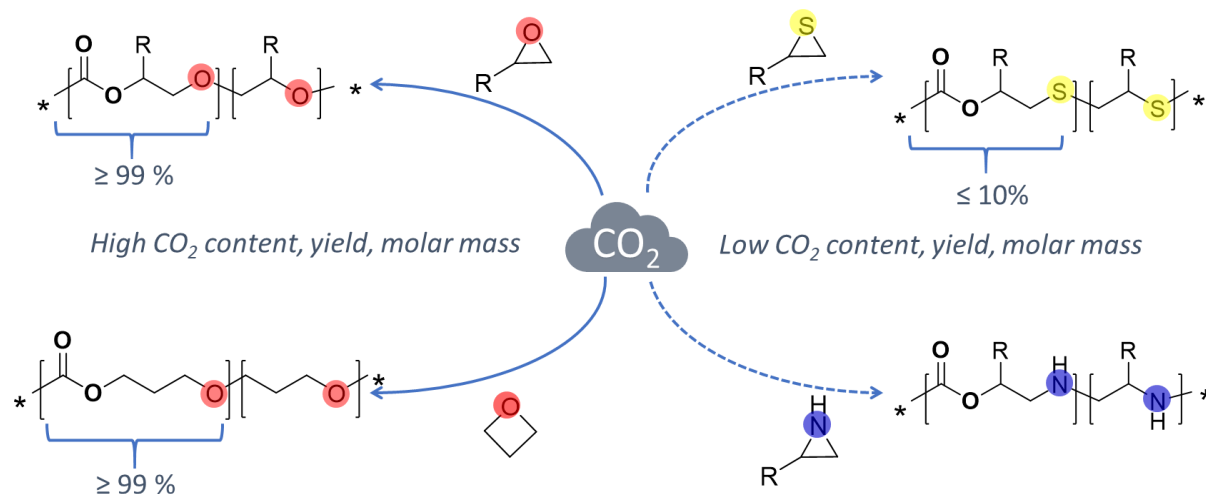
Hence, the efforts have been made to homopolymerize CO₂ into poly(CO₂)^{6, 7}. While direct polymerization is possible by requiring formidably high temperature and pressure (4 × 10⁴ MPa, 1800 K)⁸, the process is entropically disfavoured converting ineluctably poly(CO₂) into CO₂ gas under normal conditions of temperature and lower pressure. For those reasons, using CO₂ as a comonomer remains the only practical approach to incorporate CO₂ into polymer structures.

To prepare CO₂-based copolymer, two technics have been developed in past coming years consisting on (i) preparing CO₂-based monomer followed by a polymerization process ("monomer to

polymer” technic, M to P) and (ii) a direct “chain up” process of the CO₂ with other comonomers. The “M to P” technic provides a wide range of polymer precursors⁹⁻¹¹ associated with the advantage of using sublimed dry ice as CO₂ resource. In return, by-products and uneconomical purification processes are generally involved in a time-consuming approach.¹⁰ As far as the CO₂ “chain up” technic is concerned, polycondensation and ring-opening copolymerization (ROcP) have been used and reported. Although polycondensation methodology allow to prepare various product by the copolymerization CO₂ with corresponding substrates such as diols,¹² diamines, and dihalides,¹²⁻¹⁴ the drawbacks of uncontrollable polymerization, alongside with the concomitant by-products, plague the development of such method for potential industrial applications. In contrast, ring opening copolymerization CO₂ with heterocycles are highly desirable¹⁵ since few small molecule by-products is produced in a controlled manner.

Typically, three or four-membered heterocyclic molecules (HC) such as epoxide (EP), oxetane, episulfide (ES) or aziridine (AD) which feature high ring strain are suitable comonomers in CO₂-based ROcP. The association of CO₂ and those comonomers by a “chain up” process requires a repeated cycle of two steps consisting on a nucleophilic attack of the ring-straight HC and the addition of CO₂ from the ring-opened HC. (Scheme 1.1a). The driving force of the process is then entirely based on the cleavage of the C-X (X = N, O, S) bond which depends on the nature of the heterocyclic molecule ring strain energy (E_r). As compared to the other comonomers, ES molecules present the lowest E_r value ($\sim 74.05 \text{ kJ}\cdot\text{mol}^{-1}$)¹⁶. which considerably reduces its reactivity with CO₂.¹⁷ Comparatively EP ($E_r = 115.8 \text{ kJ}\cdot\text{mol}^{-1}$),¹⁸ oxetane ($E_r = 103.7 \text{ kJ}\cdot\text{mol}^{-1}$)¹⁹ and AD comonomers ($E_r = 108.7 \sim 112.9 \text{ kJ}\cdot\text{mol}^{-1}$)²⁰ are sufficiently reactive to theoretically expect a “chain up” process with CO₂ (Scheme 1.1b). Comparatively to others, the main drawback of a CO₂/AD copolymerization, alongside with the issue of CO₂-catalyzed homopolymerization of AD²¹, remains in the carbamic acid species produced during the process and resulting an uncontrollable copolymerization by the appearance of cyclic side-products and some branched copolymer structures,²²⁻²⁴ Hence, the copolymerization of CO₂ with EP

and oxetane to form aliphatic polycarbonates represent the most common routes to prepare polymers due to the high reactivity and the chemical tunability of oxygen heterocycles (Scheme 1.1b).^{25, 26}



Scheme 1.1. (a) Step-wise copolymerization of CO₂ with heterocyclic monomer (b) The corresponding copolymer from CO₂ and various heterocyclic monomers including general characteristics of those processes.

Probably due to the relative high price of the raw materials and an inherent low reactivity of oxetane molecules (as compared to their 3-membered homologues, i.e. oxiranes),²⁷⁻³¹ only few studies have been focused on oxetane/CO₂ coupling processes and reported so far in the state-of-the-art^{32, 33}. In contrast, EP/CO₂ copolymerizations have been studied extensively, not only for the superior ring-opening activity of EP, but also for the economical synthesis of EP based on petroleum³⁴ and biological resource³⁵.

The presented review will then focus on the progress realized in the preparation of cyclic carbonate synthons and aliphatic polycarbonate preparation from EP/CO₂ copolymerization as catalyzed by metal- and organo-based catalytic systems. Very interestingly, such a field of activities is quite young since the first example of CO₂/EP copolymerization dated back to 1969³⁶ and that the pioneering work of Baba *et al.* in oxetane involved CO₂ copolymerization was reported in 1984.³⁷

1.2 Organometallic Catalysts

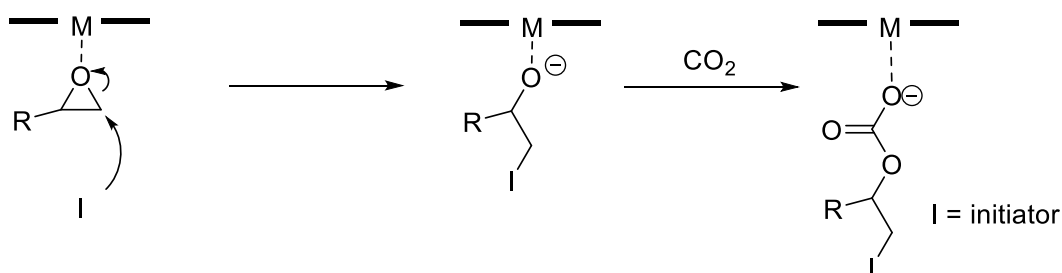
To improve material properties and to lower the associated costs, catalyst development has become a primary focus in the synthesis of aliphatic polycarbonates from CO₂ synthons. Metal-based catalysts have garnered the most attention since they often display superior catalytic activities, remain active under mild conditions, and are easily tuneable. Metals are particularly attractive as catalysts due to their versatile oxidation states and bonding modes (e.g. variability of co-ordination number and the ability to form both σ - and π -bonds).³⁸ Moreover, such catalysts can be easily tuned to modulate activity and/or selectivity via ligand substitution where the electronics at the metal-center and overall coordination sphere can be altered. As such, both main group and transition metal catalysts have been extensively developed for CO₂-based polymer synthesis. Before reviewing updates of metal-based catalysts, mechanism and kinetics should be discussed for the clear view of synthesis.

1.2.1 Mechanism and kinetics of copolymerization

General mechanism

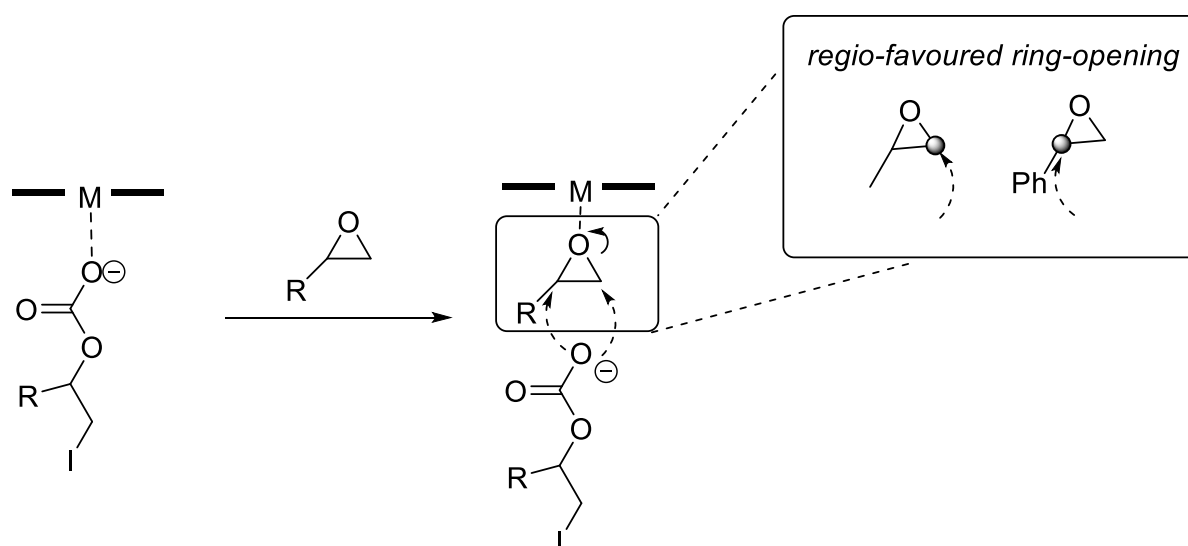
The mechanistic aspects of metal-catalyzed CO₂/EP copolymerisation were first investigated by Tsuruta and coworkers using diethylzinc (ZnEt₂) as catalyst where the oxygen-metal (O-M) species (alkoxide) was found to be of prime importance in initiating the copolymerization.³⁹ Briefly, direct copolymerization of CO₂ and EP is initiated by a ring-opened EP (alkoxide) that can subsequently attack CO₂ resulting in the formation of carbonate species (Scheme 1.2).

Initiation



Scheme 1.2. The initiation of CO₂/EP copolymerization.

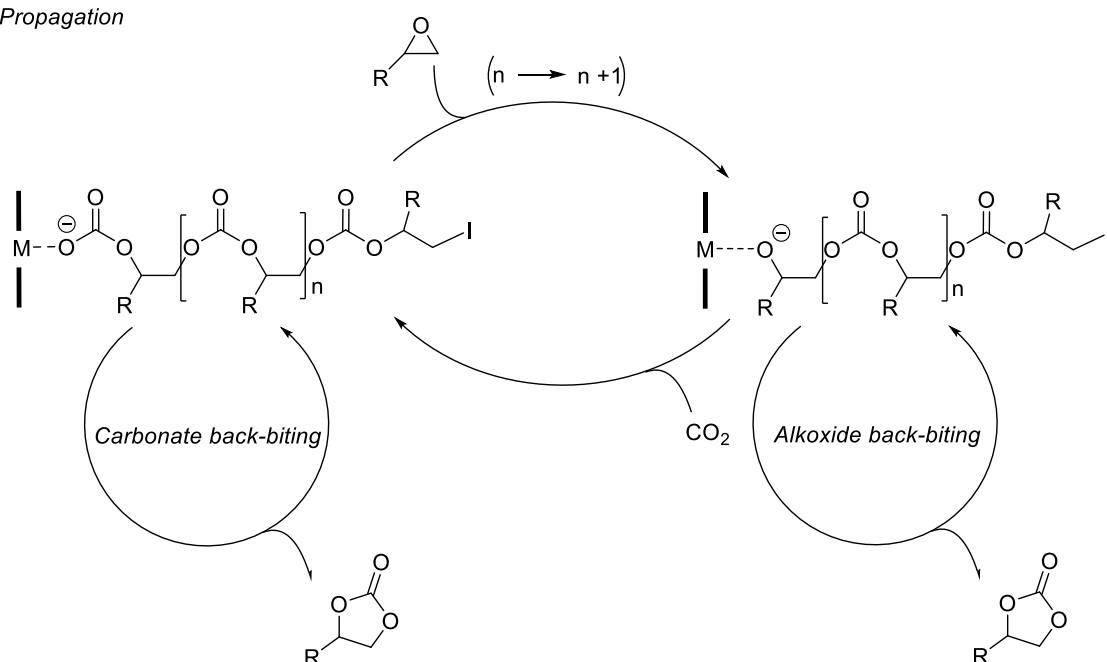
The ring-opening of the EP may experience different pathways depending on the nature of the terminal group regarding the electron donating or the electron withdrawing effects of dandling functions present on the 3-membered cyclic monomer. As examples, the electron-donating methyl function present on the propylene oxide (PO) will favor the EP to be opened by a methylene C-O bond cleavage, while electron withdrawing groups such as the aromatic phenyl of styrene oxide will prompt the methine C-O bond cleavage (Scheme 1.3).⁴⁰ Note also that such cleavages may occur simultaneously during a polymerization process leading to the production of regioirregular structures.⁴¹



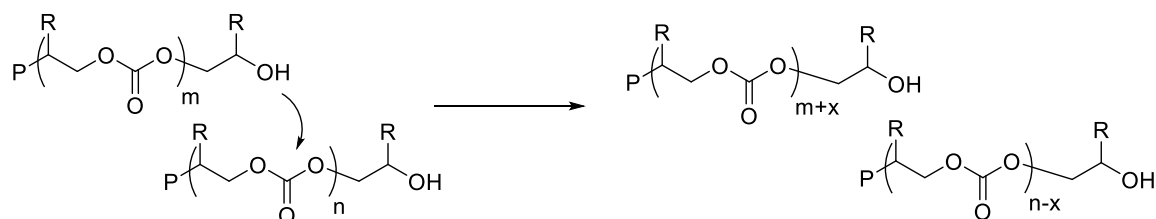
Scheme 1.3. regio-favored C-O bond cleavage of EP with different substituents.

Idealized copolymerization involves the cycling between these two species (alkoxide and carbonate) from the alternative insertion of EP and CO₂ correspondingly to form the polycarbonates while undesired cyclic by-production, ether linkages and chain transfer reactions occur practically (Scheme 1.4).

Propagation

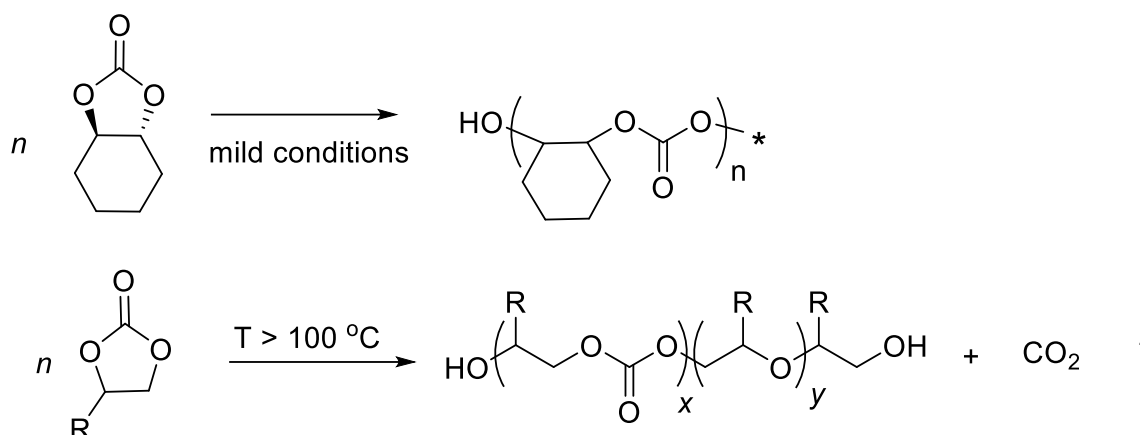


Chain transfer reaction



Scheme 1.4. The idealized propagation pathway of CO₂/EP copolymerization.

A common by-product in such co-polymerizations are five-membered cyclic carbonates (5CCs) that are often produced by back-biting reactions from the activated polymer chain (Scheme 1.4).⁴²⁻⁴⁴ The formation of 5CCs can be detrimental since they are thermodynamically stable (apart from *trans*-cyclohexane carbonate (*trans*-CHC) species with large dihedral angle (29.7°, -O-C-C-O-)⁴⁵ leading to high ring strain⁴⁶⁻⁴⁸). However, 5CCs favor entropically driven polymerization at high temperatures (> 100 °C), resulting in poly(carbonate-co-ether) with the concomitant release of CO₂ (Scheme 1.5).^{49, 50}

Ring-opening polymerisation**Scheme 1.5.** The schematically representation of polymerization of 5CCs.**Kinetic perspective**

Organometallic-based systems generally yield small amounts of 5CCs since the activation energy barrier of polymerisation (E_p) is lower than cyclic formation (E_c) (96.8 vs 137.5 kJ·mol⁻¹ for E_p vs E_c)²⁶. The coupling of EP/CO₂ is a first-order process related to catalyst and EP concentration, while zero order dependence with respect to CO₂ pressure.⁵¹⁻⁵³ However, in Rieger's dinuclear catalytic system, CO₂ pressure dramatically affects the kinetic behavior of copolymerization. For low pressure conditions (0.5-2.5 MPa), the CO₂ insertion is rate limiting as the reaction displays first-order dependence on CO₂ pressure and zero order dependence on EP assuming constant catalyst concentration. For 2.5 – 4 MPa, the order with respect to CO₂ turns to zero while EP's reaction order value is one. Conversely, in high pressure conditions (≥ 5 MPa), ring-opening of the EP monomer becomes the rate limiting step.⁵²

1.2.2 Main-group metal catalysts

Main group metals, Mg, Al and Zn for instance, are attractive alternatives to transition metal-based systems due to their low toxicity and relatively high abundance. Recently, main group-based homogeneous catalysts that display sufficient activity for EP and CO₂ co-polymerizations have been developed.

Mg Catalysts

Williams and co-workers developed a sophisticated bimetallic complex with macrocyclic ancillary ligands (**Mg-I**, Chart 1.1) displaying high activity for the cyclohexane oxide (CHO) and CO₂ copolymerization to yield poly (cyclohexane carbonate) (PCHC).⁵⁴ Up to 750 h⁻¹ TOF was observed, which is 20 times greater than previous Mg-based catalysts,⁵⁵ at 0.01 mol% **Mg-I** catalyst loading (1.2 MPa CO₂ pressure at 100 °C) and without the production of the cyclohexane carbonate (CHC) by-product. The decreased Lewis acidity and electropositive nature of magnesium contributes to a strong metal-carbonate bond that enhances the chain propagation over cyclic by-product formation. Notably, high carbonate content in the resultant polymer (> 99%) and near quantitative yields are even observed in the presence of excess exogenous water. This result is particularly important for industrial scale applications where air and moisture free processes are difficult and costly since many organometallic systems (e.g., cobalt-salen complexes) are deactivated in the presence of water.⁵⁶⁻⁵⁸

Very recently, the commercially available dialkylmagnesium species (**Mg-II**, Chart 1.1) effectively catalyzed the isoselective CHO/CO₂ copolymerization (up to 82% isotacticity), which is the first report of using an achiral catalyst to synthesize a stereo-controlled polycarbonate.⁵⁹ The TOF was modest at 0.1 MPa (6 h⁻¹) and could be increased approximately tenfold (TOF = 62 h⁻¹ at 1 MPa CO₂), but with the cost of diminished tacticity control.

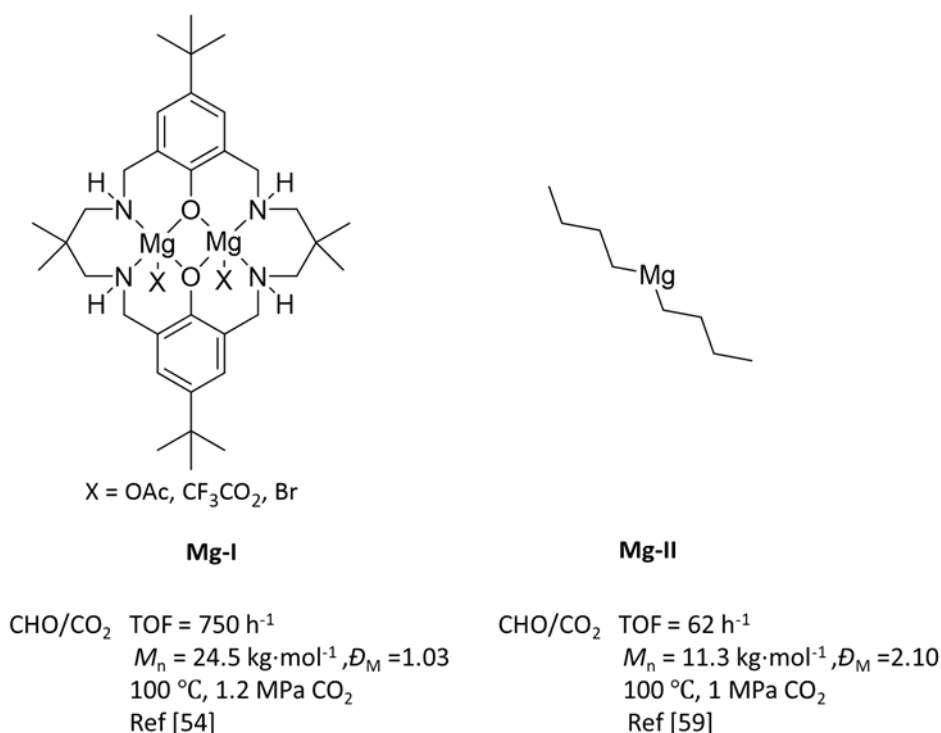


Chart 1.1. Representative magnesium-based catalysts for CO₂/EP copolymerization.

Al Catalysts

After a triethylaluminium catalyzed EP/CO₂ copolymerization was reported,⁶⁰ numerous Al-based catalysts were developed with various ligands such as porphyrin,⁶¹ salophen,⁶² salen,⁶³ dihydroxy-*p*-tert-butylcalix[4]arene (DMCA).⁶⁴ Porphyrin ligands have been ubiquitous in metal complexes for CO₂ copolymerizations because of their well-defined coordination modes and superior reactivity of the axial bond on the metal center that is perpendicular to porphyrin plane. Bifunctional porphyrin-Al complexes (**AI-I**, Chart 1.2) successfully yielded polycarbonates incorporating CO₂.^{65, 66} By introducing electron donating substituents on the porphyrin ligand to modulate Lewis acidity at the aluminium center yielded high molecular weight polymers with decreased cyclic by-products as compared to ligands bearing electron withdrawing groups. Previously, aluminium-porphyrin systems produced low molecular weight polymers ($M_n = 4.5 \text{ kg}\cdot\text{mol}^{-1}$).⁶¹ However, in another study, aluminium complexes bearing porphyrin ligands substituted with electron withdrawing fragments were more active and afforded polycarbonates with higher molecular weights ($M_n = 33.5 \text{ kg}\cdot\text{mol}^{-1}$, $\mathcal{D}_M = 1.05$).⁶⁷ Sugimoto and

coworkers investigated a series of aluminum chiral catalysts for the enantioselective copolymerization of CO₂ and CHO.⁶⁸ Al-salen complexes (**AI-II**, Chart 1.2) activated with tetraethyl acetate (Et₄NOAc) afforded highly alternating copolymers, but with low molecular weights ($M_n = 1.9 - 6.8 \text{ kg}\cdot\text{mol}^{-1}$, $\bar{D}_M = 1.14 - 1.22$) and modest enantiomeric excesses (ee) up to 23%. Using similar reaction conditions, the selectivity of the reaction was increased by using Al β -ketoiminate complexes (**AI-III**, Chart 1.2) paired with a Lewis base (N,N-dimethyl-4-aminopyridine) co-catalyst (ee = 49%). The enantioselectivity was further improved to 80% ee by implementing a bisamine Lewis base co-catalyst conditions, however high molecular weight polymers remained elusive. More recently the synthetically simple triisobutylaluminium (TiBA) (**AI-IV**, Chart 1.2) catalyst coupled with lithium ions as an initiator catalyzed the synthesis of alternating polycarbonates in a controlled manner with moderate molecular weights ($M_n = 19.6 \text{ kg}\cdot\text{mol}^{-1}$, $\bar{D}_M = 1.10$).⁶⁹ Another aluminium-based catalyst featuring aminephenolate ligands (**AI-V**, Chart 1.2) produced moderate molecular weight copolymers from CHO and CO₂ ($M_n = 29 \text{ kg}\cdot\text{mol}^{-1}$, $\bar{D}_M = 3.16$) although only 54% carbonate content was found in the resultant materials.⁷⁰ This non-alternating structure with enhanced ether content is likely a result of the off-target coordination between the aluminum center and heteroatoms of the ligand that serve to inhibit insertion of carbonate anion.

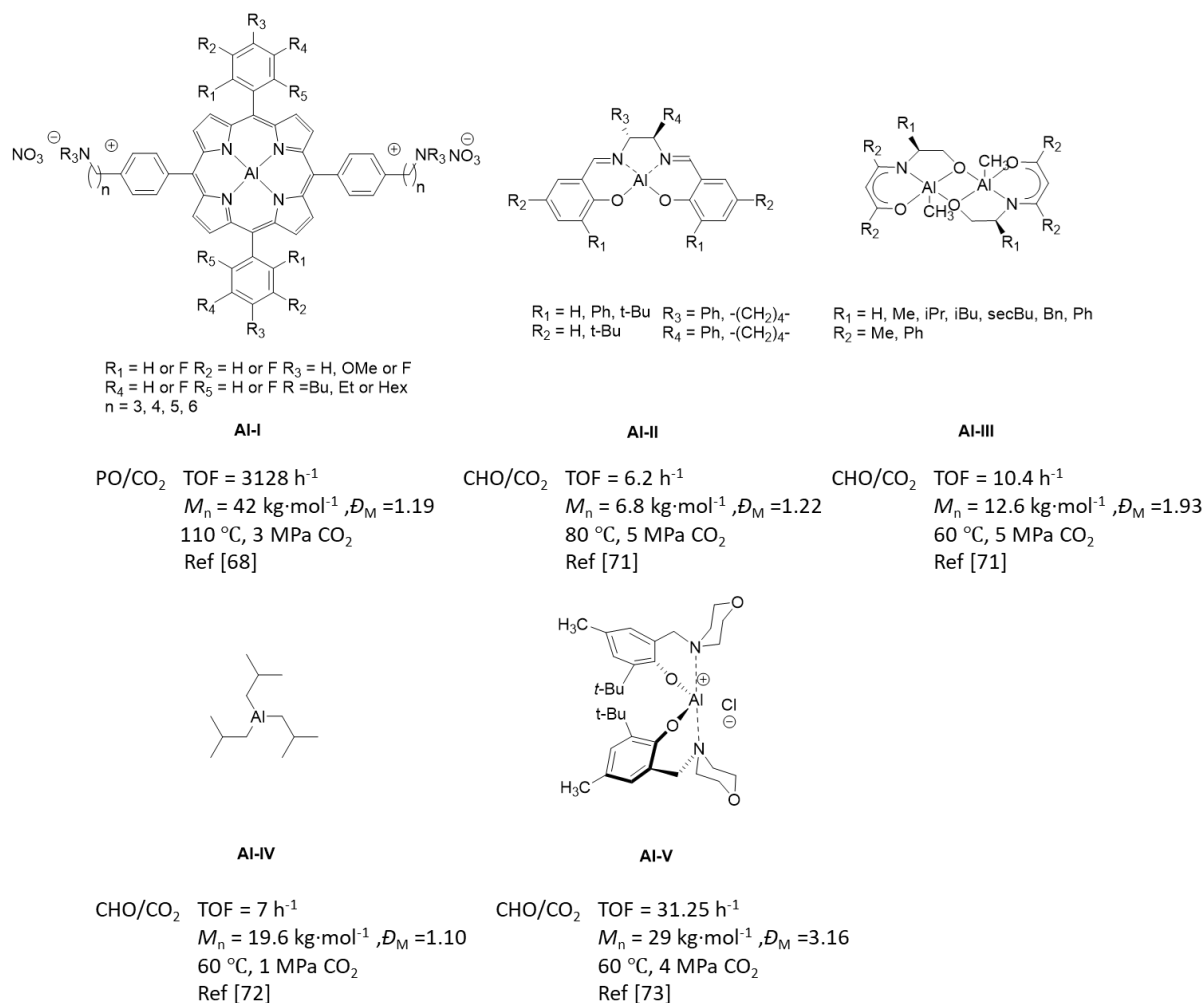


Chart 1.2. Representative aluminium-based catalysts for CO₂/EP copolymerization.

Zn Catalysts

Although zinc shares characteristics of both main-group and transition metals, it is better defined as main-group metal due to similarities with magnesium in terms of atomic size and preferred oxidation state.⁷¹ Zinc-based catalysts (diethyl zinc/H₂O) were already used for the CO₂/EP copolymerisation in 1969 and their related interest continued to grow due to the abundance of such a metal.³⁹ The dinuclear zinc structure bearing a macrocyclic ancillary ligand (**Zn-I**, Chart 1.3) demonstrates remarkable activity in the CO₂/CHO copolymerization at only 0.1 MPa CO₂.⁷²⁻⁷⁶ Attempts to probe the mechanism of **Zn-I** catalyzed processes by experimental and computational methods have revealed that the coordinated epoxide undergoing the nucleophilic attack from carbonate group

bound to the zinc metal center is the rate-determining step.^{77, 78} The continue work using heterodinuclear (Mg and Zn) catalyst is benefitted with co-catalysts free, lack of colours and high activities in comparison with homodinuclear center.⁷⁹ Asymmetrical β -diketiminato-based Zn catalysts (**Zn-II**, Chart 1.3) have also displayed high efficiencies in CO₂/CHO copolymerizations (TOF = 814 h⁻¹) when using modest CO₂ pressure c.a. 1 MPa.^{80, 81} More recently, Rieger and co-workers developed β -diiminato containing Zn complexes (**Zn-III**, Chart 1.3) active in copolymerization of CO₂ with various epoxides including CHO, propylene oxide (PO), styrene oxide (SO), limonene oxide (LO), octene oxide (OO) and epichlorohydrin (ECH) with CO₂.^{52, 82, 83} Extremely high catalytic activity (TOF = 5520 h⁻¹) was observed at moderate pressure (4 MPa CO₂) which is a promising result for potential industrial applications. A reported novel di-zinc catalyst bearing heteroscorpionate ligands (**Zn-IV**, Chart 1.3) yielded CHO/CO₂ copolymers with $M_n = 39 \text{ kg}\cdot\text{mol}^{-1}$ at 4 MPa CO₂ after 48 h.⁸⁴

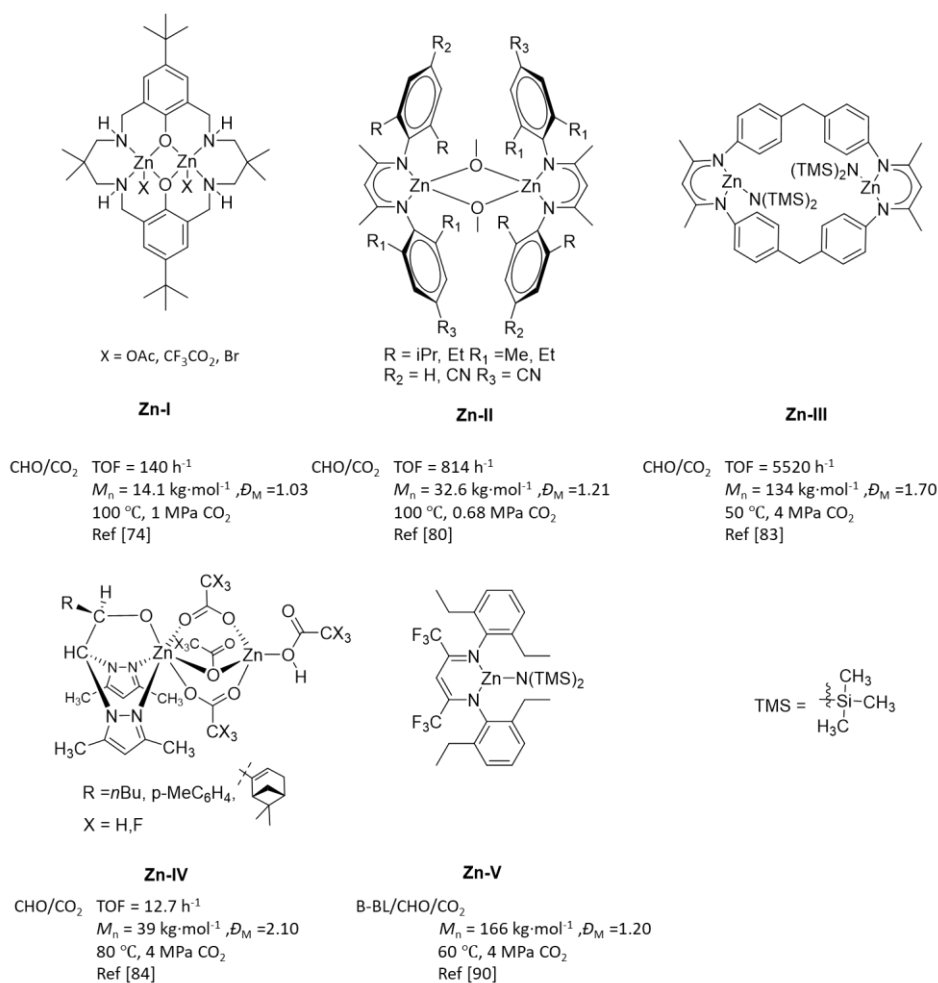
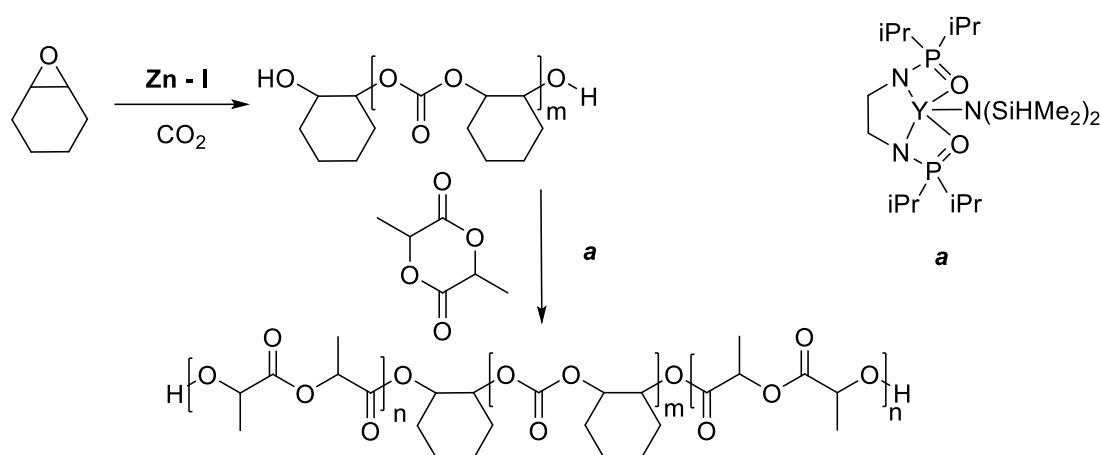


Chart 1.3. Representative zinc-based catalysts for CO₂/EP copolymerization.

Although CO₂/CHO copolymers are often used as a standard in academic investigations, they are not likely to replace commodity plastics because of inferior thermal and mechanical properties (Low T_g and elasticity).^{85, 86} However, the introduction of a third comonomer to produce terpolymeric architectures provides access to materials with a broader range of thermal and mechanical properties that could compete with modern thermoplastics (polypropylene for instance). Consequently, interest in terpolymer structures is increasing and Zn based catalysts have shown great promise in this area. Using **Zn-I** complexes in presence of an yttrium initiator, a novel triblock copolymer (poly(lactide)-*b*-poly(cyclohexane carbonate)-*b*-poly(lactide)) was successfully prepared featuring two distinct glass transition temperatures (T_g = 60 & 80 °C)(Scheme 1.6).⁸⁷

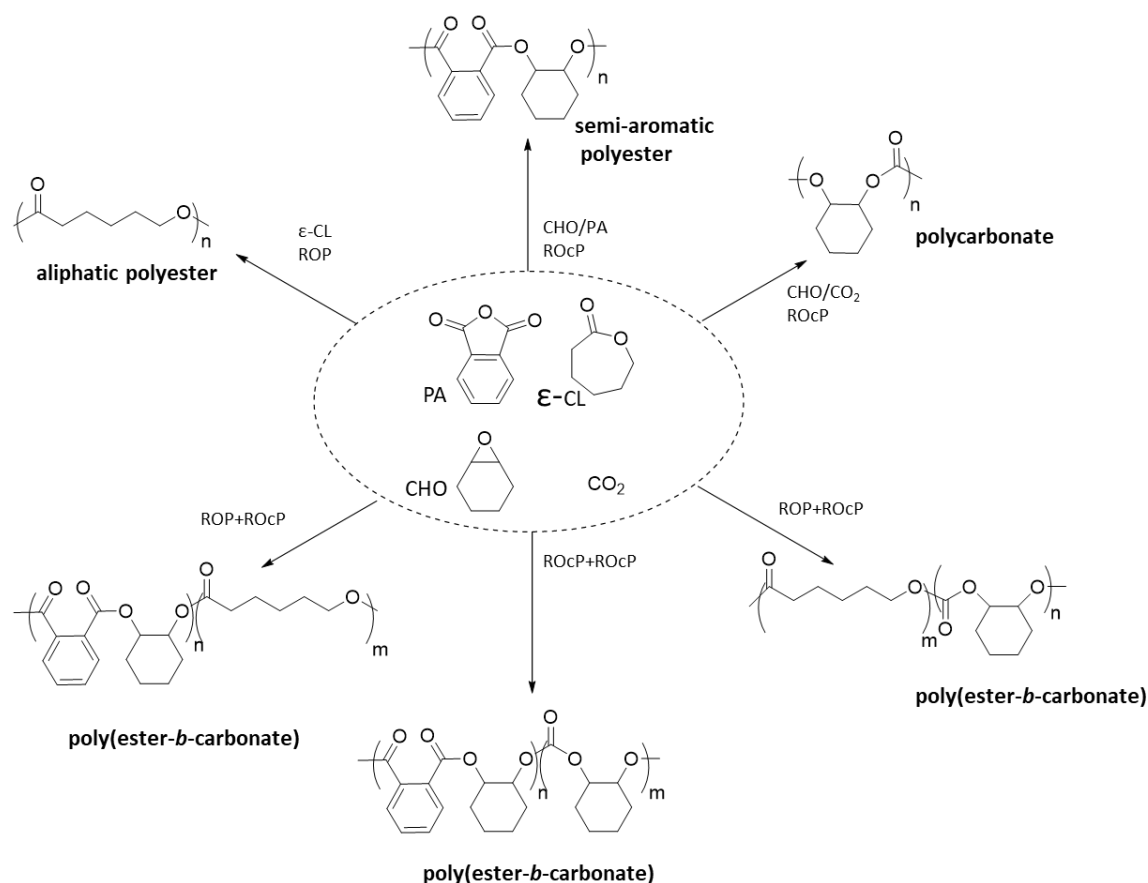


Scheme 1.6. Copolymerization of CHO and subsequent block copolymerization with lactide.

A similar study of poly(ϵ -caprolactone)-*b*-poly(cyclohexane carbonate)-*b*-poly(ϵ -caprolactone) was carried out in one-pot, two steps synthesis by combining CHO, CO₂, and ϵ -caprolactone (CL) in presence of **Zn-I**.⁸⁸ Rieger reported the synthesis of flexible triblock poly(cyclohexane carbonate)-*b*-poly(dimethylsiloxane)-*b*-poly(cyclohexane carbonate) using poly(dimethylsiloxane) as chain transfer agent catalyzed by **Zn-III** to overcome the brittleness of poly(cyclohexane carbonate).⁸⁹

Usually a triblock CO₂ copolymer synthesis requires a multi-step manipulation and poly-diol as a macro-initiator resulting in fixed sequent block component which are, to some extent, uneconomic and time-wasted approaches with limited applications. Finding block copolymer in the way simple manipulation is promising to industrial scale utilization of the CO₂ resource. Thanks to the catalyst developments, tuning CO₂ pressure to control the sequence of copolymer turns out to be a reality. Moreover, **Zn-V** complexes have been applied to the synthesis of sequence controlled terpolymers where CO₂ pressure was leveraged as a chemoselective agent in a one-pot synthesis.⁹⁰ When subjecting the mixture to low pressure (0.3 MPa CO₂), a statistical terpolymer consisting of β -butyrolactone (β -BL), CO₂, and CHO was produced ($M_n = 69 \text{ kg}\cdot\text{mol}^{-1}$, $\mathcal{D}_M = 1.60$). The block terpolymer (poly(β -BL)-*b*-poly(CHC)) ($M_n = 146 \text{ kg}\cdot\text{mol}^{-1}$, $\mathcal{D}_M = 1.20$) was obtained by tuning CO₂ pressure in the way of presenting high pressure (4 MPa) and releasing CO₂ atmosphere.

Williams and coworkers have leveraged **Zn-I** and similar dinuclear catalysts to afford control over the polycarbonate microstructure when using a mixed monomer feedstock where monomer reactivity was dependent upon nature of the polymer chain-end (Zn-O bond).⁹¹⁻⁹³ Similarly, Williams and coworkers reported a series of sequence-controlled copolymers from a four component mixture containing CL, CHO, phthalic anhydride (PA) and CO₂. Various copolymers were obtained in a one-pot methodology including semi-, full aliphatic polyesters, poly (ester-*b*-ester), polycarbonates and poly (ester-*b*- carbonate) by the advantage that the catalyst can switch between distinct polymerization cycles (Scheme 1.7).⁹³ The ability to rationally tune the polymer microstructure from monomer mixtures is a significant advancement and is particularly suited for industry applications since it affords access to numerous architectures in a straightforward and, potentially, cost-effective manner.



Scheme 1.7. Four exemplary monomers and the range of polymer products produced using chemoselective catalysis.⁹³

1.2.3 Transition metal catalysts

Transition metal catalysis continues to be a cornerstone in most synthetic applications because of the high versatility imparted by predictable oxidation-state switching and easy structural tuning enabled by ligand development and substitution.⁹⁴ Furthermore, transition metal complexes are generally more resistant to oxidative and/or hydrolytic degradation that plague many main-group catalytic systems. The glaring weakness of transition metal catalysis is that the natural abundance of transition metals is extremely low making them quite expensive and hampering their sustainability.⁹⁵ Nevertheless, efforts to improve the recyclability of such catalysts and increase catalytic efficiencies should lessen raw material requirements.

Co catalysts

Organometallic cobalt complexes have been particularly effective at catalyzing CO₂ copolymerisations since cobalt possesses a strong Lewis acidity and adopts a variety of oxidation states. Some of the most studied complexes feature tetradentate – salen ligands^{58, 96-101} and tetraaza macrocycles – porphyrin^{67, 102-107} with Co^{III} metal centers.

Lu and Darensbourg first reported the preparation of moderate molecular weight ($M_n = 25.9 \text{ kg}\cdot\text{mol}^{-1}$, $D_M = 1.07$) alternating CO₂/epichlorohydrin (ECH) copolymers using Co^{III}-based catalysts (Chart 1.4, **Co-I** and **Co-II**).¹⁰⁸ ECH is a notoriously challenging monomer since under high temperature (25 °C) chloride elimination is significant contributing to the formation of cyclic carbonate species so the activity of the cobalt species was critical with polymerization occurring below ambient temperatures (0 °C).

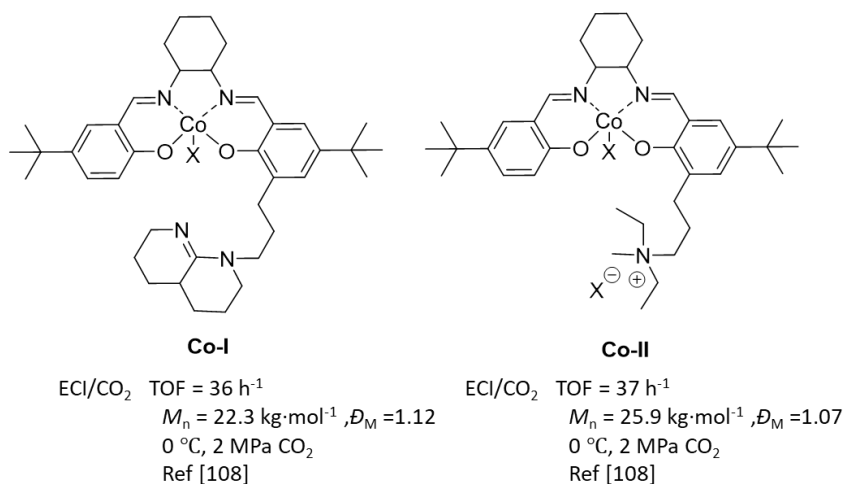
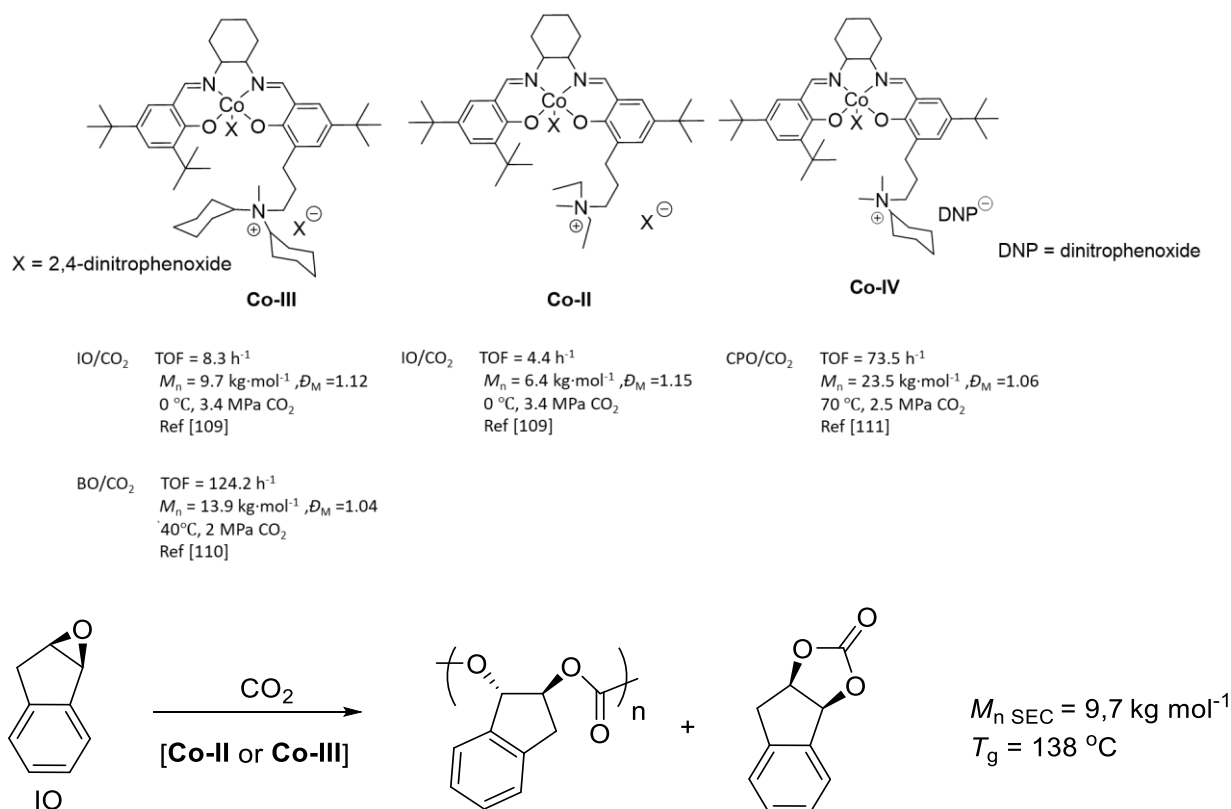


Chart 1.4. Representative cobalt-salen complexes.

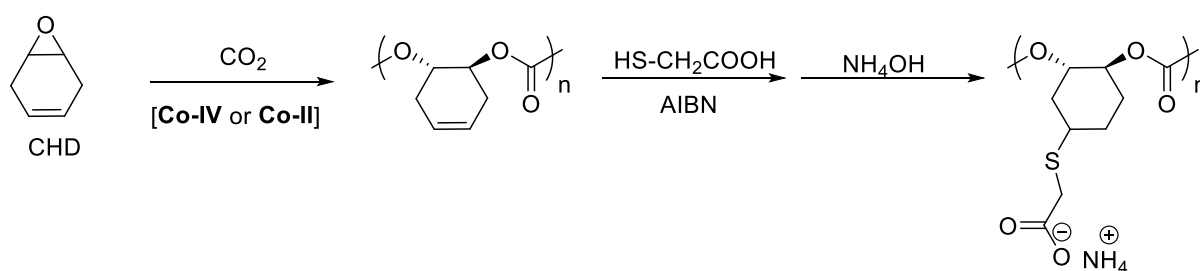
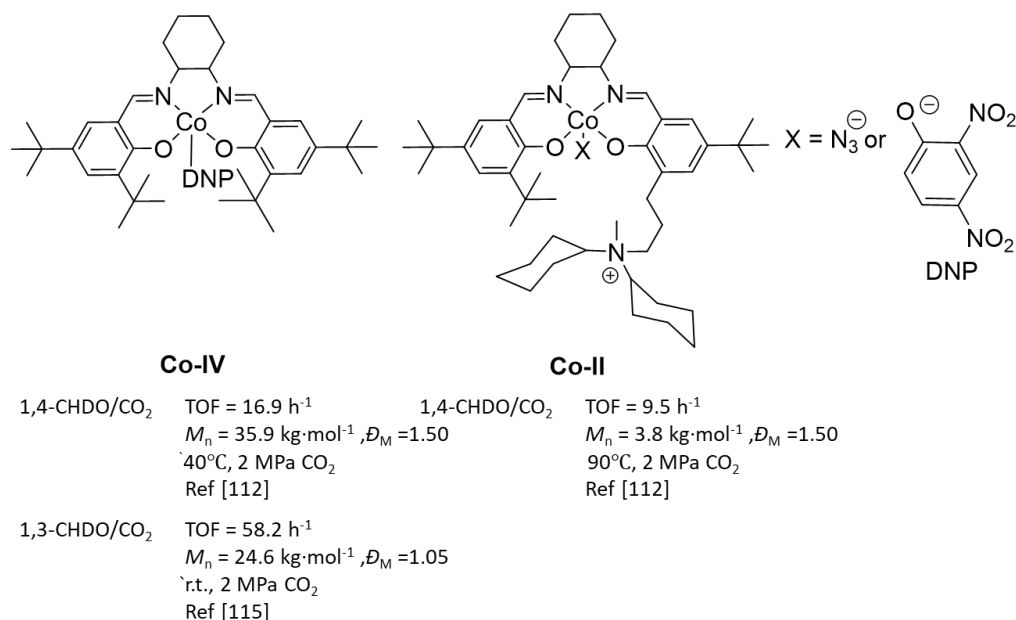
Copolymerization of indene oxide (IO) and CO₂ with mild reaction conditions using **Co-II** & **Co-III** has also been reported (Scheme 1.8).¹⁰⁹ To obtain high molecular weight, the copolymerization was performed at 0 °C with low catalyst loading (0.1 mol%) since cyclic carbonate formation is thermodynamically favored. Although low catalyst loadings (0.1 mol%) led to correspondingly longer induction periods of such binary catalyst system, the resultant polycarbonate was still isolated with reasonable properties ($M_n = 9.7 \text{ kg}\cdot\text{mol}^{-1}$, $\bar{D}_M = 1.09$, $T_g = 138$ °C). Using **Co-III** and **Co-IV**, the substrate scope was expanded to include butene oxide (BO)/CO₂ (poly(*trans*-2-butene carbonate), $M_n = 13.9 \text{ kg}\cdot\text{mol}^{-1}$, $\bar{D}_M = 1.05$, after 24 h)¹¹⁰ and cyclopentane oxide (CPO)/CO₂¹¹¹ (poly(cyclopentane carbonate), $M_n = 23.5 \text{ kg}\cdot\text{mol}^{-1}$, $\bar{D}_M = 1.06$, after 5 h as well).



Scheme 1.8. The copolymerization of indene oxide and CO₂ in presence of **Co-II** or **Co-III**.

Although saturated analogues are not very amenable to post-polymerization modifications, the introduction of unsaturated units (e.g. alkenes) into the polymer chain¹¹² that can be derivatized via thiol-based click chemistry¹¹³ (Scheme 1.9). The cobalt catalyzed copolymerization of cyclohexadiene oxide (CHDO) and CO₂ afforded high molecular weight poly(cyclohexadiene carbonate) (M_n = 35.9 kg·mol⁻¹) with good thermal properties (T_g = 123 °C) which is slightly higher than saturated polycarbonate (T_g = 116 °C). The replacement of cobalt in **Co-IV** scaffold with zinc or magnesium was also investigated, but the cobalt catalyst displayed superior performance (TOF = 65 h⁻¹) affording a polymer with higher molecular weight and lower dispersity (M_n = 12.9 kg·mol⁻¹, Đ_M = 1.18).¹¹⁴ Regiochemistry has also been investigated in the CHDO/CO₂ system by examining the effect of the alkene placement (1,3-CHDO versus 1,4-CHDO).¹¹⁵ Co-polymerizations with 1,3-CHDO displayed increased reaction kinetics and yields (40.8% selectivity of polymer and 100% conversion for 1,3-CHDO) while the inferior catalytic activity was observed for 1,4-CHDO/CO₂ (36.6% selectivity of polymer with

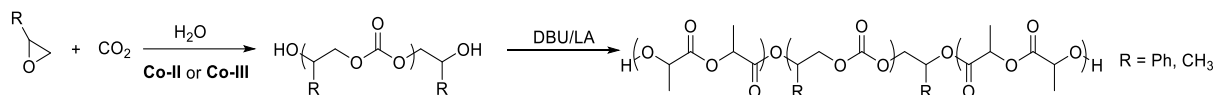
57% conversion for 1,4-CHDO), albeit poly(1,3-cyclohexadiene carbonate) features a slight lower T_g (104 – 108 °C) than poly (1,4-cyclohexadiene carbonate) (T_g = 123 °C).



Scheme 1.9. Representative functional polycarbonate synthesis using cobalt-salen complexes.

Similarly to the zinc catalyzed synthesis of poly(lactide)-*b*-poly(carbonate)-*b*-poly(lactide) materials,⁸⁷ Co^{III} catalysts have also found utility in the preparation of triblock CO₂-based polymeric materials (Scheme 1.10). Both propylene oxide (PO)¹¹⁶ and styrene oxide (SO)¹¹⁷ were copolymerized with CO₂ to form ABA-type block copolymers with a degradable carbonate-containing block, respectively. Building upon this concept more complex co-monomers such as allyl glycidyl ether¹¹⁸ or cyclic phosphates¹¹⁹ were also successfully copolymerized with CO₂ to form the polycarbonate block. These studies highlight a promising route to CO₂ incorporation into functional materials. Moreover,

the advantages imbued by the simple one-pot synthesis and monomer diversity should make this method attractive to industry interests.

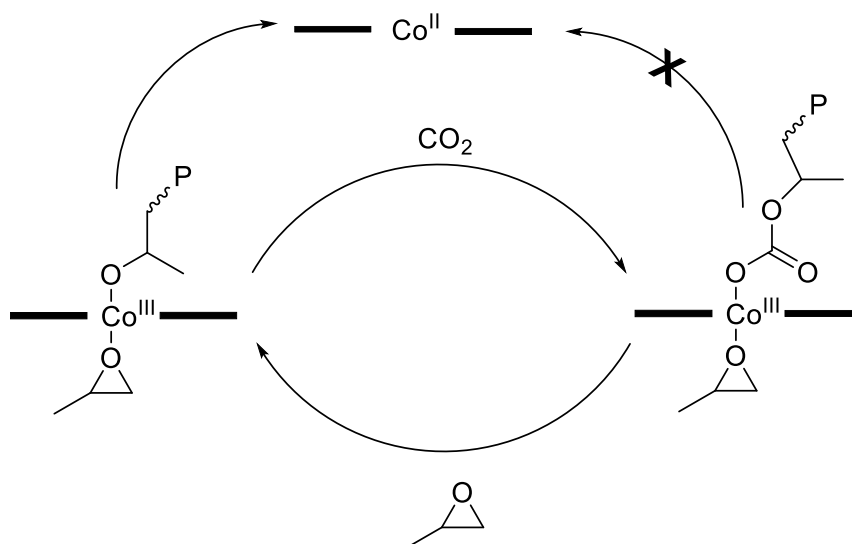


Scheme 1.10. One pot synthesis of poly carbonate-*b*-ester from CO₂, epoxide, and lactide.

While Co^{III}-salen complexes have been widely used for epoxide/CO₂ copolymerizations, dinuclear systems also demonstrate high activity yet operate by a distinct mechanism relative to the single-site cobalt complexes. A dinuclear cobalt catalyst with a macrocyclic ancillary ligand yielded a copolymer from CO₂/CHO under mild conditions (0.1 MPa CO₂).¹²⁰ Unlike the alternating insertion of CO₂ and alkoxide in single site systems, Williams and coworkers have proposed a different catalytic cycle when dinuclear catalysts are employed where the ligated epoxide on one metal center attacks the neighboring cobalt ligated to the carbonate polymer chain-end.

Due to their facile synthesis and ease of handling porphyrin ligands have been widely investigated in cobalt complexes for CO₂ copolymerizations. Rieger and coworkers demonstrated facile tuning of catalytic activity in single metal cobalto-porphyrin complexes where electron withdrawing substituents on the periphery of the porphyrin led to only cyclic carbonate formation while substitution with electron donating groups (e.g. alkoxy group) afforded a catalyst that yielded high molecular PO/CO₂ copolymers ($M_n = 46.5 \text{ kg} \cdot \text{mol}^{-1}$, $D_M = 1.20$) at 30 °C. Following the studies involving single-site cobalt-porphyrin complexes, dinuclear complexes were synthesized and examined in CO₂ copolymerizations.¹²¹ In contrast to dinuclear cobalt-salen species, unfortunately, no rate enhancement or increase in polymer formation was observed when bis-para-tethered dinuclear complexes were employed for the CO₂/PO copolymerization suggesting that polymer growth proceeds from one metal center. For the bis-ortho-tethered porphyrin, due to steric constraints, the polymerization was even more sluggish, and the cyclic carbonate was the predominant product. As

suggested by UV/Vis and NMR experiments it is likely the Co^{III}-alkoxide species hydrolyzes and forms an inactive Co^{II} species.^{121, 122} Polymer formation is still possible if CO₂ insertion occurs and forms the more stable cobalt-carbonate complex (Scheme 1.11), which is not as pronounced as in Co^{III}-salen complexes.⁴⁵

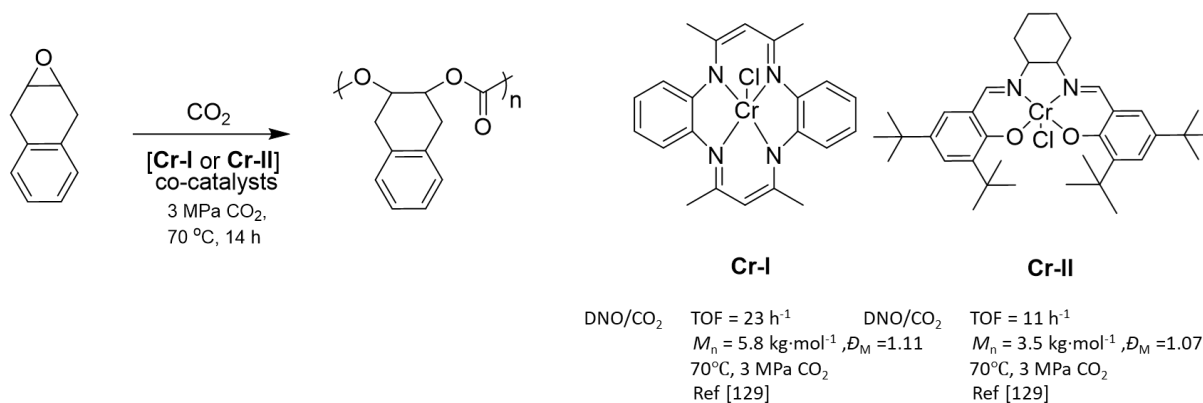


Scheme 1.11. The possible propagation route and deactivation pathways for Co^{III} catalyzed CO₂/PO polymerizations (where P represents the growing polymer chain).¹²³

Cr catalysts

Salen-chromium complexes^{109-112, 124, 125} perform markedly worse often leading to lower amounts of polymer formation and diminished catalytic activity as compared to their cobalt analogs. The same general observation is apparent for thio-ligated chromium catalysts as well.^{126, 127} It has been hypothesized that this is a consequence of the larger spherical volume of six-coordinate Cr relative to Co that serves to assist back-biting along the polymer chain.¹²⁸ To overcome this issue, a chromium catalyst featuring a less sterically hindered salen-type ligand (**Cr-I**) was investigated in the copolymerization of 1,4-dihydronaphthalene oxide (DNO) and CO₂ (Scheme 1.12).¹²⁹ The planar geometry of the azaannulene ligand opened up the coordination sphere around the metal center and allowed the polymerization to proceed to 63% conversion with only 11 % cyclic carbonate formation

(TOF = 23 h⁻¹). A chromium complex bearing the classic salen ligand (tert-butyl substituents) (**Cr-II**) resulted in poor conversion (32 %) and larger amounts of cyclic carbonate by-product (39 %) with low TOF (11 h⁻¹).



Scheme 1.12. The copolymerization of 1,4-dihydronaphthalene oxide and CO₂ using **Cr-I** or **Cr-II**.

Kozak developed a series of Cr^{III} amine-bis(phenolato) (ABP) catalysts (**Cr-III**, Chart 1.5) for CO₂/CHO copolymerizations to yield moderate molecular weight polycarbonate ($M_n = 13.1 \text{ kg}\cdot\text{mol}^{-1}$, $\bar{D}_M = 1.40$) in just 24h at low catalyst loading (0.2 mol% Cr and 0.1 mol% co-catalyst).^{130, 131} Both *trans* and *cis* geometries feature an accessible, vacant coordination site that allows an ionic species to coordinate with the metal center. Although the chloride-bridged dimer was isolated and confirmed by X-ray diffraction, it is likely that the monometallic, five-coordinate complex that is ligated by ionic cocatalysts (e.g. azide, chloride) is involved in the catalytic cycle since the cocatalyst and Cr^{III} dimer afford a heterogenous mixture in CHO. **Cr-III** with co-catalysts are also active in the copolymerization of CO₂ with PO with decent activity (TOF = 48 h⁻¹) at low temperature (25 °C).¹³²

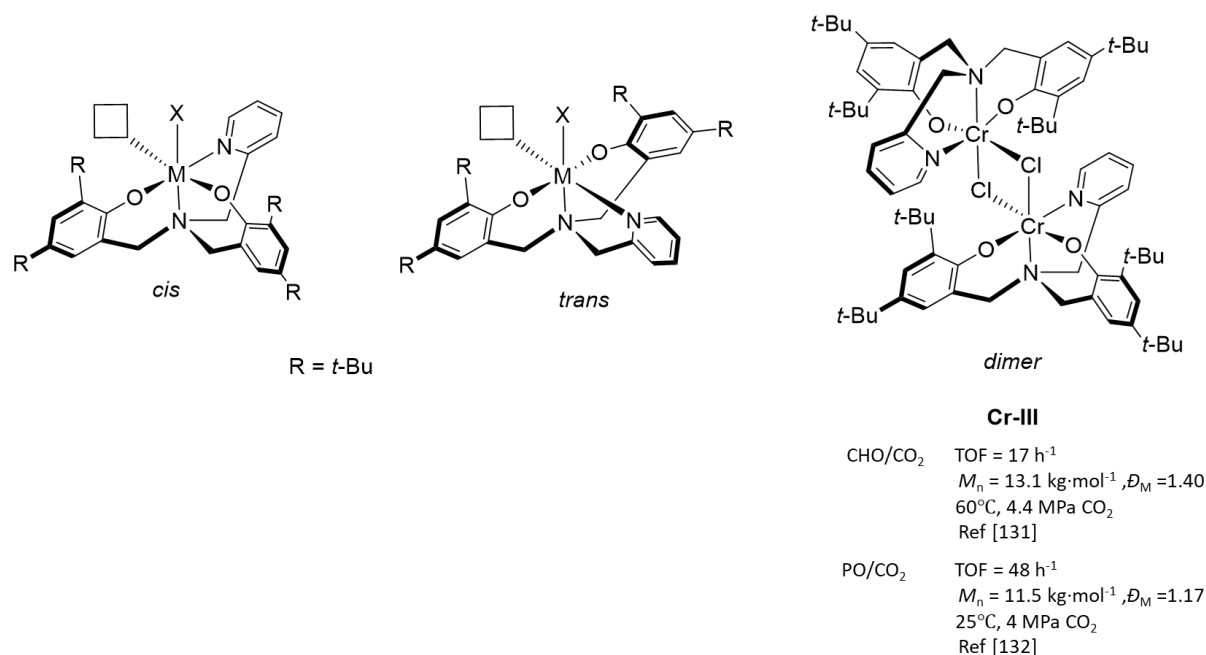


Chart 1.5. The steric formation of Cr-III catalyst and proposed monometallic geometries.

In a follow-up study two similar chromium complexes featuring either a tridentate and tetradentate ligand were synthesized by replacing the pridyl arm of **Cr-III** with either a non-coordinating benzyl moiety (**Cr-IV**, Chart 1.6) or a weaker tetrahydrofuranyl donating group (**Cr-V**, Chart 1.6) in 2014.¹³³ Overall, the tridentate complex resulted in lower molecular weight polymers ($M_n = 3.8 \text{ kg}\cdot\text{mol}^{-1}$, $\bar{D}_M = 1.48$) likely due catalyst instability while the tetradentate ligand afforded better results ($M_n = 6.4 \text{ kg}\cdot\text{mol}^{-1}$, $\bar{D}_M = 1.42$). Notably, **Cr-V** still performed worse than **Cr-III** likely due to the weaker donating ability of the ethereal oxygen in the tethering group, thus highlighting the critical importance of ligand tuning. A recent work from Kozak and co-workers described a new complex where the tetrafuranyl moiety in **Cr-IV** was replaced with a more donating amino group (**Cr-VI**, Chart 1.6) which led to an improvement of the CO₂/CHO copolymerization furnishing a controlled, high molecular weight polycarbonate ($M_n = 35 \text{ kg}\cdot\text{mol}^{-1}$, $\bar{D}_M = 1.12$).¹³⁴

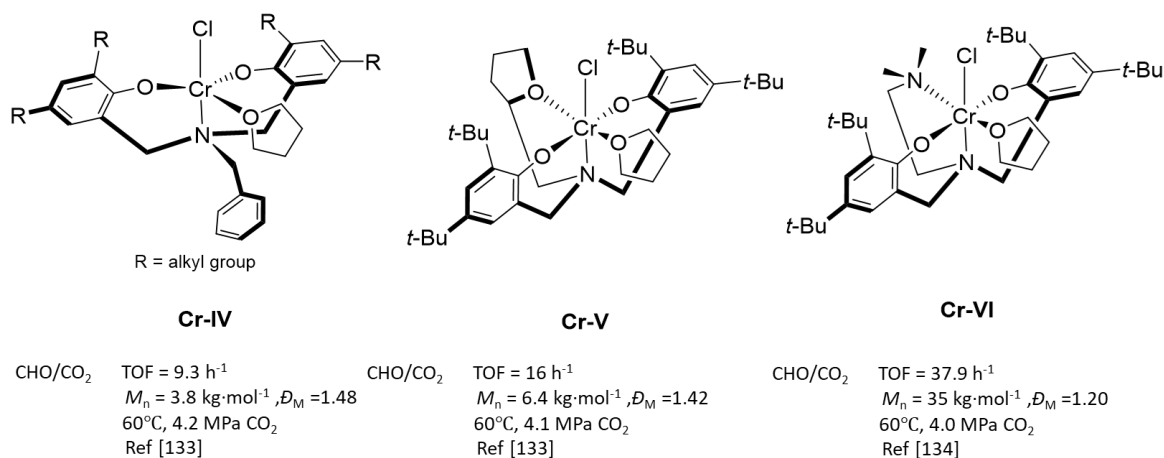


Chart 1.6. Representative complexes of chromium with tridentate and tetradentate ligands.

Cr-porphyrin complexes have also been screened in the synthesis of CO₂-based polycarbonates.^{107, 135} When compared to the main-group containing Al-porphyrin counterparts⁶⁶, the catalytic activity of chromium complexes are less dependent upon CO₂ pressure since CO₂ insertion is more favorable due to the high oxidation state (III) of the chromium in the organometallic complex (3 MPa CO₂ Al-porphyrin vs 0.1 MPa CO₂ Cr-porphyrin).¹⁰⁷ Furthermore, porphyrin containing chromium catalysts generally display better kinetics (TOF = 150 h⁻¹) than similarly structured aluminum (TOF = 73 h⁻¹) or cobalt analogues (TOF = 140 h⁻¹) which is probably due to higher polarity, and thus reactivity, of the M-O bond.¹⁰⁵

Fe catalysts

Since iron is one of the most Earth-abundant metals, there are considerable financial and environmental motivations to develop catalytic systems with comparable activity to the robust transition metal-based catalysts. Nozaki has reported the copolymerization of various epoxides such as PO, CHO, and glycidyl phenyl ether (GPE) with CO₂ in presence of Fe-corrole catalysts (**Fe-I**, Chart 1.7).¹³⁶ However, the CO₂ incorporation in the resultant polymers is minimal (9%) at 60 °C, under 2 MPa CO₂ for 1 h resulting in a polymer backbone that resembles a polyether. Another Fe-based catalyst (**Fe-II**, Chart 1.7) displayed switchable polymerization behaviour (selectivity for cyclic vs. linear

topology).¹³⁷ By increasing the ratio of co-catalyst (tetrabutylammonium halide, Bu₄NX, X = Cl, Br, I), a cyclic polymer was preferred as the nucleophile rapidly replaced the M-OCO₂ adduct, thus inhibiting propagation. In contrast, low catalyst loading of both Fe-complexes and corresponding halide (**Fe-II**: TBACl = 1:1, 0.5 mol%) promoted a linear structure even when supercritical CO₂ (8 MPa) was employed as the reaction medium at 85 °C for 3 h.

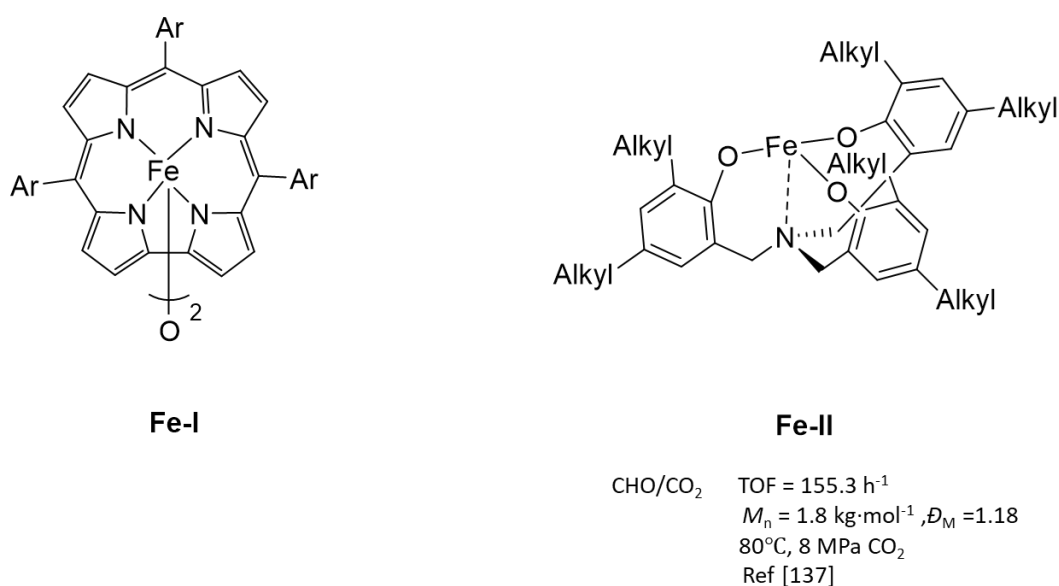


Chart 1.7. Representative complexes of iron with corrole (**Fe-I**) and triphenolate ligands.

Ni catalysts

Ko and co-workers pioneered nickel-catalysed epoxide/CO₂ co-polymerizations.¹³⁸⁻¹⁴² The imine-chelated complex (**Ni-I**, Chart 1.8) proved remarkably active, without a co-catalyst, in the ROcP of CO₂/CHO (TON = 2484, TOF = 38.7 h⁻¹, $M_n = 47.7 \text{ kg} \cdot \text{mol}^{-1}$, $D_M = 1.19$).¹³⁸ By modifying the imine moiety to a tertiary amine, the resultant nickel catalyst (**Ni-II**, Chart 1.8) displayed increased the stability and efficiency (TON > 4000) under similar reaction conditions.¹³⁹ The same catalyst (**Ni-II**) also performed well when the alkene containing monomer 4-vinyl-1,2-cyclohexane oxide (VCHO) was used thus showing the potential to create a functional polycarbonate. Following this study, the acetate bridge in **Ni-I** was substituted with a trifluoroacetate linker (**Ni-III**, Chart 1.8) and higher efficiency was observed (TON = 1728, TOF = 432 h⁻¹).¹⁴⁰ Other modified Ni-based catalysts with Schiff base ligands (**Ni-IV**, Chart

8)¹⁴¹ or carbene ligands (**Ni-V**, Chart 1.8)¹⁴² have displayed some catalytic activity in CHO/CO₂ copolymerizations (**Ni-IV**, TON = 840 and **Ni-V**, TON = 280) but these metrics are relatively low compared to the salen-type Ni complexes (**Ni-I**, **Ni-II** and **Ni-III**).

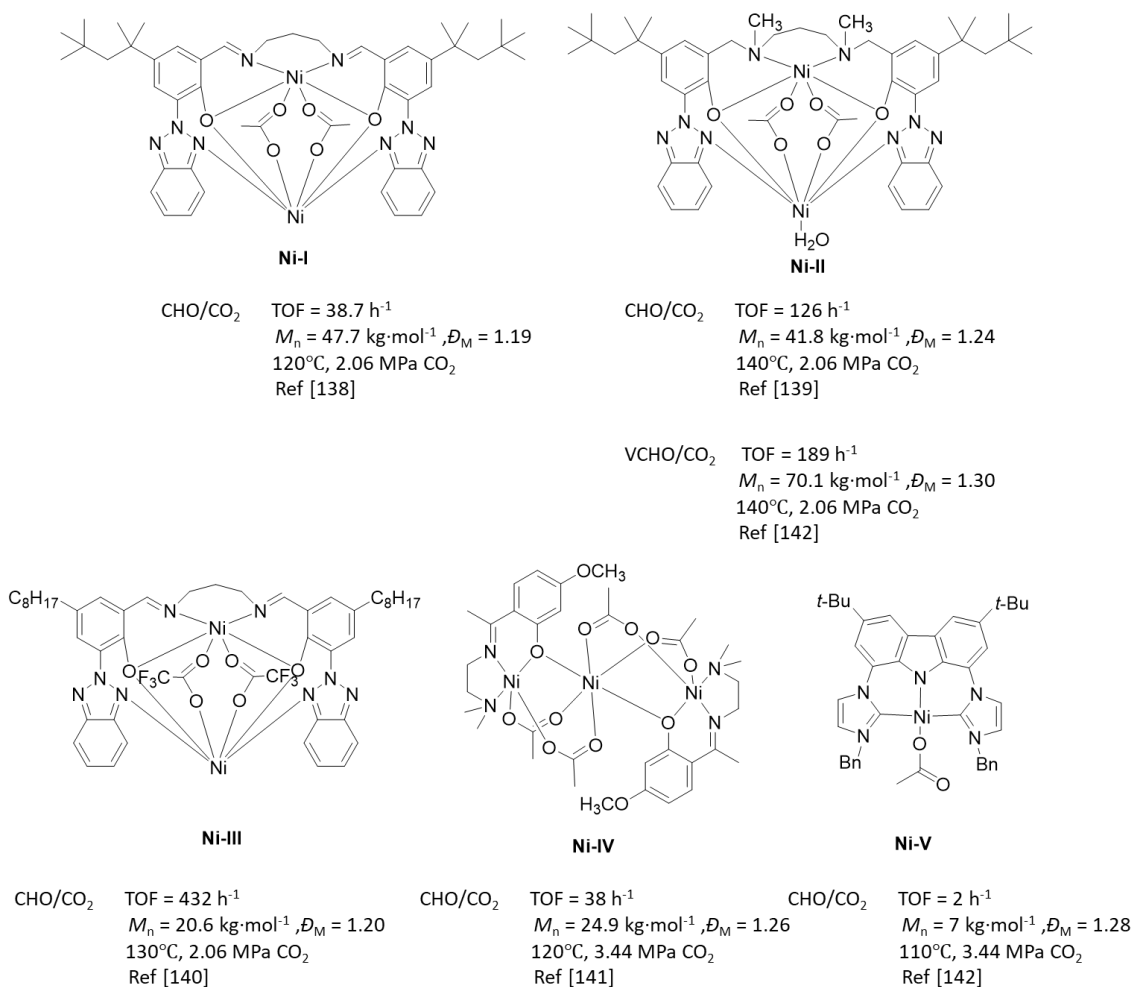


Chart 1.8. Representative Ni-based complexes for CO₂/epoxide copolymerization.

Ti, Zr, Hf Catalysts

Group IV transition metal complexes (Ti, Zr, and Hf) were only recently explored in CO₂-based copolymerization reactions, but they have proven remarkably effective thus far. The first use of tetravalent group IV catalyzed copolymerization of CO₂/PO was demonstrated in 2011.¹⁴³ Although N-heterocyclic carbene (NHC) bears lone electron pair which can serve as a ligand, ease of dissociation from metal center to destabilize metal-ligand complexes hinders the utilization of NHC in

organometallics.¹⁴⁴ Such dissociation can be overcome by the introduction of anionic tethers moieties to NHC.¹⁴⁵ Ti catalysts bearing bisanionic NHC pincer ligands (**Ti-I**, Chart 1.9) or (**Ti-II**, Chart 1.9) were investigated in CO₂-based copolymerizations and in the absence of co-catalysts (organic halide), only the polyether was observed.^{146, 147}

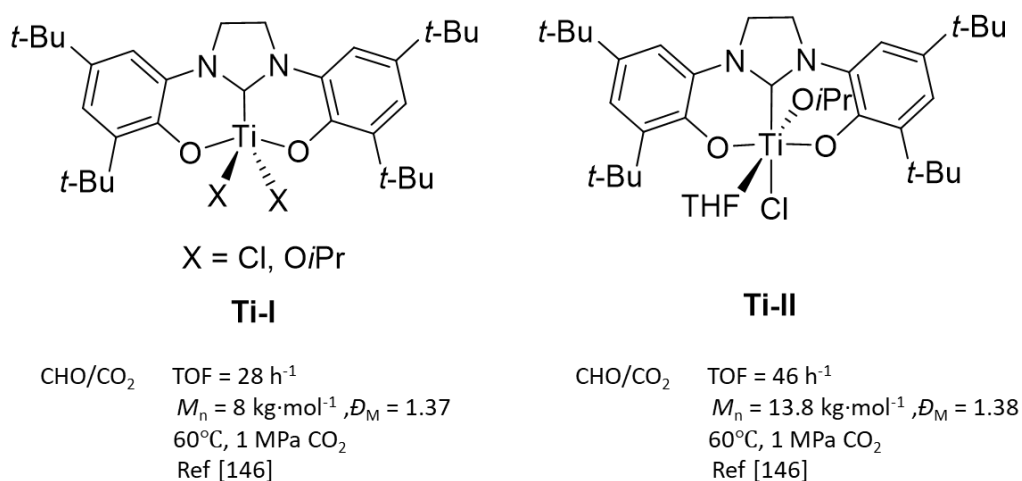
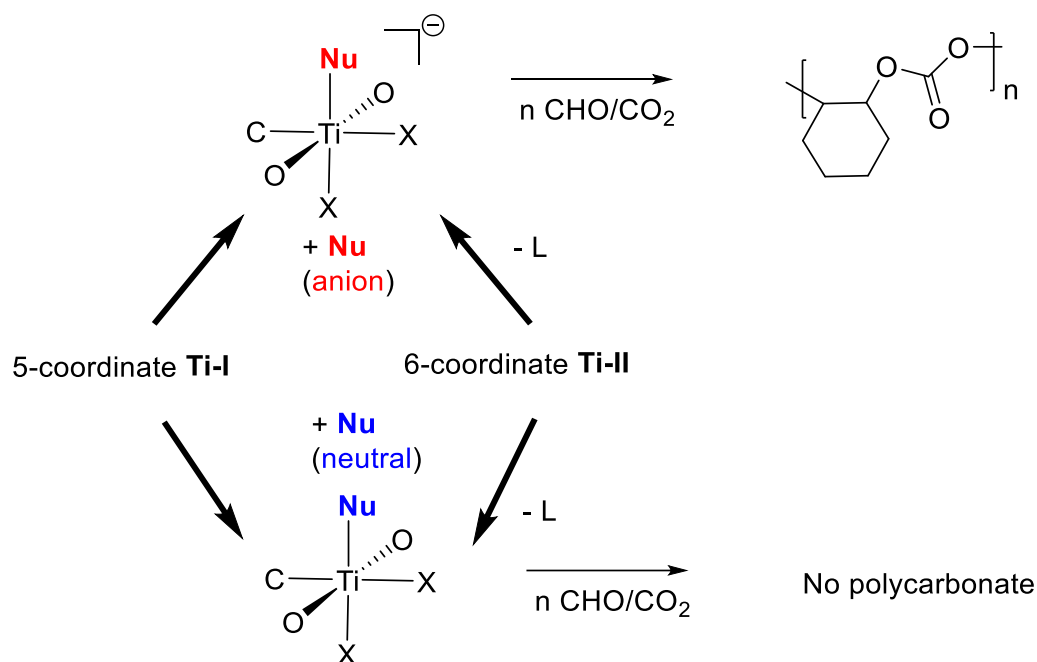


Chart 1.9. Representative Ti-NHC complexes for CO₂/CHO copolymerisation.

Le Roux postulated that six-coordinate Ti complex served as a crucial intermediate species in the mechanism of polycarbonate formation after anion exchange (Cl or OiPr from the co-catalyst), since the addition of neutral co-catalysts like 4-Dimethylaminopyridine (DMAP) did not afford a polycarbonate (Scheme 1.13).¹⁴⁶



Scheme 1.13. The proposed mechanism of Ti-catalyzed CO₂/CHO copolymerization

The catalytic system was further improved by substituting the halide co-catalyst with bulkier anions including benzyl oxide (OBn), acetate (OAc), azide (N₃) and tri-tert-butyl silicate oxide (OSi(OtBu)₃) (Figure 1.1).¹⁴⁸ In the presence of large organic salts - bis(triphenylphosphine)iminium (PPN) chloride or azide (PPNCl or PPNN₃), the copolymerization CHO and CO₂ was carried out under low CO₂ pressure (0.05 MPa) resulting in polycarbonate ($M_n = 7.7 \text{ kg} \cdot \text{mol}^{-1}$, $D_M = 1.54$) within 15 minutes, albeit the overall conversion remained low (< 35%) even after prolonged reaction times.

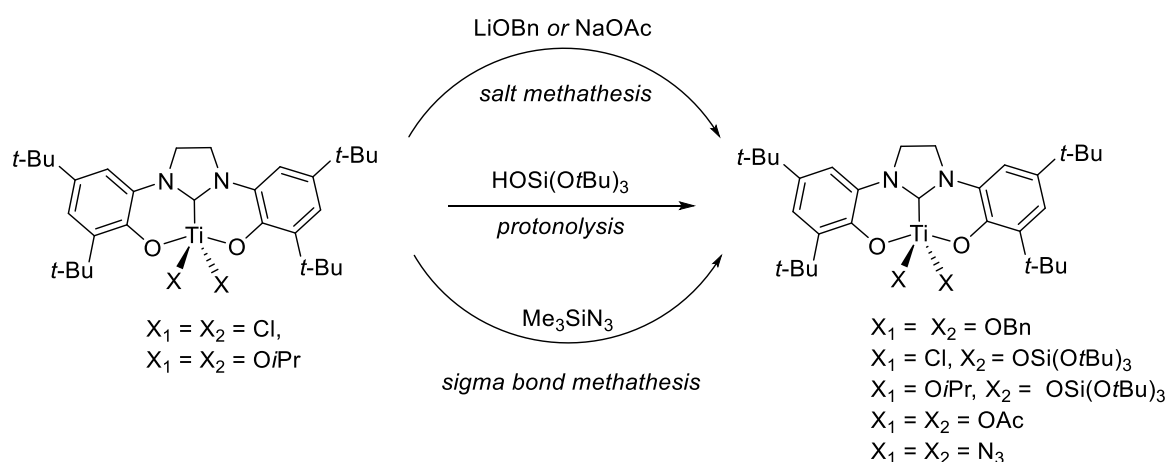


Figure 1.1. Synthetic route of Ti-based catalysts with various anions.

The scope of salen-based catalysts was expanded by introducing Ti as the active metal center (**Ti-III**, Chart 1.10).¹⁴⁹ However, when applied in a CO₂/CHO copolymerization, only modest molecular weight polycarbonate was observed (M_n up to 6.3 kg·mol⁻¹) at 4 MPa CO₂ and 60 °C after 20 h. Moreover, the coordinatively saturated Ti-salen complex (**Ti-IV**, Chart 1.10) only afforded cyclic carbonate, even in the presence of PPNCl. It confirmed the conclusion of Erwan and coworkers who had also implicated this nucleophile exchange from co-catalysts as a crucial pathway toward chain propagation.¹⁴⁶ They also found that Ti with dianionic ligand served as salen complexes (**Ti-V**, Chart 1.10) bring more considerable catalytic activity (TOF = 577 h⁻¹ for 1 h) than the complexes of Ti with trianionic ligand (**Ti-III**) (TOF = 41 h⁻¹ for 8 h).¹⁵⁰

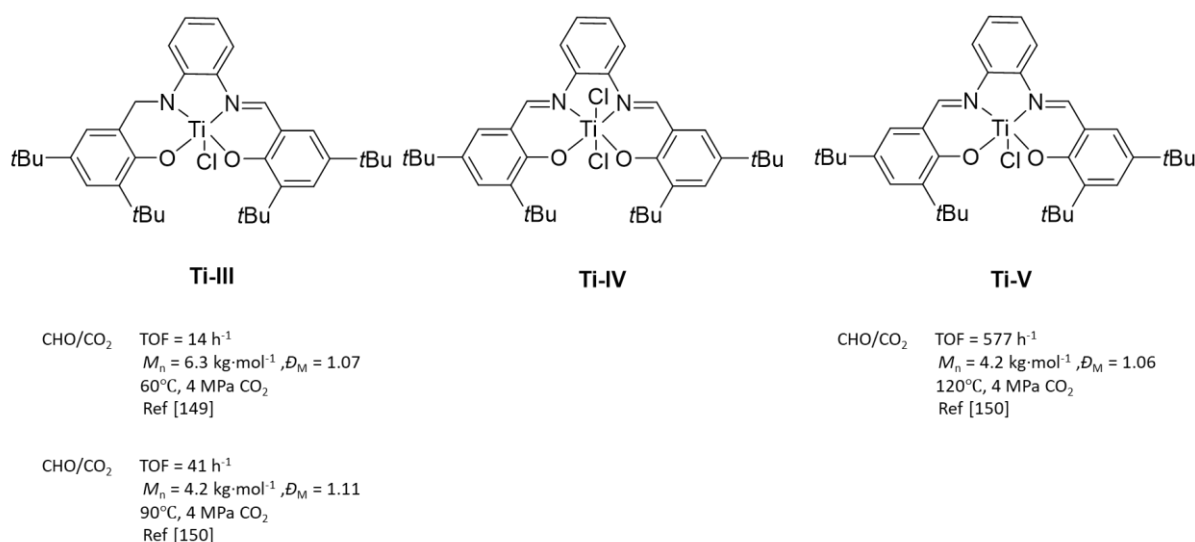


Chart 1.10. Representative Ti-salen complexes for CO₂/CHO copolymerisation.

A heterodinuclear Ti/Zn catalyst was recently reported, however, only low molecular weight polycarbonates were produced ($M_n = 2 \text{ kg}\cdot\text{mol}^{-1}$, $\bar{D}_M = 1.35$).¹⁵¹ It is possible that the poor activity is due to minimal active polymer chain exchange between the Ti and Zn center similarly to the dinuclear mechanism proposed for the dinuclear zinc catalysts.¹⁵¹ Nevertheless, other complexes that feature half salen ligands paired with Ti, Ti-Ti, or Zr-Zr metal centers (**Ti-VI**, **Ti-VII** or **Zr-I**, Chart 1.11) have exhibited better activity and control (for polyCHC, $M_n = 15.2 \text{ kg}\cdot\text{mol}^{-1}$ and 84% carbonate content) for a wide substrate scope (including LA, ϵ -CL, CHO, PO and SO).¹⁵²

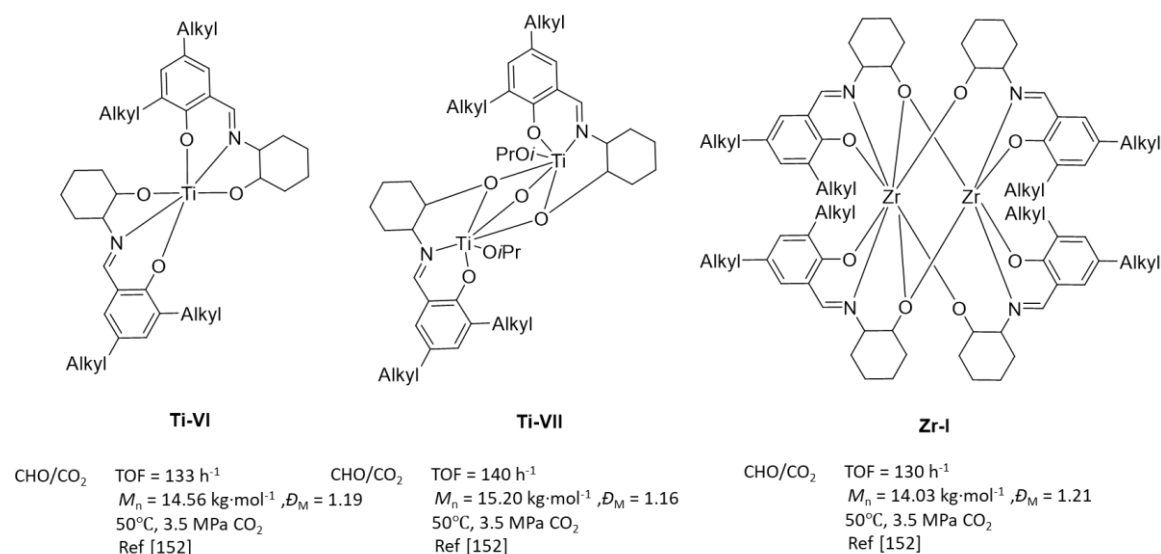


Chart 1.11. Representative dinuclear complexes of Ti, Zr for CO₂/epoxide copolymerisation.

Le Roux and coworkers have reported Zr-NHC complexes (**Zr-II**, Chart 1.12) for the synthesis of poly(CHC).¹⁵³ Unlike the sluggish performance of the Ti-NHC/DMAP catalytic system, the Zr-NHC/DMAP species was more active potentially due to the larger coordination sphere of zirconium where both anion and neutral co-ligand were accommodated to form a stable six-coordinate species. A Zr-salen catalyst (**Zr-III**, Chart 1.12) was also active for various polymerization pathways, including the ROP of LA, ϵ -CL and epoxides or the ROCp of CO₂/epoxides where moderate molecular weight polycarbonates ($M_n = 16.02 \text{ kg}\cdot\text{mol}^{-1}$, $\text{Đ}_M = 1.09$) were produced under relatively mild reaction conditions (50 °C, 3.5 MPa CO₂).¹⁵⁴

The benzotriazole phenolate (bis-BZH) chelating species was used to form various group IV (Ti, Zr, Hf) complexes possessing ethereal bridges. The catalysts were assessed for activity in both ROP of LA and ROCp of CO₂/CHO and Zr-bis-BZH complexes displayed decent performance (TOF = 6.8 h⁻¹) for CO₂-based polycarbonate synthesis as compared to Hf analogues (TOF = 3 h⁻¹).¹⁵⁵ Tetra-benzotriazole phenolate(BZH) group IV complexes were also investigated in CO₂/CHO copolymerizations with the Zr-based catalyst (**Zr-IV**) again outperforming the group IV analogues to afford a controlled ($\text{Đ}_M = 1.28$) polycarbonate with moderate molecular weight (**Zr-IV** $M_n = 8.6 \text{ kg}\cdot\text{mol}^{-1}$, 93 % carbonate content vs Hf-BZH $M_n = 4 \text{ kg}\cdot\text{mol}^{-1}$ 76 % carbonate content vs Ti-BZH, $M_n = 0 \text{ kg}\cdot\text{mol}^{-1}$). The order of reactivity for

the complexes follows Zr ~ Hf > Ti possibly explained by the larger atomic radii of Zr and Hf opening up the coordination sphere relative to the smaller Ti metal center.¹⁵⁶

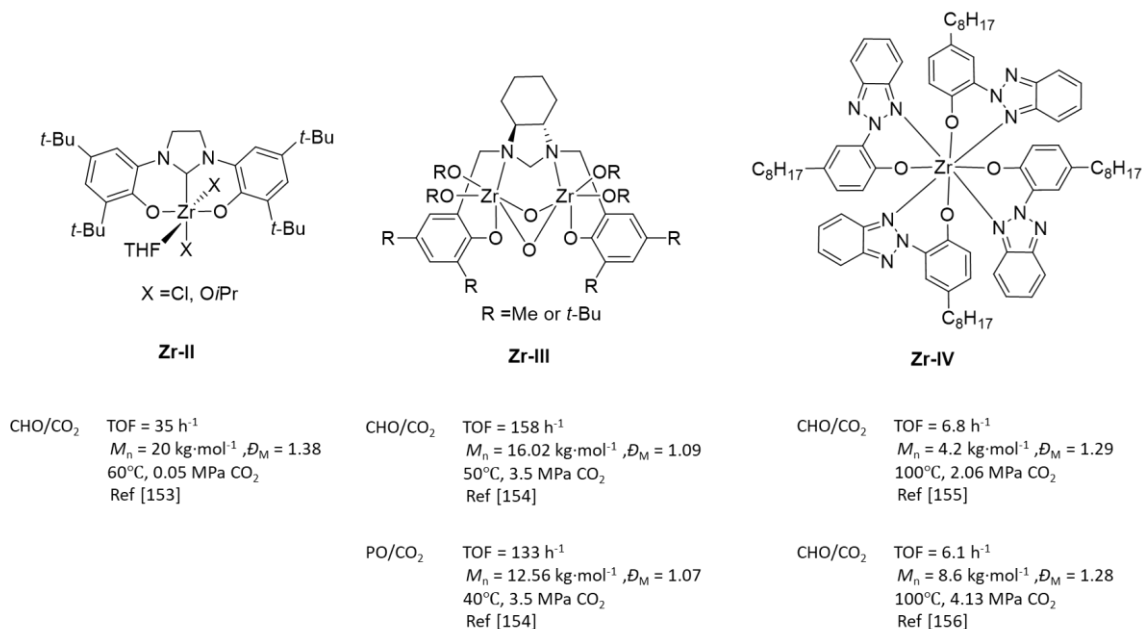
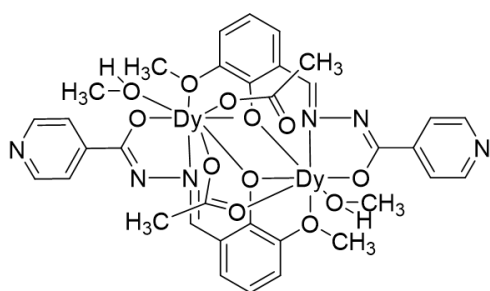


Chart 1.12. Representative Zr-based complexes for CO₂/epoxide copolymerization.

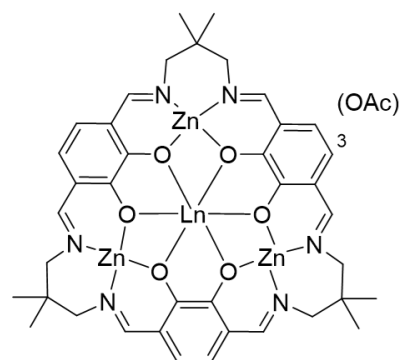
Lanthanide Catalysts

Compared to the large amount of investigations involving transition metal complexes, lanthanide catalysts have been largely ignored. Nevertheless, many lanthanide complexes can possess superior air-stability relative to transition metal species and this should provide a great advantage in CO₂ copolymerization processes. Dy Schiff-base complexes (**Dy-I**, Chart 1.13) were robust catalysts (TON = 1620) for CO₂/CHO copolymerization yielding moderate molecular weight polycarbonate ($M_n = 22 \text{ kg}\cdot\text{mol}^{-1}$) under optimized conditions (3.44 MPa CO₂, 100 °C), albeit the dispersity ($\mathcal{D}_M = 2.02\sim 5.69$) was quite high indicating some chain termination or transfer processes.¹⁵⁷



Dy-I

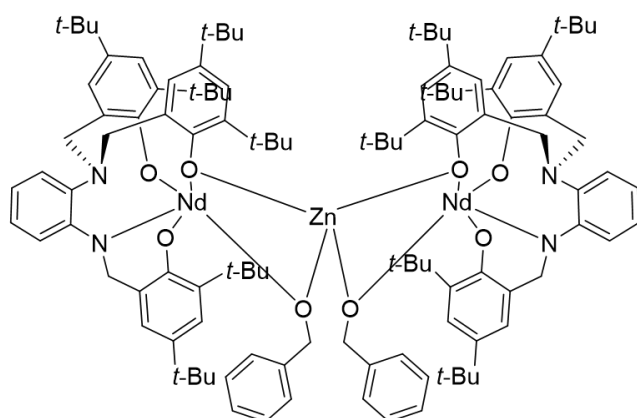
CHO/CO₂ TOF = 17 h⁻¹
 $M_n = 22 \text{ kg} \cdot \text{mol}^{-1}$, $\mathcal{D}_M = 5.12$
 100°C, 3.44 MPa CO₂
 Ref [157]



Ln = La, Ce, Pr, Nd, Sm, Eu, Gd,
 Dy

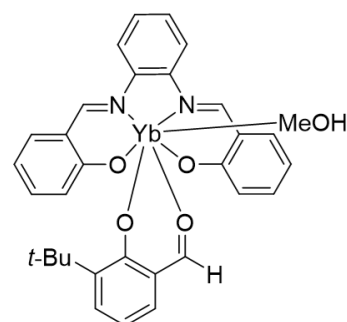
La-I

CHO/CO₂ TOF = 370 h⁻¹
 $M_n = 14 \text{ kg} \cdot \text{mol}^{-1}$, $\mathcal{D}_M = 1.30$
 100°C, 0.6 MPa CO₂
 Ref [158]



Nd-I

CHO/CO₂ TOF = 82 h⁻¹
 $M_n = 295.8 \text{ kg} \cdot \text{mol}^{-1}$, $\mathcal{D}_M = 1.65$
 25°C, 0.7 MPa CO₂
 Ref [159]



Yb-I

CHO/CO₂ TOF = 12 h⁻¹
 $M_n = 11.4 \text{ kg} \cdot \text{mol}^{-1}$, $\mathcal{D}_M = 1.35$
 70°C, 2 MPa CO₂
 Ref [160]

Chart 1.13. Representative lanthanide-based catalysts for CO₂/epoxide copolymerization.

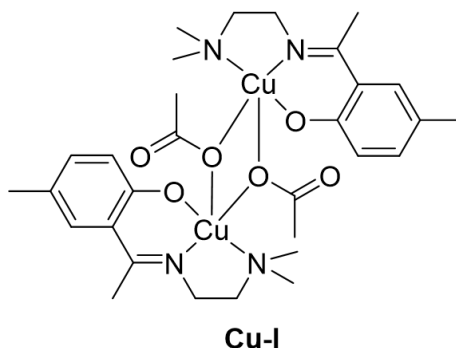
Inspired by the salen dinuclear complexes from Williams' group, mixed heterometallic structures featuring a lanthanide (Ln) and main group metal (Zn) paired with a macrocyclic tri(salen) ligand (**La-I**, Chart 1.13) were discovered to possess the unique property of rapid inter-/intra-molecular acetate ligand exchange.¹⁵⁸ By screening lanthanide metals the Ce/Zn complex exhibited superior catalytic

performance (TOF = 370 h⁻¹). Telomerization of CO₂/CHO copolymerization was successful by adjusting the amount of acetate counterion resulting in a polymer with “controllable” molecular weight.

The heterometallic (Nd/Zn) complex (**Nd-I**, Chart 1.13) afforded extremely high molecular weight ($M_n = 295 \text{ kg}\cdot\text{mol}^{-1}$, $\bar{D}_M = 1.65$) polycarbonates in 12 h under mild conditions (25 °C, 0.7 MPa CO₂).¹⁵⁹ The molecular weight of the resultant polymer was found to be extremely sensitive to reaction temperature with $M_n \sim 50 \text{ kg}\cdot\text{mol}^{-1}$ at 70 °C and even lower at higher temperatures. It was surmised that at elevated temperatures, the catalyst could also degrade the polymer backbone since there is an equilibrium between propagation and depolymerization favours the latter as the temperature increases. Ytterbium-salen complexes (**Yb-I**, Chart 1.13) paired with halide co-catalysts were active for CO₂/CHO copolymerizations yielding with optimized conditions yielding a polycarbonate with $M_n = 11.4 \text{ kg}\cdot\text{mol}^{-1}$ at 2 MPa CO₂ and 70 °C.¹⁶⁰ Other lanthanides (Sc, Y) were also substituted for Yb in the same organometallic framework, but they displayed inferior activity.

Cu Catalysts

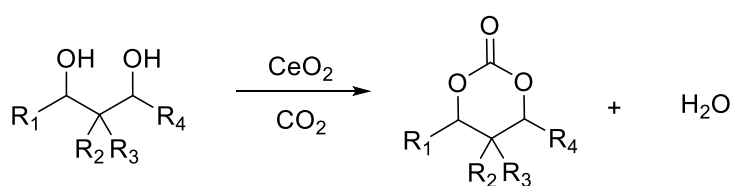
Although Cu organometallic complexes have been widely studied as both small molecule and polymerization catalysts, they are relatively unexplored as CO₂/epoxide co-polymerization catalysts with only one such study reported by Ko and co-workers that demonstrated unremarkable results (TOF = 11.5 - 18.8 h⁻¹).¹⁶¹



CHO/CO₂ TOF = 18.8 h⁻¹
 $M_n = 3.4 \text{ kg}\cdot\text{mol}^{-1}$, $\bar{D}_M = 1.31$
120°C, 2.06 MPa CO₂
Ref [161]

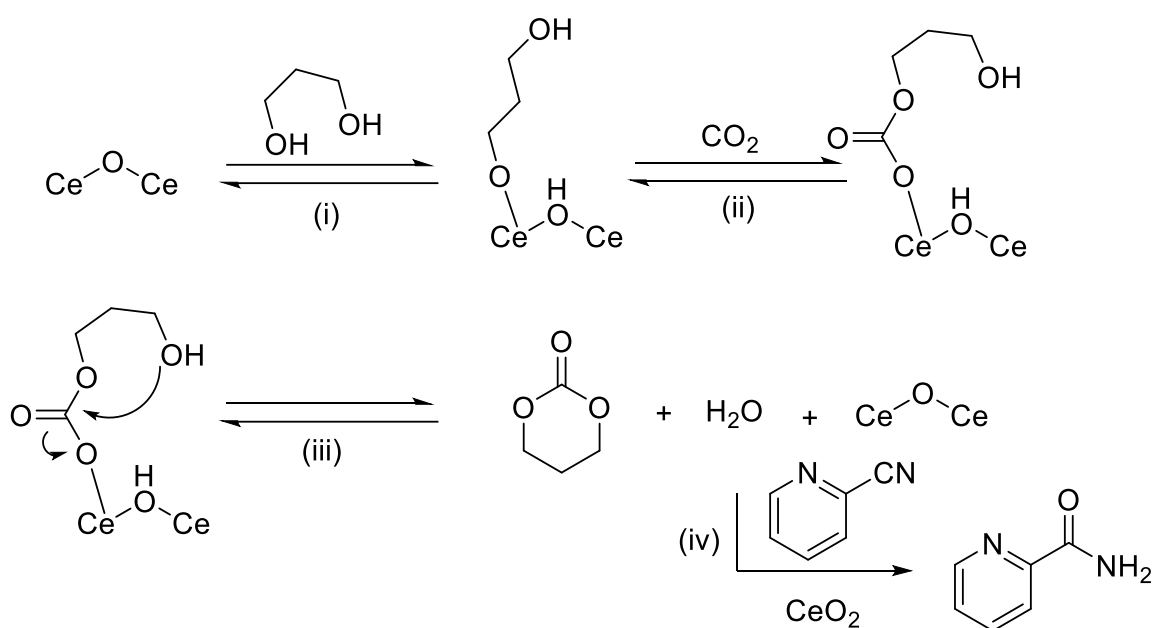
1.2.4 Novel Cyclic Carbonate Monomers derived from CO₂

Although direct incorporation of CO₂ into macromolecular architectures by copolymerization strategies is a straightforward strategy to sustainable polymers, an alternative method to incorporate CO₂ into polymers is to use it as a reagent in the synthesis of cyclic carbonate monomers from naturally-derived alcohols. Initially, five-membered cyclic carbonates (5CC) were investigated as precursors to polycarbonates, however, the ring opening is unfavorable without the elimination of CO₂. As such, attention has turned to six-membered cyclic carbonates (6CCs) that can undergo controlled ROP using either metal- or organo- catalysts.^{162, 163} The strategy does not simply increase the valorization of CO₂, but broadens the functional group scope of the resultant polycarbonates potentially leading to new materials with interesting thermal and/or mechanical properties.



Scheme 1.14. Synthesis of six-membered cyclic carbonates from the corresponding diol substrates.

One of the most common routes to 6CCs is the Cerium(IV) oxide (CeO₂)/2-cyanopyridine catalyzed coupling of CO₂ and various diols (Scheme 1.14).^{9, 11} The mechanism was proposed as the deprotonation of one OH group by Lewis acid sites of CeO₂ forming cerium alkoxide in first, following with the carbonation of alkoxide from CO₂ insertion and the nucleophilic attack of the other OH resulting in cyclic carbonate and H₂O, side product, that was diminished by 2-cyanopyridine hydration over CeO₂ (Scheme 1.15). Many substrates with CO₂ are converted to 6CC in presence of CeO₂ (Chart 1.14) which can be transformed into polycarbonate potentially.



Scheme 1.15. Proposed mechanism of 6CC synthesis from diol and CO₂.⁹

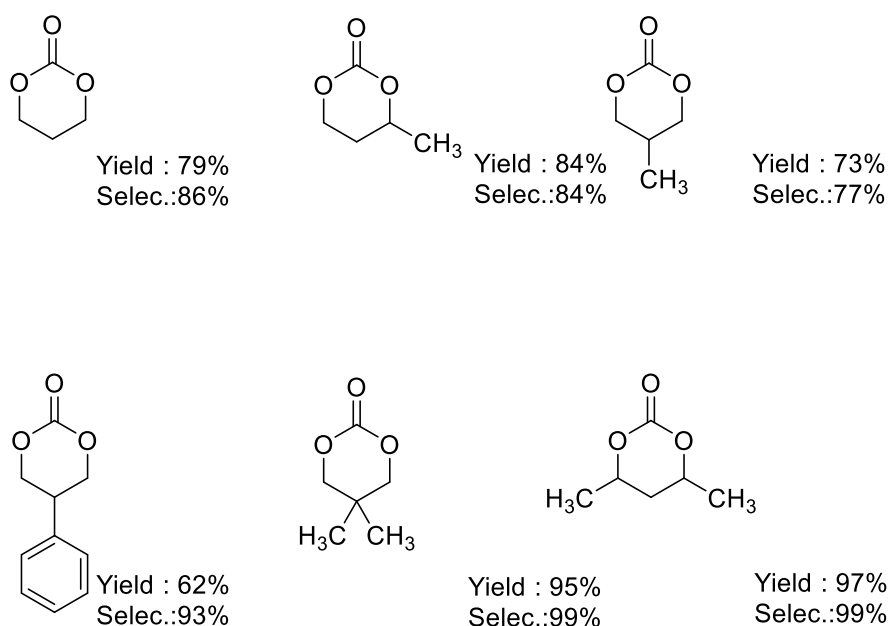


Chart 1.14. The library of six-membered cyclic carbonate from CO₂ and diol substrates.⁹

After the pioneering trimethylene carbonate (TMC) synthesis using oxetane and CO₂ from Baba^{37, 164} and Darensbourg¹⁶⁵, Kleij's group developed an aluminum (**Al-VI**, Chart 1.15) catalysed coupling reaction between a heterocyclic oxide and CO₂.³³ The reaction method is particularly effective for the synthesis of functional 5CCs and TMC. However, the coupling reaction to produce a 6CC using CO₂ and

3,3-dimethyloxetane is not very selective (54%) and low yielding to 6CC formation (yield: 26%) presumably due to steric inhibition from the adjacent methyl groups.

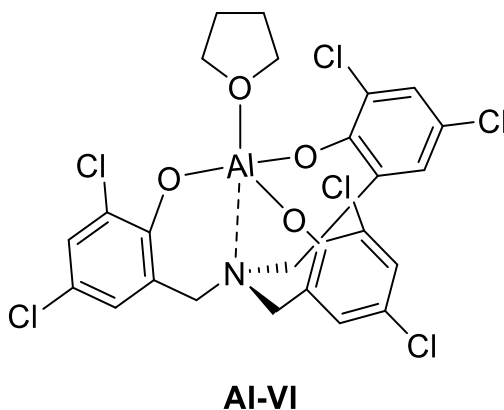


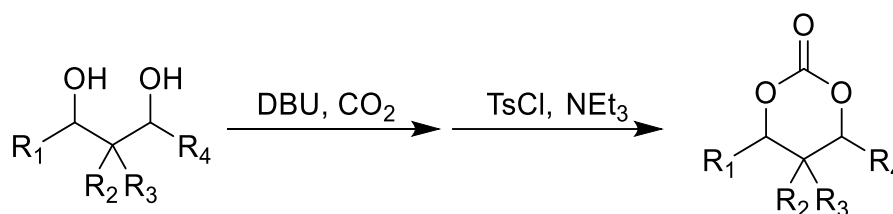
Chart 1.15. Representative aluminum catalyst for 6CC synthesis.

1.3 Organocatalysts

In efforts to address environmental concerns, health impacts, high costs and the inherent oxygen and moisture lability of metal-based catalysts, metal-free methods for CO₂-based polycarbonate synthesis have been developed contemporaneously. Although organocatalysts present essential green chemistry benefits, they have traditionally lagged behind their metal counterparts in terms of stability and activity. Nevertheless, the development of robust organocatalysts for polycarbonate synthesis remains a priority.

Organocatalysts have been successfully employed to activate CO₂ for the synthesis of cyclic carbonate monomers such as 5CCs, but these monomers are not particularly suitable for ring-opening protocols. Furthermore, efforts aimed at incorporating CO₂ into copolymeric structures while suppressing the formation of 5CC products have traditionally yielded predominantly cyclic by-products instead (Scheme 1.3). As previously mentioned, the synthesis of 6CCs (from CO₂ and oxetane substrates mentioned in section 1.2.4), is an alternative approach to using CO₂ in polycarbonate synthesis. However, the dramatic difference of acidity between epoxide and oxetane has precluded

organocatalyzed approaches.^{29, 30} Nevertheless, Buchard and coworkers reported the first instance of 6CCs synthesised from corresponding diols and CO₂ at very low pressure (0.1 MPa CO₂) (Scheme 1.16).¹⁶⁶



Scheme 1.16. Organocatalytic synthesis of six-membered cyclic carbonates from CO₂ and diol substrates.

The mechanism was hypothesised to begin with a mono CO₂ insertion at an alcohol to form the carbonate after the deprotonation by 1,8-Diazabicyclo(5.4.0)undec-7-ene (DBU). Following this, intramolecular attack from the second alcohol completes the cyclization process to form the corresponding 6CC. Interestingly, the cyclization step was ineffective without the addition of tosyl chloride to form a good leaving group and density functional theory (DFT) studies corroborated this high energy barrier in the cyclization step. After the successful synthesis of 6CCs, numerous other green CO₂-based copolymer from renewable feedstocks were explored. Mannopyranose derivative¹⁶⁷, thymidine¹⁶⁸ and 2-deoxy-D-ribose¹⁶⁹ derivatives were coupled directly to CO₂ affording cyclic monomers that were polymerized to form novel polycarbonates that are promising biomaterial applications.

Recently, the first metal-free CO₂-based polycarbonate synthesis was achieved by activating an epoxide with a strong Lewis acid (triethyl borane). The presence of the Lewis acid is crucial to lower the activation barrier for of the epoxide ring-opening to compete with the back-biting of carbonate species. Both PO and CHO were copolymerized with CO₂, to obtain polycarbonates ($M_n = 43 \text{ kg}\cdot\text{mol}^{-1}$, $D_M = 1.10$) with high carbonate content (99%).¹⁷⁰ An organocatalyzed approach featuring a binary system composed of 1,3-bis(2-hydroxyhexafluoroisopropyl)benzene and tetrabutylammonium iodide was also effective for the CO₂ copolymerization with trimethylene oxide (TMO), a traditionally

challenging monomer³². An oligocarbonate ($M_n = 2 \text{ kg}\cdot\text{mol}^{-1}$) was obtained after 24h under 10 MPa CO_2 and 130 °C, demonstrating one of the only instances of organocatalyzed CO_2 /TMO copolymerization.

1.4. Conclusion and Outlooks

The copolymerization of CO_2 /EP offers an efficient approach to sustainable polycarbonates and has accordingly drawn a great deal of attention in recent decades. Currently, the process is becoming more economical do to the development of better catalysts that serve to afford a diverse array of polycarbonates under increasingly mild conditions. Nevertheless, modern non-degradable plastics still remain comparatively inexpensive, but environmental concerns are exponentially increasing. Thus, it is imperative to continue the development of sustainable polymers and lower the cost of such materials. As it stands, the issue remains a great challenge to the chemistry community. Further improvements will certainly be gained from more efficient organometallic catalysts, but the maturation of organocatalysts could provide a breakthrough and further drive the production price down while offering a more sustainable approach.

The renewable plastics from bio-based monomer and CO_2 could be another interesting research field to compete with petroleum products, for instance, the breakthrough from poly (limonene carbonate) (PLO) ¹⁷¹⁻¹⁷³ and 2,5-furandicarboxylic acid (FDCA),^{174, 175} a monomer from biomass waste/ CO_2 , lead to various methodologies of CO_2 utilisation. Although both metal- and organic- based catalysts present several respective advantages that viable options for CO_2 -based polymer synthesis, overcoming the sensitive against contamination (e.g. oxygen, moisture) and using air as CO_2 resource would allow CO_2 -based fabrication step forward industrial scale globally.

References

1. A. L. Andrady and M. A. Neal, *Philos Trans R Soc Lond B Biol Sci*, 2009, **364**, 1977-1984.
2. T. J. Crowley and R. A. Berner, *Science*, 2001, **292**, 870-872.
3. T. Janes, Y. Yang and D. Song, *Chem. Commun.*, 2017, **53**, 11390-11398.
4. Q. Liu, L. Wu, R. Jackstell and M. Beller, *Nat. Commun*, 2015, **6**, 5933.
5. J. Wei, Q. Ge, R. Yao, Z. Wen, C. Fang, L. Guo, H. Xu and J. Sun, *Nat. Commun*, 2017, **8**, 15174.
6. S. Ghosh and A. Barron, *C*, 2016, **2**, 5.
7. X. Yong, J. S. Tse and C. S. Yoo, *J. Phys. Chem. C*, 2017, **121**, 115-122.
8. V. Iota, C. S. Yoo and H. Cynn, *Science*, 1999, **283**, 1510.
9. M. Honda, M. Tamura, K. Nakao, K. Suzuki, Y. Nakagawa and K. Tomishige, *ACS Catal.*, 2014, **4**, 1893-1896.
10. M. Tamura, H. Wakasugi, K.-i. Shimizu and A. Satsuma, *Chem. Eur. J*, 2011, **17**, 11428-11431.
11. T. M. McGuire, E. M. López-Vidal, G. L. Gregory and A. Buchard, *J. CO₂ Util.*, 2018, **27**, 283-288.
12. M. Tamura, K. Ito, M. Honda, Y. Nakagawa, H. Sugimoto and K. Tomishige, *Sci. Rep*, 2016, **6**, 24038.
13. Z. Chen, N. Hadjichristidis, X. Feng and Y. Gnanou, *Macromolecules*, 2017, **50**, 2320-2328.
14. Z. Chen, N. Hadjichristidis, X. Feng and Y. Gnanou, *Polym. Chem.*, 2016, **7**, 4944-4952.
15. E. J. Beckman, *Science*, 1999, **283**, 946.
16. W. Ando, N. Choi and N. Tokitoh, in *Comprehensive Heterocyclic Chemistry II*, eds. A. R. Katritzky, C. W. Rees and E. F. V. Scriven, Pergamon, Oxford, 1996, DOI: <https://doi.org/10.1016/B978-008096518-5.00005-8>, 173-240.
17. I. Palard, M. Schappacher, B. Belloncle, A. Soum and S. M. Guillaume, *Chem. Eur. J*, 2007, **13**, 1511-1521.

18. I. Erden, in *Comprehensive Heterocyclic Chemistry II*, eds. A. R. Katritzky, C. W. Rees and E. F. V. Scriven, Pergamon, Oxford, 1996, DOI: <https://doi.org/10.1016/B978-008096518-5.00003-4>, 97-144.
19. R. J. Linderman, in *Comprehensive Heterocyclic Chemistry II*, eds. A. R. Katritzky, C. W. Rees and E. F. V. Scriven, Pergamon, Oxford, 1996, DOI: <https://doi.org/10.1016/B978-008096518-5.00022-8>, 721-753.
20. W. H. Pearson, B. W. Lian and S. C. Bergmeier, in *Comprehensive Heterocyclic Chemistry II*, eds. A. R. Katritzky, C. W. Rees and E. F. V. Scriven, Pergamon, Oxford, 1996, DOI: <https://doi.org/10.1016/B978-008096518-5.00001-0>, 1-60.
21. G. D. Jones, A. Langsjoen, S. M. M. C. Neumann and J. Zomlefer, *J. Org. Chem.*, 1944, **09**, 125-147.
22. O. Ihata, Y. Kayaki and T. Ikariya, *Macromolecules*, 2005, **38**, 6429-6434.
23. K. Soga, S. Hosoda and S. Ikeda, *Makromol. Chem.*, 1974, **175**, 3309-3313.
24. W. Kuran, A. Rokicki and D. Romanowska, *J. Polym. Sci. Polym. Chem. Ed.*, 1979, **17**, 2003-2011.
25. Y. Tanaka, *J. Macromol. Sci. A*, 1967, **1**, 1059-1068.
26. G. Trott, P. K. Saini and C. K. Williams, *Philos. Trans. Royal Soc. A*, 2016, **374**, 20150085.
27. H. K. Eigenmann, D. M. Golden and S. W. Benson, *J. Phys. Chem.*, 1973, **77**, 1687-1691.
28. B. S. Ringnér, Stig; Watanabe, Haruhiko, *Acta Chem. Scand.*, 1971, **25**, 141-146.
29. S. Aoshima, T. Fujisawa and E. Kobayashi, *J. Polym. Sci. A Polym. Chem.*, 1994, **32**, 1719-1728.
30. J. A. Burkhard, G. Wuitschik, M. Rogers-Evans, K. Müller and E. M. Carreira, *Angew. Chem. Int. Ed.*, 2010, **49**, 9052-9067.
31. J. A. Bull, R. A. Croft, O. A. Davis, R. Doran and K. F. Morgan, *Chem. Rev.*, 2016, **116**, 12150-12233.
32. M. Alves, B. Grignard, A. Boyaval, R. Méreau, J. De Winter, P. Gerbaux, C. Detrembleur, T. Tassaing and C. Jérôme, *ChemSusChem*, 2017, **10**, 1128-1138.

33. C. J. Whiteoak, N. Kielland, V. Laserna, E. C. Escudero-Adán, E. Martin and A. W. Kleij, *J. Am. Chem. Soc.*, 2013, **135**, 1228-1231.
34. W. M. H. Sachtler, C. Backx and R. A. Van Santen, *Catal. Rev.*, 1981, **23**, 127-149.
35. J. Marco-Contelles, M. T. Molina and S. Anjum, *Chem. Rev.*, 2004, **104**, 2857-2900.
36. S. Inoue, H. Koinuma and T. Tsuruta, *J. Polym. Sci. B Polym. Lett.*, 1969, **7**, 287-292.
37. A. Baba, H. Meishou and H. Matsuda, *Makromol. Chem., Rapid Commun.*, 1984, **5**, 665-668.
38. C. Masters, *Homogeneous Transition Metal Catalysis: A Gentle Art*, Routledge, Chapman & Hall, Incorporated, 1981.
39. S. Inoue, H. Koinuma and T. Tsuruta, *J. Polym. Sci. B Polym. Lett.*, 1969, **7**, 287-292.
40. W.-M. Ren, T.-J. Yue, X. Zhang, G.-G. Gu, Y. Liu and X.-B. Lu, *Macromolecules*, 2017, **50**, 7062-7069.
41. M. H. Chisholm, D. Navarro-Llobet and Z. Zhou, *Macromolecules*, 2002, **35**, 6494-6504.
42. D. J. Darensbourg and S.-H. Wei, *Macromolecules*, 2012, **45**, 5916-5922.
43. D. J. Darensbourg, S.-H. Wei, A. D. Yeung and W. C. Ellis, *Macromolecules*, 2013, **46**, 5850-5855.
44. D. J. Darensbourg, A. D. Yeung and S.-H. Wei, *Green Chem.*, 2013, **15**, 1578-1583.
45. D. J. Darensbourg and S. J. Wilson, *Green Chem.*, 2012, **14**, 2665-2671.
46. K. Tezuka, K. Komatsu and O. Haba, *Polym J*, 2013, **45**, 1183.
47. W. Guerin, A. K. Diallo, E. Kirilov, M. Helou, M. Slawinski, J.-M. Brusson, J.-F. Carpentier and S. M. Guillaume, *Macromolecules*, 2014, **47**, 4230-4235.
48. S. E. Felder, M. J. Redding, A. Noel, S. M. Grayson and K. L. Wooley, *Macromolecules*, 2018, **51**, 1787-1797.
49. L. Vogdanis, B. Martens, H. Uchtmann, F. Hensel and W. Heitz, *Makromol. Chem.*, 1990, **191**, 465-472.
50. J.-C. Lee and M. H. Litt, *Macromolecules*, 2000, **33**, 1618-1627.
51. D. J. Darensbourg and J. C. Yarbrough, *J. Am. Chem. Soc.*, 2002, **124**, 6335-6342.

52. M. W. Lehenmeier, S. Kissling, P. T. Altenbuchner, C. Bruckmeier, P. Deglmann, A.-K. Brym and B. Rieger, *Angew. Chem. Int. Ed.*, 2013, **52**, 9821-9826.
53. F. Jutz, A. Buchard, M. R. Kember, S. B. Fredriksen and C. K. Williams, *J. Am. Chem. Soc.*, 2011, **133**, 17395-17405.
54. M. R. Kember and C. K. Williams, *J. Am. Chem. Soc.*, 2012, **134**, 15676-15679.
55. Y. Xiao, Z. Wang and K. Ding, *Macromolecules*, 2006, **39**, 128-137.
56. X.-B. Lu and D. J. Darensbourg, *Chem. Soc. Rev.*, 2012, **41**, 1462-1484.
57. S. J. Na, S. S. A. Cyriac, B. E. Kim, J. Yoo, Y. K. Kang, S. J. Han, C. Lee and B. Y. Lee, *Inorg. Chem.*, 2009, **48**, 10455-10465.
58. X.-B. Lu, L. Shi, Y.-M. Wang, R. Zhang, Y.-J. Zhang, X.-J. Peng, Z.-C. Zhang and B. Li, *J. Am. Chem. Soc.*, 2006, **128**, 1664-1674.
59. S. Ghosh, D. Pahovnik, U. Kragl and E. Mejía, *Macromolecules*, 2018, **51**, 846-852.
60. H. Koinuma and H. Hirai, *Makromol. Chem.*, 1977, **178**, 1283-1294.
61. T. Aida, M. Ishikawa and S. Inoue, *Macromolecules*, 1986, **19**, 8-13.
62. H. Sugimoto, H. Ohtsuka and S. Inoue, *J. Polym. Sci. A Polym. Chem.*, 2005, **43**, 4172-4186.
63. D. J. Darensbourg and D. R. Billodeaux, *Inorg. Chem.*, 2005, **44**, 1433-1442.
64. W. Kuran, T. Listos, M. Abramczyk and A. Dawidek, *J. Macromol. Sci. Part A*, 1998, **35**, 427-437.
65. W. Wu, X. Sheng, Y. Qin, L. Qiao, Y. Miao, X. Wang and F. Wang, *J. Polym. Sci. Part A: Polym. Chem.*, 2014, **52**, 2346-2355.
66. X. Sheng, W. Wu, Y. Qin, X. Wang and F. Wang, *Polym. Chem.*, 2015, **6**, 4719-4724.
67. C. Chatterjee and M. H. Chisholm, *Inorg. Chem.*, 2011, **50**, 4481-4492.
68. K. Nishioka, H. Goto and H. Sugimoto, *Macromolecules*, 2012, **45**, 8172-8192.
69. D. Zhang, H. Zhang, N. Hadjichristidis, Y. Gnanou and X. Feng, *Macromolecules*, 2016, **49**, 2484-2492.

70. N. Ikpo, S. M. Barbon, M. W. Drover, L. N. Dawe and F. M. Kerton, *Organometallics*, 2012, **31**, 8145-8158.
71. C. W. Bock, A. K. Katz, G. D. Markham and J. P. Glusker, *J. Am. Chem. Soc.*, 1999, **121**, 7360-7372.
72. P. K. Saini, C. Romain and C. K. Williams, *Chem. Commun.*, 2014, **50**, 4164-4167.
73. N. Yi, J. Unruangsri, J. Shaw and C. K. Williams, *Faraday Discuss.*, 2015, **183**, 67-82.
74. M. R. Kember, P. D. Knight, P. T. R. Reung and C. K. Williams, *Angew. Chemie Int. Ed.*, 2009, **48**, 931-933.
75. A. M. Chapman, C. Keyworth, M. R. Kember, A. J. J. Lennox and C. K. Williams, *ACS Catal.*, 2015, **5**, 1581-1588.
76. A. Thevenon, J. A. Garden, A. J. P. White and C. K. Williams, *Inorg. Chem.*, 2015, **54**, 11906-11915.
77. A. Buchard, F. Jutz, M. R. Kember, A. J. P. White, H. S. Rzepa and C. K. Williams, *Macromolecules*, 2012, **45**, 6781-6795.
78. C. Romain, J. A. Garden, G. Trott, A. Buchard, A. J. P. White and C. K. Williams, *Chem. Eur. J.*, 2017, **23**, 7367-7376.
79. J. A. Garden, P. K. Saini and C. K. Williams, *J. Am. Chem. Soc.*, 2015, **137**, 15078-15081.
80. N. M. Rajendran, A. Haleel and N. D. Reddy, *Organometallics*, 2014, **33**, 217-224.
81. M. Kröger, C. Folli, O. Walter and M. Döring, *Adv. Synth. Catal.*, 2006, **348**, 1908-1918.
82. S. Kissling, P. T. Altenbuchner, M. W. Lehenmeier, E. Herdtweck, P. Deglmann, U. B. Seemann and B. Rieger, *Chem. Eur. J.*, 2015, **21**, 8148-8157.
83. M. Reiter, S. Vagin, A. Kronast, C. Jandl and B. Rieger, *Chem. Sci.*, 2017, **8**, 1876-1882.
84. J. Martínez, J. A. Castro-Osma, A. Lara-Sánchez, A. Otero, J. Fernández-Baeza, J. Tejeda, L. F. Sánchez-Barba and A. Rodríguez-Diéguez, *Polym. Chem.*, 2016, **7**, 6475-6484.

85. G.-p. Wu, S.-d. Jiang, X.-b. Lu, W.-m. Ren and S.-k. J. C. J. o. P. S. Yan, *Chinese J. Polym. Sci.*, 2012, **30**, 487-492.
86. G. A. Luinstra and E. Borchardt, in *Synthetic Biodegradable Polymers*, eds. B. Rieger, A. Künkel, G. W. Coates, R. Reichardt, E. Dinjus and T. A. Zevaco, Springer Berlin Heidelberg, Berlin, Heidelberg, 2012, DOI: 10.1007/12_2011_126, 29-48.
87. M. R. Kember, J. Copley, A. Buchard and C. K. Williams, *Polym. Chem.*, 2012, **3**, 1196-1201.
88. S. Paul, C. Romain, J. Shaw and C. K. Williams, *Macromolecules*, 2015, **48**, 6047-6056.
89. M. Reiter, A. Kronast, S. Kissling and B. Rieger, *ACS Macro Lett.*, 2016, **5**, 419-423.
90. S. Kernbichl, M. Reiter, F. Adams, S. Vagin and B. Rieger, *J. Am. Chem. Soc.*, 2017, **139**, 6787-6790.
91. P. K. Saini, G. Fiorani, R. T. Mathers and C. K. Williams, *Chem. Eur. J.*, 2017, **23**, 4260-4265.
92. C. Romain and C. K. Williams, *Angew. Chem. Int. Ed.*, 2014, **53**, 1607-1610.
93. C. Romain, Y. Zhu, P. Dingwall, S. Paul, H. S. Rzepa, A. Buchard and C. K. Williams, *J. Am. Chem. Soc.*, 2016, **138**, 4120-4131.
94. F. P. P. S. A. Duraj, *Organometallic Chemistry of the Transition Elements*, 1990, DOI: 10.1007/978-1-4899-2076-8.
95. Q.-L. Zhou, *Angew. Chem. Int. Ed.*, 2016, **55**, 5352-5353.
96. W.-M. Ren, Z.-W. Liu, Y.-Q. Wen, R. Zhang and X.-B. Lu, *J. Am. Chem. Soc.*, 2009, **131**, 11509-11518.
97. E. K. Noh, S. J. Na, S. S. S.-W. Kim and B. Y. Lee, *J. Am. Chem. Soc.*, 2007, **129**, 8082-8083.
98. C. T. Cohen, T. Chu and G. W. Coates, *J. Am. Chem. Soc.*, 2005, **127**, 10869-10878.
99. O. M. Chukanova, G. P. J. K. Belov and Catalysis, *Kinet. Catal.*, 2016, **57**, 821-825.
100. B. Liu, X. Zhao, H. Guo, Y. Gao, M. Yang and X. Wang, *Polymer*, 2009, **50**, 5071-5075.
101. H. Li and Y. Niu, *Polym. J.*, 2010, **43**, 121.
102. H. Sugimoto and S. Inoue, *Pure Appl. Chem.*, 2006, **78**, 1823-1834.

103. X. Jiang, F. Gou and H. Jing, *J. Catal.*, 2014, **313**, 159-167.
104. H. Sugimoto and K. Kuroda, *Macromolecules*, 2008, **41**, 312-317.
105. C. Chatterjee, M. H. Chisholm, A. El-Khalidy, R. D. McIntosh, J. T. Miller and T. Wu, *Inorg. Chem.*, 2013, **52**, 4547-4553.
106. C. E. Anderson, S. I. Vagin, W. Xia, H. Jin and B. Rieger, *Macromolecules*, 2012, **45**, 6840-6849.
107. C. Chatterjee and M. H. Chisholm, *Inorg. Chem.*, 2012, **51**, 12041-12052.
108. G.-P. Wu, S.-H. Wei, W.-M. Ren, X.-B. Lu, T.-Q. Xu and D. J. Darensbourg, *J. Am. Chem. Soc.*, 2011, **133**, 15191-15199.
109. D. J. Darensbourg and S. J. Wilson, *Macromolecules*, 2013, **46**, 5929-5934.
110. D. J. Darensbourg and W.-C. Chung, *Macromolecules*, 2014, **47**, 4943-4948.
111. D. J. Darensbourg, W.-C. Chung and S. J. Wilson, *ACS Catal.*, 2013, **3**, 3050-3057.
112. D. J. Darensbourg, W.-C. Chung, C. J. Arp, F.-T. Tsai and S. J. Kyran, *Macromolecules*, 2014, **47**, 7347-7353.
113. P. Derboven, D. R. D'hooge, M. M. Stamenovic, P. Espeel, G. B. Marin, F. E. Du Prez and M.-F. Reyniers, *Macromolecules*, 2013, **46**, 1732-1742.
114. M. Winkler, C. Romain, M. A. R. Meier and C. K. Williams, *Green Chem.*, 2015, **17**, 300-306.
115. D. J. Darensbourg, W.-C. Chung, A. D. Yeung and M. Luna, *Macromolecules*, 2015, **48**, 1679-1687.
116. D. J. Darensbourg and G.-P. Wu, *Angew. Chem. Int. Ed.*, 2013, **52**, 10602-10606.
117. G.-P. Wu, D. J. Darensbourg and X.-B. Lu, *J. Am. Chem. Soc.*, 2012, **134**, 17739-17745.
118. Y. Wang, J. Fan and D. J. Darensbourg, *Angew. Chem. Int. Ed.*, 2015, **54**, 10206-10210.
119. G.-P. Wu and D. J. Darensbourg, *Macromolecules*, 2016, **49**, 807-814.
120. M. R. Kember, F. Jutz, A. Buchard, A. J. P. White and C. K. Williams, *Chem. Sci.*, 2012, **3**, 1245-1255.

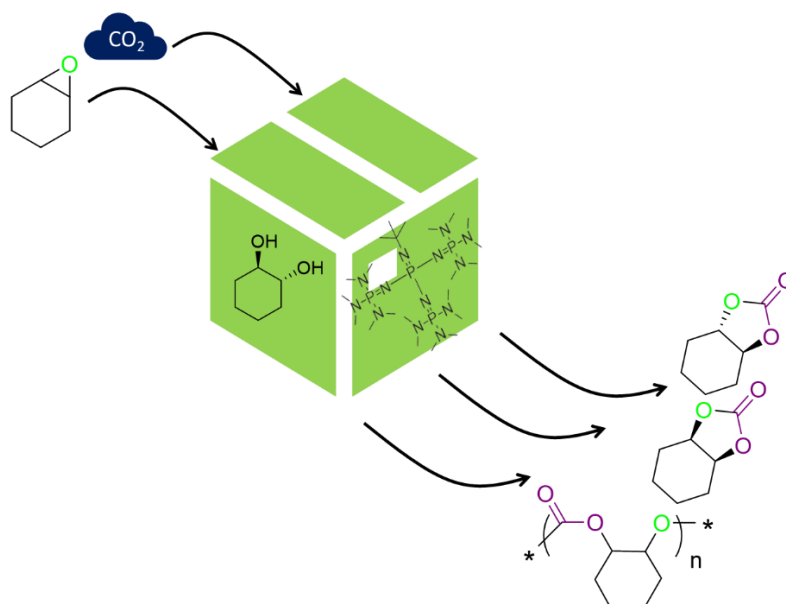
121. C. E. Anderson, S. I. Vagin, M. Hammann, L. Zimmermann and B. Rieger, *ChemCatChem*, 2013, **5**, 3269-3280.
122. W. Xia, S. I. Vagin and B. Rieger, *Chem. Eur. J.*, 2014, **20**, 15499-15504.
123. W. Xia, K. A. Salmeia, S. I. Vagin and B. Rieger, *Chem. Eur. J.*, 2015, **21**, 4384-4390.
124. K. A. Salmeia, S. Vagin, C. E. Anderson and B. Rieger, *Macromolecules*, 2012, **45**, 8604-8613.
125. D. J. Darensbourg, R. R. Poland and C. Escobedo, *Macromolecules*, 2012, **45**, 2242-2248.
126. B. Han, L. Zhang, S. J. Kyran, B. Liu, Z. Duan and D. J. Darensbourg, *J. Polym. Sci. Part A: Polym. Chem.*, 2016, **54**, 1938-1944.
127. G. Si, L. Zhang, B. Han, H. Zhang, X. Li and B. Liu, *RSC Adv.*, 2016, **6**, 22821-22826.
128. R. Shannon, *Acta Crystallogr. Sect. A*, 1976, **32**, 751-767.
129. D. J. Darensbourg and S. J. Kyran, *ACS Catal.*, 2015, **5**, 5421-5430.
130. K. Devaine-Pressing and C. M. Kozak, *ChemSusChem*, 2017, **10**, 1266-1273.
131. R. K. Dean, L. N. Dawe and C. M. Kozak, *Inorg. Chem.*, 2012, **51**, 9095-9103.
132. R. K. Dean, K. Devaine-Pressing, L. N. Dawe and C. M. Kozak, *Dalton Trans.*, 2013, **42**, 9233-9244.
133. H. Chen, L. N. Dawe and C. M. Kozak, *Catal. Sci. Technol.*, 2014, **4**, 1547-1555.
134. K. Ni and C. M. Kozak, *Inorg. Chem.*, 2018, **57**, 3097-3106.
135. N. D. Harrold, Y. Li and M. H. Chisholm, *Macromolecules*, 2013, **46**, 692-698.
136. K. Nakano, K. Kobayashi, T. Ohkawara, H. Imoto and K. Nozaki, *J. Am. Chem. Soc.*, 2013, **135**, 8456-8459.
137. M. Taherimehr, S. M. Al-Amsyar, C. J. Whiteoak, A. W. Kleij and P. P. Pescarmona, *Green Chem.*, 2013, **15**, 3083-3090.
138. C.-H. Li, H.-J. Chuang, C.-Y. Li, B.-T. Ko and C.-H. Lin, *Polym. Chem.*, 2014, **5**, 4875-4878.
139. P.-M. Lin, C.-H. Chang, H.-J. Chuang, C.-T. Liu, B.-T. Ko and C.-C. Lin, *ChemCatChem*, 2016, **8**, 984-991.

140. L.-S. Huang, C.-Y. Tsai, H.-J. Chuang and B.-T. Ko, *Inorg. Chem.*, 2017, **56**, 6141-6151.
141. C.-Y. Tsai, F.-Y. Cheng, K.-Y. Lu, J.-T. Wu, B.-H. Huang, W.-A. Chen, C.-C. Lin and B.-T. Ko, *Inorg. Chem.*, 2016, **55**, 7843-7851.
142. T.-Y. Lee, Y.-J. Lin, Y.-Z. Chang, L.-S. Huang, B.-T. Ko and J.-H. Huang, *Organometallics*, 2017, **36**, 291-297.
143. K. Nakano, K. Kobayashi and K. Nozaki, *J. Am. Chem. Soc.*, 2011, **133**, 10720-10723.
144. E. Peris, *Chem. Rev.*, 2018, **118**, 9988-10031.
145. L. Benhamou, E. Chardon, G. Lavigne, S. Bellemin-Laponnaz and V. César, *Chem. Rev.*, 2011, **111**, 2705-2733.
146. C. C. Quadri and E. Le Roux, *Dalton Trans.*, 2014, **43**, 4242-4246.
147. J. Hessevik, R. Lalrempuia, H. Nsiri, K. W. Törnroos, V. R. Jensen and E. Le Roux, *Dalton Trans.*, 2016, **45**, 14734-14744.
148. C. C. Quadri, R. Lalrempuia, J. Hessevik, K. W. Törnroos and E. Le Roux, *Organometallics*, 2017, **36**, 4477-4489.
149. Y. Wang, Y. Qin, X. Wang and F. Wang, *Catal. Sci. Technol.*, 2014, **4**, 3964-3972.
150. Y. Wang, Y. Qin, X. Wang and F. Wang, *ACS Catal.*, 2015, **5**, 393-396.
151. J. A. Garden, A. J. P. White and C. K. Williams, *Dalton Trans.*, 2017, **46**, 2532-2541.
152. M. Mandal, U. Monkowius and D. Chakraborty, *New J. Chem.*, 2016, **40**, 9824-9839.
153. R. Lalrempuia, F. Breivik, K. W. Törnroos and E. Le Roux, *Dalton Trans.*, 2017, **46**, 8065-8076.
154. M. Mandal, D. Chakraborty and V. Ramkumar, *RSC Adv.*, 2015, **5**, 28536-28553.
155. C.-K. Su, H.-J. Chuang, C.-Y. Li, C.-Y. Yu, B.-T. Ko, J.-D. Chen and M.-J. Chen, *Organometallics*, 2014, **33**, 7091-7100.
156. H.-J. Chuang and B.-T. Ko, *Dalton Trans.*, 2015, **44**, 598-607.
157. C.-H. Ho, H.-J. Chuang, P.-H. Lin and B.-T. Ko, *J. Polym. Sci. Part A: Polym. Chem.*, 2017, **55**, 321-328.

158. H. Nagae, R. Aoki, S.-n. Akutagawa, J. Kleemann, R. Tagawa, T. Schindler, G. Choi, T. P. Spaniol, H. Tsurugi, J. Okuda and K. Mashima, *Angew. Chem. Int. Ed.*, 2018, **57**, 2492-2496.
159. J. Qin, B. Xu, Y. Zhang, D. Yuan and Y. Yao, *Green Chem.*, 2016, **18**, 4270-4275.
160. A. Decortes, R. M. Haak, C. Martín, M. M. Belmonte, E. Martin, J. Benet-Buchholz and A. W. Kleij, *Macromolecules*, 2015, **48**, 8197-8207.
161. C.-Y. Tsai, B.-H. Huang, M.-W. Hsiao, C.-C. Lin and B.-T. Ko, *Inorg. Chem.*, 2014, **53**, 5109-5116.
162. S. Tempelaar, L. Mespouille, O. Coulembier, P. Dubois and A. P. Dove, *Chem. Soc. Rev.*, 2013, **42**, 1312-1336.
163. L. Mespouille, O. Coulembier, M. Kawalec, A. P. Dove and P. Dubois, *Prog. Polym. Sci.*, 2014, **39**, 1144-1164.
164. A. Baba, H. Kashiwagi and H. Matsuda, *Organometallics*, 1987, **6**, 137-140.
165. D. J. Darensbourg, A. Horn Jr and A. I. Moncada, *Green Chem.*, 2010, **12**, 1376-1379.
166. G. L. Gregory, M. Ulmann and A. Buchard, *RSC Adv.*, 2015, **5**, 39404-39408.
167. G. L. Gregory, L. M. Jenisch, B. Charles, G. Kociok-Köhn and A. Buchard, *Macromolecules*, 2016, **49**, 7165-7169.
168. G. L. Gregory, E. M. Hierons, G. Kociok-Köhn, R. I. Sharma and A. Buchard, *Polym. Chem.*, 2017, **8**, 1714-1721.
169. G. L. Gregory, G. Kociok-Köhn and A. Buchard, *Polym. Chem.*, 2017, **8**, 2093-2104.
170. D. Zhang, S. K. Boopathi, N. Hadjichristidis, Y. Gnanou and X. Feng, *J. Am. Chem. Soc.*, 2016, **138**, 11117-11120.
171. F. Auriemma, C. De Rosa, M. R. Di Caprio, R. Di Girolamo, W. C. Ellis and G. W. Coates, *Angew. Chemie Int. Ed.*, 2015, **127**, 1231-1234.
172. F. Parrino, A. Fidalgo, L. Palmisano, L. M. Ilharco, M. Pagliaro and R. Ciriminna, *ACS Omega*, 2018, **3**, 4884-4890.

173. O. Hauenstein, M. Reiter, S. Agarwal, B. Rieger and A. Greiner, *Green Chem.*, 2016, **18**, 760-770.
174. G. R. Dick, A. D. Frankhouser, A. Banerjee and M. W. Kanan, *Green Chem.*, 2017, **19**, 2966-2972.
175. A. Banerjee, G. R. Dick, T. Yoshino and M. W. Kanan, *Nature*, 2016, **531**, 215.

Organocatalyzed coupling of epoxide and CO₂ using a phosphazene superbases



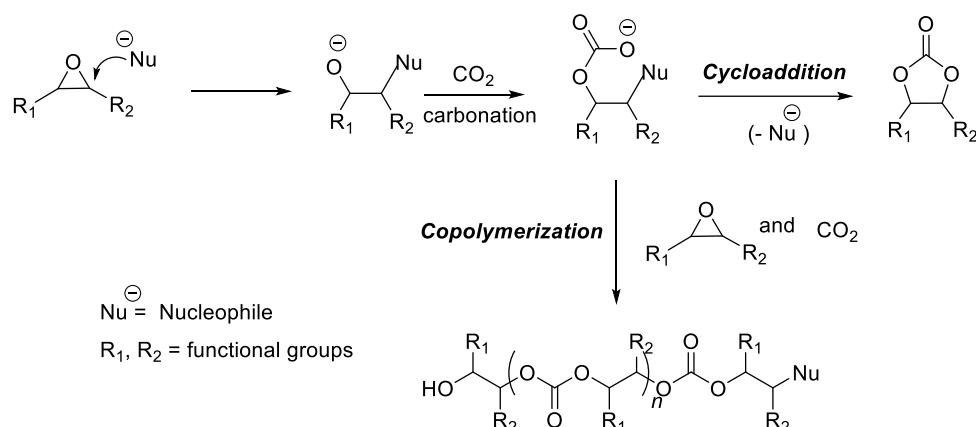
Keywords: Organocatalysis, carbon dioxide, cyclic carbonate, oligomerization, phosphazene

As already presented in the introduction of this thesis, carbon dioxide (CO₂) is considered as a non-toxic and renewable C1 feedstock to deal in long term with the depletion of fossil fuel in our society. The coupling of CO₂ and epoxides to yield poly and cyclic carbonates by using the organocatalysis provides an economical and green route to produce important reagent for further applications such as biomaterials and microelectronic devices.

Herein, we report a halogen-free catalytic system based on the association of *trans*-cyclohexane diol and an organic superbases to efficiently couple CO₂ and a representative epoxide. Such catalytic system allows a mixture of *cis* and *trans* 5-membered cyclic carbonate as well as oligo-carbonates to be obtained in very mild conditions.

2.1 Introduction

The increasing awareness of CO₂ levels in the atmosphere, that result from a massive deforestation and the combustion of fossil fuels, has motivated scientists to develop strategies and technologies for CO₂ valorization.¹ The transformation of CO₂ into fine chemicals has received a great deal of attention since such abundant and non-toxic C1 feedstock is promising to replace highly toxic phosgene.² Due to a fully oxidized state and a symmetric molecular structure, CO₂ is characterized by an inert activity requiring the development of catalytic tools to valorize it. Coupling CO₂ with epoxides, EPs, by using either metal-based or organic catalytic systems to produce polycarbonate^{3,4} and cyclic analogues^{5,6} is the most favorable approach to valorize CO₂. Since the inherent structure of those 3-membered cyclic EPs features a high ring strain energy (112 kJ·mol⁻¹)⁷, they can undergo, in presence of carbon dioxide, either a copolymerization⁸ or a simple cycloaddition⁹ reaction under mild conditions (Scheme 2.1).



Scheme 2.1. Two pathways of CO₂ valorization by reaction with epoxides.

While metal-based catalysis is associated with drawbacks of potential metallic pollution, multi-step synthesis and pharmaceutical toxicity, the organocatalysis efficiently utilizes (preferably renewable) raw materials, eliminates waste and avoids the use of toxic and/or hazardous reagents. In 1956, Lichtenwalter and Cooper pioneered the synthesis of cyclic carbonates prepared by organocatalysis.¹⁰ They developed a catalytic process enable to efficiently induce the preparation of ethylene carbonate (EC) from a CO₂/ethylene oxide (EO) mixture using quaternary ammonium halides (tetrabutylammonium bromide, TBABr). At 200 °C and under 3.4 MPa CO₂ pressure, EC was produced in a 97% yield. Later on, such harsh experimental conditions were overcome by Calo *et al.* who used a catalytic mixture of TBABr and tetrabutylammonium iodide (TBAI) (used in a 1:1 ratio) to fully convert styrene oxide (SO) in cyclic carbonate, at 60 °C and under 0.1 MPa pressure in CO₂.¹¹ Next to the ammonium-based structures, other halide-based catalysis such as phosphonium salts and imidazolium salts were also investigated. Recently, Dufaud *et al.* reported some researches on the cycloaddition of EP with CO₂ as catalyzed by azaphosphatane allowing the production of cyclic carbonate under ambient pressure.¹²⁻¹⁴ In 2014, Cokoja *et al.* reported the use of an imidazolium halide-based catalyst for the conversion of a CO₂/EP mixture under mild conditions (*e.g.* 70 °C, 0.4 MPa CO₂).^{15, 16} In their studies, the authors demonstrated that the acidity of the imidazolium cation dictates the activity of

the entire catalytic system since high conversions in EP were only obtained when imidazolium salts of high acidity were used.¹⁷ Recently, our group described a dual catalytic system based on iodine and the use of a 1,8-diazabicyclo[5.4.0]undec-7-ene (DBU) superbases to valorize and transform CO₂ in bulk, providing cyclic carbonates at 60 °C and for a 0.1 MPa CO₂ pressure. (Chart 2.1)¹⁸

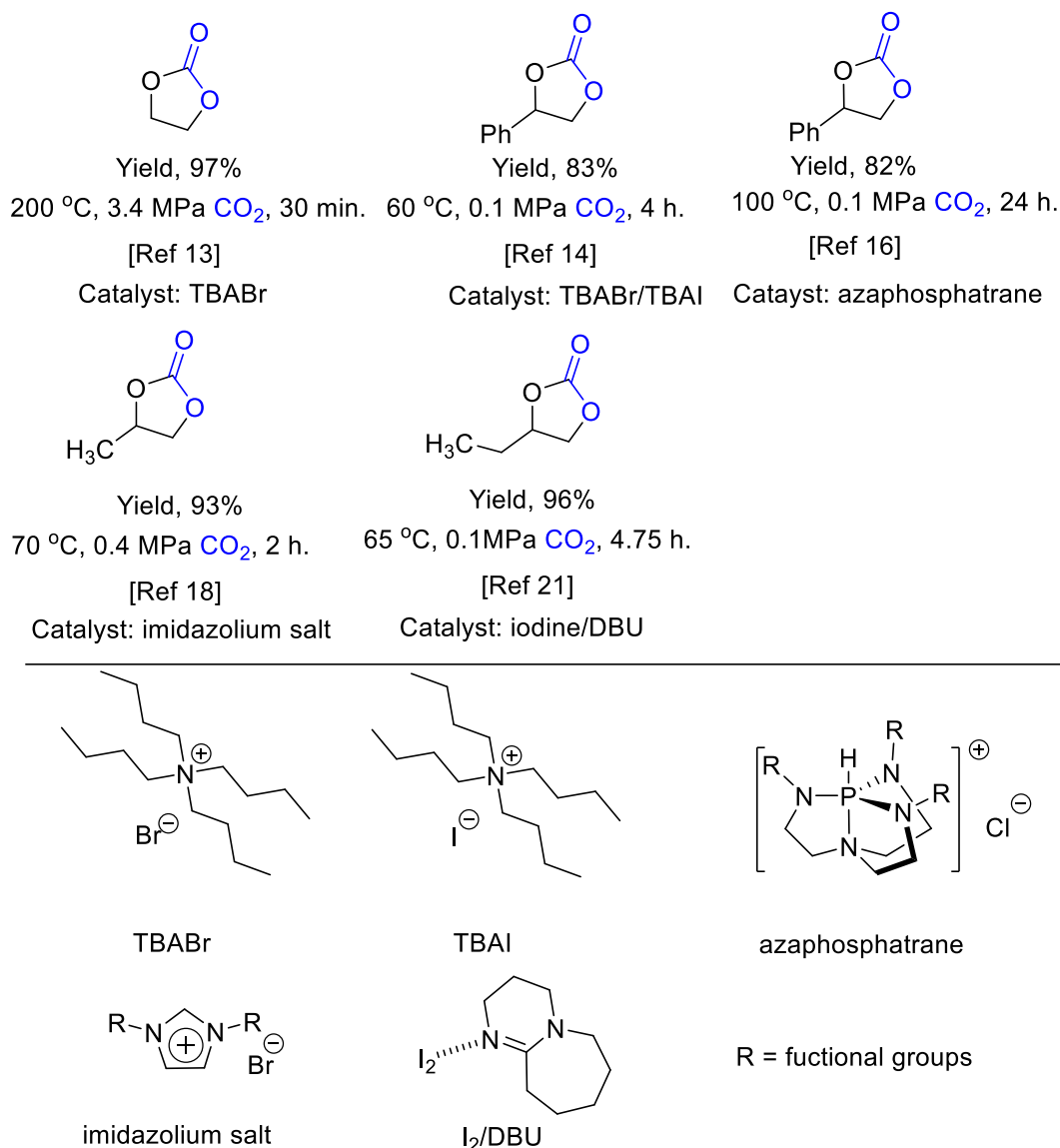
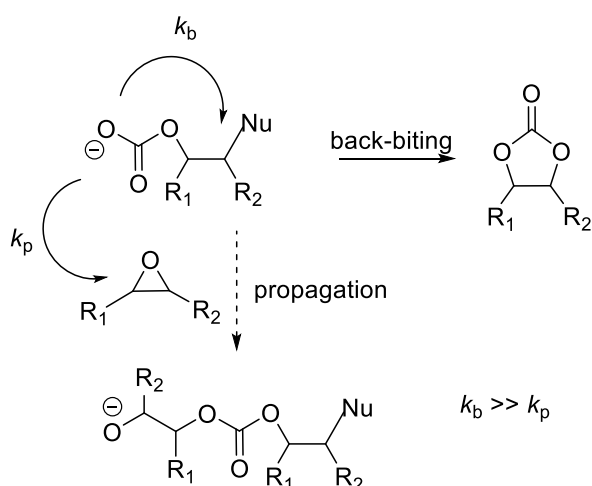


Chart 2.1. Various catalysts used for the preparation of cyclic carbonates from CO₂ and epoxides.

While the pronounced progress in the organocatalytic cycloaddition between CO₂ and EP is growing, the copolymerization of both CO₂ and EP using an organocatalysis is, to date, rarely addressed since

the rate constant of back-biting (k_b) occurring after addition of CO_2 from the generated alkoxide in the anionic ring-opening process is much higher than the copolymer chain propagation (k_p) which eventually generates a thermodynamic favored cyclic carbonate instead of a copolymer (Scheme 2.2).¹⁹ Recently, Gnanou reported the first example of CO_2 and EP copolymerization in presence of triethylene borane (TEB) as catalyst.¹⁹ High molar masses polycarbonates (M_n of $76.3 \text{ kg}\cdot\text{mol}^{-1}$, \bar{M}_{SEC} of 1.20) were obtained 80°C and 1 MPa CO_2 in tetrahydrofuran (THF). Although organocatalytic copolymerization of CO_2 and EP is not explored extensively due to the inevitable back-biting reactions, the utilization of polycarbonates as biomaterials^{20, 21} or in the microelectronic^{22, 23} field is promising.

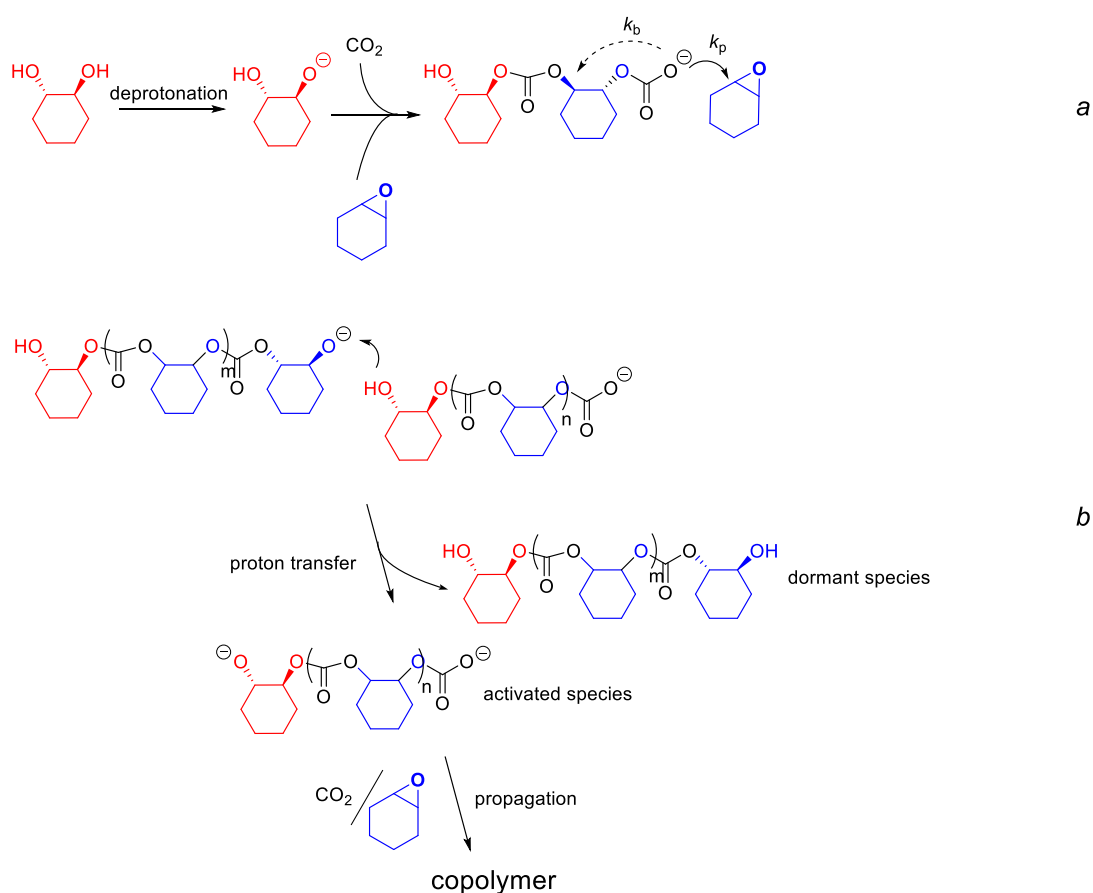


Scheme 2.2. Kinetic comparison of CO_2 and EP coupling reaction.

Herein, we report a novel procedure to produce oligo-(cyclohexane carbonate) (OCC), *trans*-cyclohexane carbonate (*trans*-CHC) and its *cis*-analogue (*cis*-CHC) from cyclohexane oxide (CHO) and CO_2 in a one pot process. Such a reaction was catalyzed by a *trans*-cyclohexane diol (*trans*-CHD) and 1-*tert*-butyl-4,4,4-tris(dimethylamino)-2,2-bis[tris(dimethylamino)-phosphoranylideneamino]-2 λ^5 ,4 λ^5 -catenadi(phosphazene) (*tert*-Bu- P_4) under mild conditions.

As mentioned in the introduction, the *trans*-CHC is a polymerizable monomer (cf. Chapter I, Scheme 1.5)²⁴⁻²⁶ due to its large dihedral angle.²⁷ Such characteristics render *trans*-CHC interesting to be

prepared *in situ* from CHO and CO₂ and further polymerized in a one pot procedure. To realize such a reaction, *trans*-CHD was used as co-catalyst and in presence of a *tert*-Bu-P₄ superbases to hypothetically prepare poly(cyclohexane carbonate). In an ideal situation, the introduction of *trans*-CHD would suppress k_b and hence couple another CHO for the propagation process (Scheme 2.3a). If the proton transfer exists in such coupling reaction, the generated alkoxide that retains the *trans* geometry will continue the propagation process (Scheme 2.3b).



Scheme 2.3. Schematic representation of CO₂ and CHO copolymerization in presence of *trans*-CHD

To carry out such reaction, introducing a strong base that promotes the deprotonation process is then prerequisite. As such, *tert*-Bu-P₄, one of the non-nucleophilic strongest bases, was applied to the coupling of CO₂ and CHO, while other superbases such as amidine and guanidine were also examined.

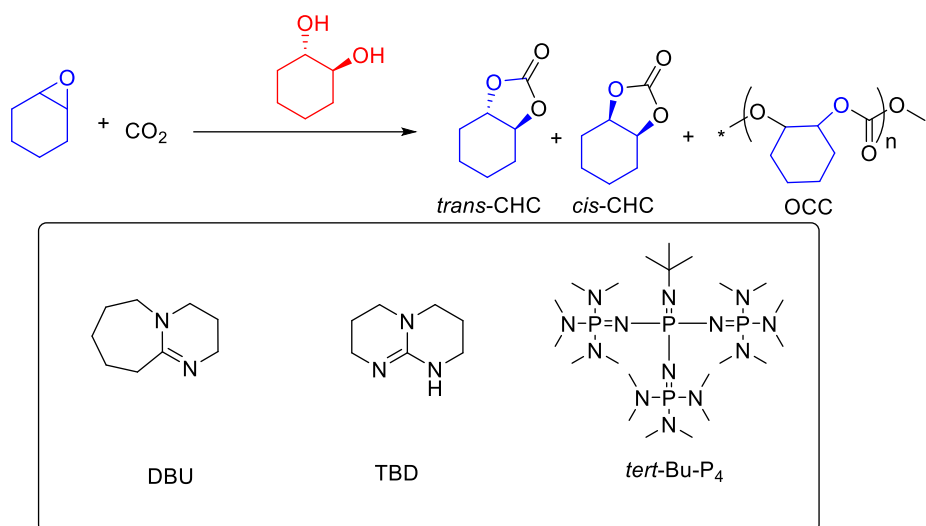
Reactions were voluntarily realized under 0.1 MPa pressure in CO₂ while experimental conditions such as temperature, reaction time and catalytic loading were varied.

2.2 Results and Discussion

Reasoning that 1,8-diazabicyclo[5.4.0]undec-7-ene (DBU) and 1,5,7-triazabicyclo[4.4.0]dec-5-ene (TBD) have been proven as effective superbases that deprotonating aliphatic alcohols and hence allowing the insertion of CO₂ to generate carbonate,²⁸ alongside with the superior performance of *tert*-Bu-P₄ for the ketone's deprotonation resulting in enolate,²⁹ these three superbases were chosen for an initial investigation.

2.2.1 Superbases efficiencies

The superbase screening experiments were performed in Schlenk tubes charged with a defined amount of CHO (5.17 mmol), *trans*-CHD (5 mol%) and superbase (SB, 5 mol%). Mixtures were frozen in liquid nitrogen for 1 min, degassed by dry N₂ and eventually charged by gaseous CO₂ under 0.1 MPa pressure. After equilibration, the mixtures were heated up to 85 °C for 24 h. The selectivity and yield of products were determined by ¹H NMR spectroscopy and reported in Table 2.1.

Table 2.1. The catalysis screening on coupling of CHO/CO₂ using SBs and diol in bulk ^[a].


| Entry | Catalysis (pK _a H ⁺) ^[b] | Conversion /% ^[g] | Selectivity / % ^[f] | | | | <i>M</i> _n SEC ^[g] g·mol ⁻¹ | <i>D</i> _M SEC [g] |
|------------------|---|---------------------------------|--------------------------------|-----------------|-----|-------------------|---|----------------------------------|
| | | | <i>trans</i> -CHC | <i>cis</i> -CHC | OCC | Ether linkages | | |
| 1 | DBU ^[c] (24.3) | 1 | >99 | 0 | 0 | 0 | N.D. ^[h] | N.D. |
| 2 | TBD ^[d] (26.0) | 2 | 50 | 0 | 50 | 0 | N.D. | N.D. |
| 3 | <i>tert</i> -Bu-P ₄ (42.7) | 46.5 | 28.7 | 33 | 22 | 16.3 | 660 | 1.38 |
| 4 ^[e] | <i>tert</i> -Bu-P ₄ (42.7) | 37 | 11.5 | 77 | 0 | 11.5 | N.D. | N.D. |

[a] Experimental conditions: 5.17 mmol of CHO, [SBs]/[*trans*-CHD]/[CHO] = 1/1/20, T = 85 °C, t = 24 h, *P*_{CO₂} = 0.1 MPa; [b] pK_aH⁺ of bases in acetonitrile³⁰; [c] DBU = 1,8-diazabicyclo-[5.4.0]-undec-7-ene; [d] TBD = 1,5,7-triazabicyclo[4.4.0]dec-5-ene; [e] *cis*-CHD was used; [f] conversion of CHO and selectivity were determined from ¹H NMR spectroscopy of crude mixture; [g] Determined by SEC in tetrahydrofuran (THF) with polystyrene standard; [h] N.D. =not determined.

The results revealed that DBU and TBD present a very poor catalytic performance by limiting the overall conversion to traces of cyclic carbonate and OCC. Such a result probably originates from a hydrogen interaction between the resulted carbonate and the protonated SB (Figure 2.1). This

interaction provides a stable ion pair leading to an inferior activity toward ring-opening of CHO, as supported by Helderant et al. who observed the formation of stable ion pairs after bubbling gaseous CO₂ through a solution of prepared neutral liquid consisting of SB and aliphatic alcohols, such as 1-hexanol and 1-octanol, under ambient pressure and at room temperature.²⁸ ¹H NMR spectroscopic analysis revealed the complete conversion of superbases and alcohol by the absent signals for free alcohol or unprotonated SBs. Moreover, the crystallographic analysis supported the generation of complexes that protonated SBs and carbonate species were held together *via* hydrogen bonds.

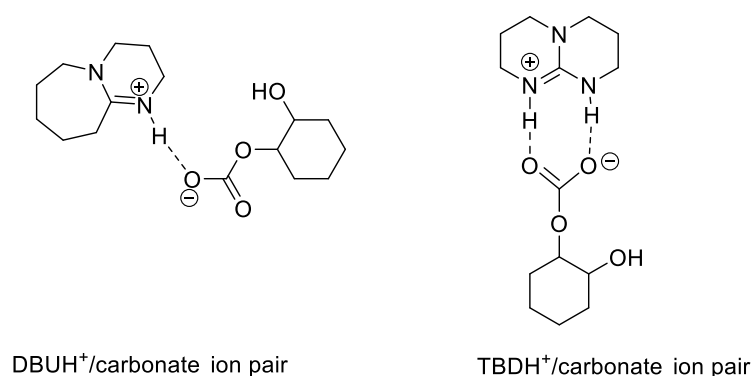


Figure 2.1. Plausible SBs carbonate ion pairs formed between protonated SBs and resulted carbonate.

Interestingly, the *tert*-Bu-P₄ phosphazene considerably improves the overall yield of reaction allowing the generation of OCC and CHCs to be produced at 47 % (entry 3). ¹H NMR spectroscopy reveals that the identical signals of CHCs (*cis*-CHC, δ = 4.66 ppm and *trans*-CHC, δ = 3.98 ppm) are present while a broad peak corresponding to OCCs shows up at δ = 4.62 ppm (Figure 2.2). As determined by SEC analysis, a number-average molar mass (M_n) of 660 g·mol⁻¹ and a dispersity value ($M_w/M_n = D_M$) of 1.38 have been calculated confirming the presence of oligomeric OCCs. Note here that such low molecular weight does not simply correspond to oligocarbonates but also to the presence of oligoethers as clearly identified at δ = 3.54 ppm in ¹H NMR spectroscopy (Figure 2.2). Substituting *trans*-CHD by *cis*-CHD does not really affect the overall yield of the reaction (Table 2.1, entry 4) but drastically limits the process to and the production of *cis*-CHC (77 mol%). Such observation

indicates that the conformation of the diol catalyst has a significant impact on the final conformation of the cyclic carbonate. Moreover, as also observed, OCC was not produced when using the *cis*-CHC which may suggest that either the *cis*-CHC is produced at the initial step of the process (being too stable to generate OCC) or is obtained by instantaneous depolymerization of the OCC.

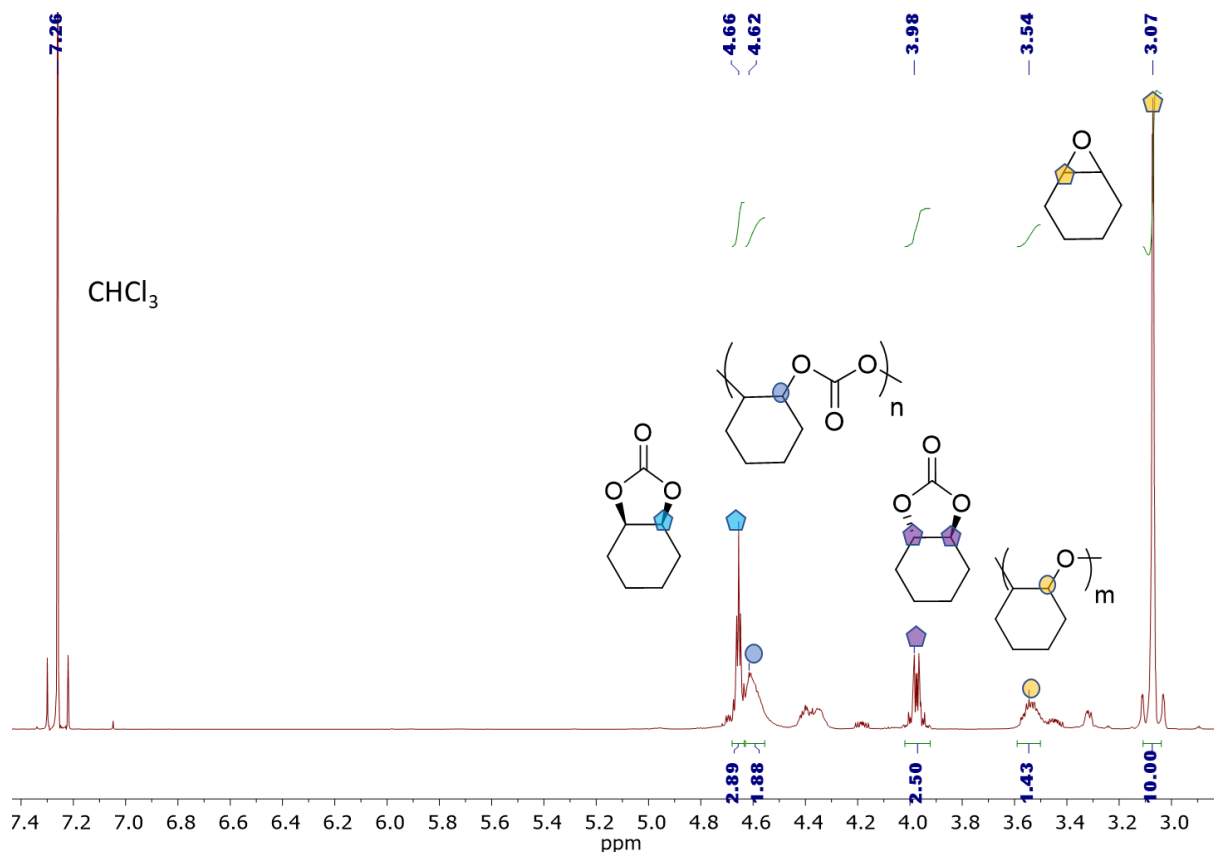


Figure 2.2. ¹H NMR spectrum [zoomed from 3.0 ppm to 7.4 ppm (CDCl₃, 500 MHz)] of the resultant mixture of coupling (Table 2.1, entry 3). Conditions: 5.17 mmol of CHO, [*tert*-Bu-P₄]/[*trans*-CHD]/[CHO] = 1/1/20, T = 85 °C, t = 24 h, P_{CO2} = 0.1 MPa.

2.2.2 Modification of the experimental conditions.

The successful generation of OCC alongside with the generation of *trans*-CHC that can be polymerized under mild conditions,²⁴⁻²⁶ motivated us to further investigate the general process by modifying the reaction conditions. As such, the influence of both temperature and reaction time were

studied, while catalyst loading was investigated for the purpose of obtaining polycarbonate with high molar mass.

- Temperature

As an important experimental parameter, the influence of the temperature on the overall reaction was first investigated. Reactions were performed following the protocol initially set retaining a catalytic *trans*-CHD/*tert*-Bu-P₄ ratio of 1:1 in a 5 mol% loading, a reaction time of 24 h and 0.1 MPa CO₂ pressure at different temperatures going from 45 to 105 °C (Table 2.2).

Table 2.2. The temperature effect on CHO/CO₂ coupling using *tert*-Bu-P₄ and *trans*-CHD in bulk ^[a].

| Entry | T / °C | conversion/% [b] | Selectivity / % [b] | | | | M_n SEC [c] g·mol ⁻¹ | \bar{D}_M SEC [c] |
|-------|--------|---------------------|---------------------|-----------------|-----|----------------|--------------------------------------|---------------------|
| | | | <i>trans</i> -CHC | <i>cis</i> -CHC | OCC | Ether linkages | | |
| 1 | 45 | 4 | 38 | 14 | 13 | 35 | N.D. [d] | N.D. |
| 2 | 65 | 13 | 32 | 24 | 15 | 29 | 430 | 1.14 |
| 3 | 85 | 46.5 | 28.7 | 33 | 22 | 16.3 | 660 | 1.38 |
| 4 | 105 | 70 | 11 | 85 | 0 | 4 | N.D. | N.D. |

[a] Experimental conditions: 5.17 mmol of CHO, [*tert*-Bu-P₄]/[*trans*-CHD]/[CHO] = 1/1/20, t = 24 h, P_{CO_2} = 0.1 MPa ;

[b] conversion of CHO and selectivity were determined from ¹H NMR spectroscopy of crude mixture; [c]

Determined by SEC in tetrahydrofuran (THF) with polystyrene standard; [d] N.D. =not determined.

As expected, increasing the temperature from 45 to 105 °C allowed the overall yield to be considerably improved (from 4 to 70 mol%). While oligomers of carbonates and ethers repeating units were always present from 45 to 85 °C , their relative amounts fluctuated when the reaction is heated up. Increasing the temperature clearly reduces the amount of ether linkages while the relative quantity in carbonate repeating units slowly increases. A further increase in temperature (from 85 to 105 °C)

does not generalize those conclusions since both amounts of carbonate and ether linkages are at their minimum. Concomitantly, the *cis*-to-*trans* CHC ratio increases with the temperature and an impressive selectivity in *cis*-CHC is obtained at 105 °C (85 mol%, entry 4, Table 2.2). Those observations indicate that the increase in temperature allows the production of *cis*-CHC in a high yield while the desired *trans*-CHC and OCC is suppressed. Concomitantly to the reaction of oligo-etherification, those *trans*-CHCs ring-open by generating oligo-carbonates possibly. When the temperature is sufficiently high (here observed at 105 °C), those oligomers start to unzip by eventually generating thermodynamically stable *cis*-CHC with a comparable high selectivity.

- Reaction time

Since the oligo-carbonate (OCC) was the highest at 85 °C and its contamination by ether linkages the lowest, the effect of the reaction time on a CO₂/CHO coupling was studied at 85 °C under the same experimental conditions that were initially set (0.1 MPa CO₂, 5 mol% catalysis loading). Two reactions were then performed for 48 and 72 h to complement the results obtained after 24 h (Table 2.2, entry 3). Results are summarized in Table 2.3.

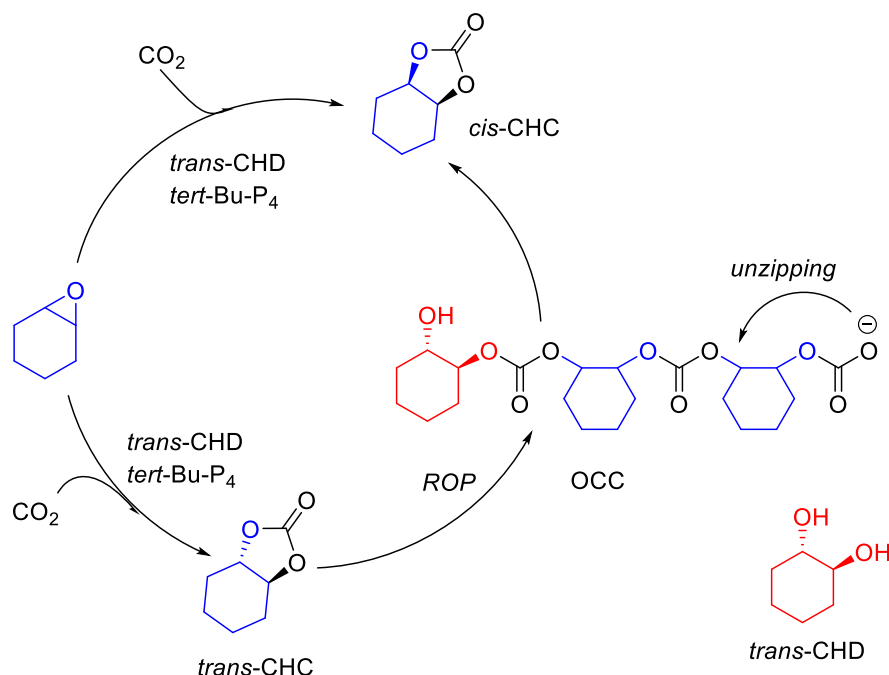
By performing the reaction with the extended times, an OCC characterized by a M_n of 500 g·mol⁻¹ (\bar{D}_{MSEC} of 1.25) was obtained after 48 h (Table 2.3, entry 2), which was slightly lower than that obtained after 24 h (M_n = 600 g·mol⁻¹, \bar{D}_{MSEC} of 1.38) (Table 2.3, entry 1). ¹H NMR spectroscopic analysis revealed that a decrease in selectivity was observed in both *trans*-CHC and OCC (*trans*-CHC from 28.7 to 24 mol%, OCC from 22 to 10 mol%), while *cis*-CHC was further enhanced correspondingly (from 33 to 50 mol%) with 77 mol% conversion of CHO (Table 2.3, entry 2). Interestingly, the extended reaction did not allow the increase of ether linkage in selectivity (16 mol%) (Table 2.3, entry 2), which supported the conclusion that temperature affected the selectivity of ether linkage pronouncedly (Table 2.2).

Table 2.3. Coupling of CO₂ and CHO with different reaction times. ^[a]

| Entry | t / h | conversion/% [b] | Selectivity / % ^[b] | | | | $M_{n\text{ SEC}}$ [c] g·mol ⁻¹ | $\bar{D}_{M\text{ SEC}}$ [c] |
|----------|-------|---------------------|--------------------------------|-----------------|-----|----------------|---|------------------------------|
| | | | <i>trans</i> -CHC | <i>cis</i> -CHC | OCC | Ether linkages | | |
| 1 | 24 | 46.5 | 28.7 | 33 | 22 | 16.3 | 660 | 1.38 |
| 2 | 48 | 77 | 24 | 50 | 10 | 16 | 500 | 1.25 |
| 3 | 72 | 83 | 20 | 51.4 | 13 | 15.6 | 460 | 1.18 |

[a] Experimental conditions: 5.17 mmol of CHO, [*tert*-Bu-P₄]/[*trans*-CHD]/[CHO] = 1/1/20, T = 85 °C, P_{CO_2} = 0.1 MPa; [b] conversion of CHO and selectivity were determined from ¹H NMR spectroscopy of crude mixture; [c] Determined by SEC in tetrahydrofuran (THF) with polystyrene standard.

Very importantly, by increasing the reaction time, the molar mass of the generated OCC decreased gradually. Such a decrease is accompanied by the consumption of the *trans*-CHC and a considerable overproduction of the *cis*-isomer. We postulate that the resulted *cis*-CHC raise from both direct coupling reaction and unzipping generated OCC. With time extension, the *in situ* generated *trans*-CHC is ring-opened yielding OCC that undergo a carbonate back-biting reaction to produce eventually the *cis*-CHC isomer (Scheme 2.4). Confirming that trend, it was anticipated that after 72 h, an increase in the overall conversion would have been accompanied by the decrease in both OCC molar masses (M_n = 460 g·mol⁻¹, $\bar{D}_{M\text{ SEC}}$ of 1.18) and *trans*-CHC content (20 mol% in selectivity) while increasing the level of *cis*-CHC isomer (Table 2.3, entry 3).



Scheme 2.4. Plausible route of products generation (ROP: ring-opening polymerization).

- Effect of co-catalyst loading

As observed, extending the reaction time does not allow high molar mass OCC to be produced but increases the propensity of their unzipping process. As such, further attempts to increase the molar mass of those oligomers were tempted by tuning the catalytic content of both co-catalysts. To examine the effect of the catalytic loading, experimental parameters such as temperature, pressure in CO₂ and reaction time were fixed to 85 °C, 0.1 MPa CO₂ and 24 h, respectively, while the catalytic loadings in both *trans*-CHD and *tert*-Bu-P₄ were varied. The results were summarized in Table 2.4.

In a first attempt, the cooperative effect of both diol and phosphazene superbases was attested by two control reactions involving either the presence of the diol only or the use of the pristine SB (Table 2.4, entries 1 – 2). A total absence of reaction was observed even after 24 hours. Results support the conclusion of the section 2.2.1 where the SB was postulated to deprotonate the *trans*-diol allowing the insertion of CO₂ and yielding (oligo)carbonates.

Table 2.4. The coupling of CHO/CO₂ using *tert*-Bu-P₄ and *trans*-CHD in various molar ratios ^[a].

| Entry | Catalysts loading /mol% | | Conversion/% ^[b] | Selectivity / % ^[b] | | | | $M_{n\text{ SEC}}^{[c]}$ g·mol ⁻¹ | $\bar{D}_{M\text{ SEC}}^{[c]}$ |
|------------------|-------------------------|--------------------------------|--------------------------------|--------------------------------|-----------------|------|----------------|---|--------------------------------|
| | <i>trans</i> -CHD | <i>tert</i> -Bu-P ₄ | | <i>trans</i> -CHC | <i>cis</i> -CHC | OCC | Ether linkages | | |
| 1 | 5 | 0 | 0 | N.D. | N.D. | N.D. | N.D. | N.D. | N.D. |
| 2 | 0 | 5 | 0 | N.D. | N.D. | N.D. | N.D. | N.D. | N.D. |
| 3 | 5 | 5 | 49 | 28.7 | 33 | 22 | 16.3 | 660 | 1.38 |
| 4 | 10 | 10 | 72 | 13 | 57 | 16 | 14 | N.D. ^[d] | N.D. |
| 5 | 15 | 15 | 83 | 13 | 69 | 6 | 12 | N.D. | N.D. |
| 6 | 5 | 10 | 89 | 2 | 98 | 0 | 0 | N.D. | N.D. |
| 7 | 10 | 5 | 48 | 35 | 11 | 7 | 47 | 470 | 1.19 |
| 8 | 40 | 5 | 48 | 43 | 24 | 33 | 0 | 660 | 1.16 |
| 9 ^[e] | 2 | 0.25 | 98 | 28 | 55 | 9 | 8 | 1040 | 1.25 |

[a] Experimental conditions: 0.258 mmol of *trans*-CHD, t = 24 h, P_{CO_2} = 0.1 MPa, T = 85 °C ; [b] conversion of CHO and selectivity were determined from ¹H NMR spectroscopy of crude mixture; [c] Determined by SEC in tetrahydrofuran (THF) with polystyrene standard; N.D. = not determined; [e] t = 216 h.

As suspected, increasing the amounts of both SB and *trans*-CHD ($[\text{SB}]_0/[\text{trans-CHD}]_0 = 1$) relative to the CHO does improve the reaction by increasing the overall conversion of the process (entries 3-5, Table 2.4). Such an increase in conversion is accompanied by a decrease in both carbonate and ether oligomers, a consumption of the as-produced *trans*-CHC as well as an increase in its *cis*-isomer. It clearly revealed that high catalyst loadings only contributed to the production of *cis*-CHC affording a low yield of *trans*-CHC and OCC products. Interestingly, a pronounced conversion of CHO (89 mol%) with unique selectivity in *cis*-CHC (98 mol%) resulted by changing the *trans*-CHD: *tert*-Bu-P₄ catalytic ratio to 1:2 as characterized by ¹H NMR spectroscopy by comparing the *cis*-CHC representing signal at δ = 4.70 ppm to the one of the *trans*-CHC isomer present at δ = 4.02 ppm (Table 2.4, entry 6). Such

ratio allows the unique production of *cis*-CHC without the concomitant presence of neither *trans*-CHC nor oligo-structures (Figure 2.3) As *cis*-CHC is an important precursor for the preparation of *cis*-CHD,³¹ such a catalyst system provides *cis*-CHC under very mild conditions will be interesting to the industrial community for the fabrication of *cis*-CHD economically.

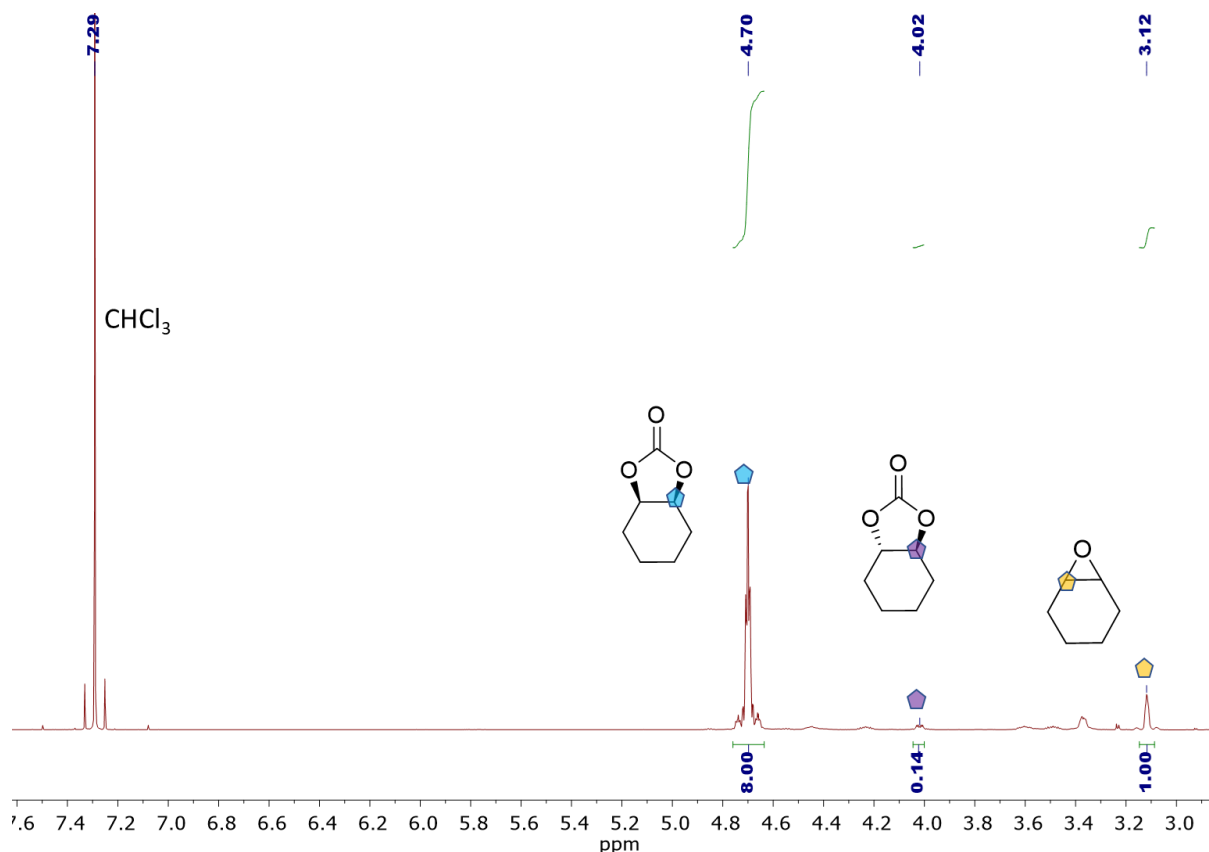


Figure 2.3. ¹H NMR spectrum (CDCl₃, 500 MHz) of the resultant mixture of coupling (Table 2.4, entry 6).

Conditions: [*tert*-Bu-P₄]/[*trans*-CHD]/[CHO] = 2/1/20, T = 85 °C, t = 24 h, P_{CO2} = 0.1 MPa.

To provide more information on the influence of the catalytic ratio, 2 equivalents of *trans*-CHD (relative to the *tert*-Bu-P₄ initial content) were also used (Table 2.4, entry 7). Although a small amount of OCC (7 mol% in selectivity) was produced under such conditions, the selectivity of *trans*-CHC reached 35 mol% that outperformed other ratios used so far. This result suggests that the excessive *trans*-CHD loading could lead to a comparable selectivity of *trans*-CHC. In order to support this postulation, 8

equivalents of *trans*-CHD were applied to the reaction and impressive provided the highest selectivity of *trans*-CHC (43 mol%) as characterized by ^1H NMR spectroscopy (Table 2.4, entry 8).

Although the mechanism of coupling CO_2 and CHO yielding *trans*-CHC is not clear in the state-of-art,³² our study evidently reveals that the excessive addition of *trans*-CHD promotes the generation of *trans*-CHC isomer and that a low content in phosphazene SB diminishes the propensity of the concomitantly produced oligomers to unzip. As it might be expected, performing the reaction by using a large excess of *trans*-CHD ($[\textit{trans}\text{-CHD}]_0/[\textit{tert}\text{-Bu-P}_4]_0 = 8$) and for a prolonged reaction time (216 h instead of 24 h) allows higher molar mass oligomers (M_n of $1,040\text{ g}\cdot\text{mol}^{-1}$; \bar{D}_{MSEC} of 1.25) to be produced from the *in situ* generated *trans*-CHC which eventually leads to an overproduction of *cis*-CHC isomers (Table 2.4, entry 9). After precipitation from *n*-hexane, the residue was dried at $40\text{ }^\circ\text{C}$ under vacuum overnight and was characterized by ^1H NMR spectroscopy. It clearly revealed the existence of carbonate ($\delta = 4.66\text{ ppm}$) and ether ($\delta = 3.55\text{ ppm}$) linkages in the oligomeric chain (Figure 2.4). This result suggests that the preparation of OCC can be realized using *trans*-CHD and *tert*-Bu-P₄ as the catalysis, albeit the inferior performance is observed. It would be interesting to explore the similar catalytic system for PCHC preparation with a high molar mass in future.

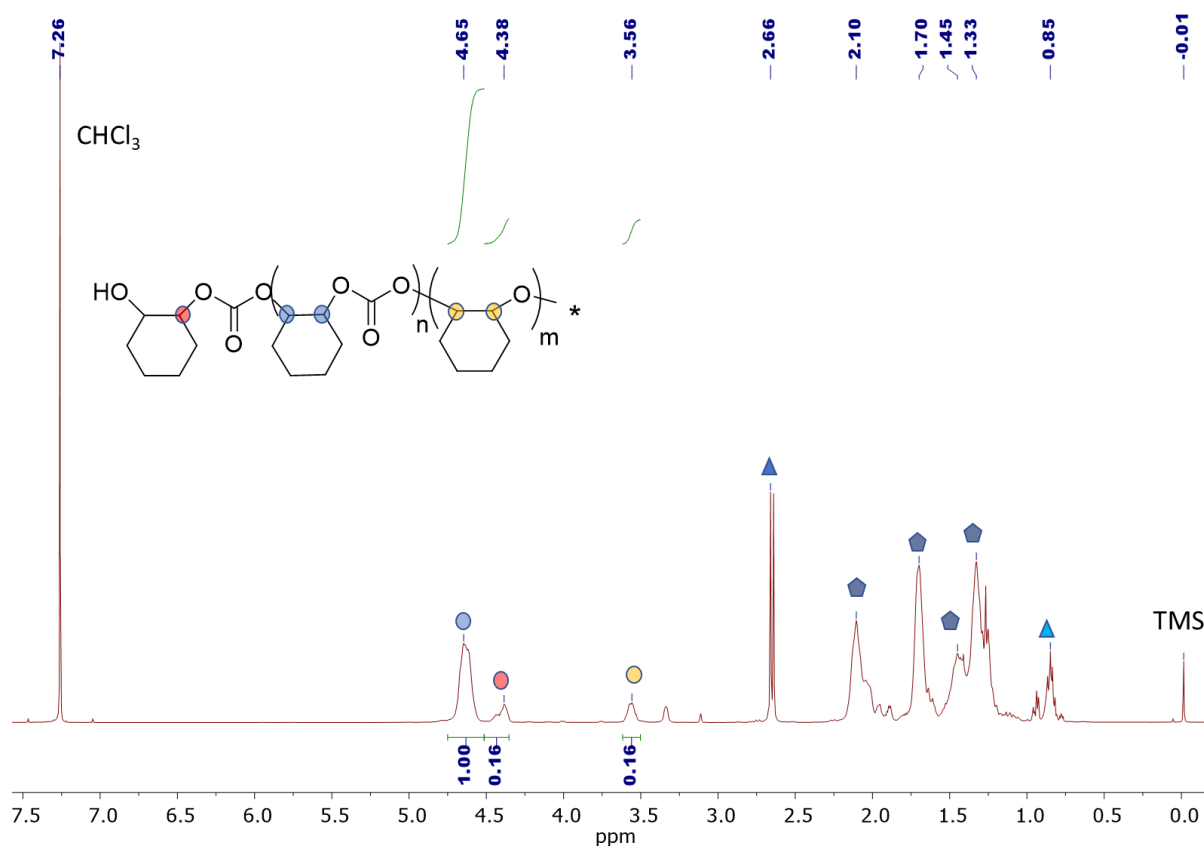

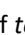
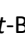


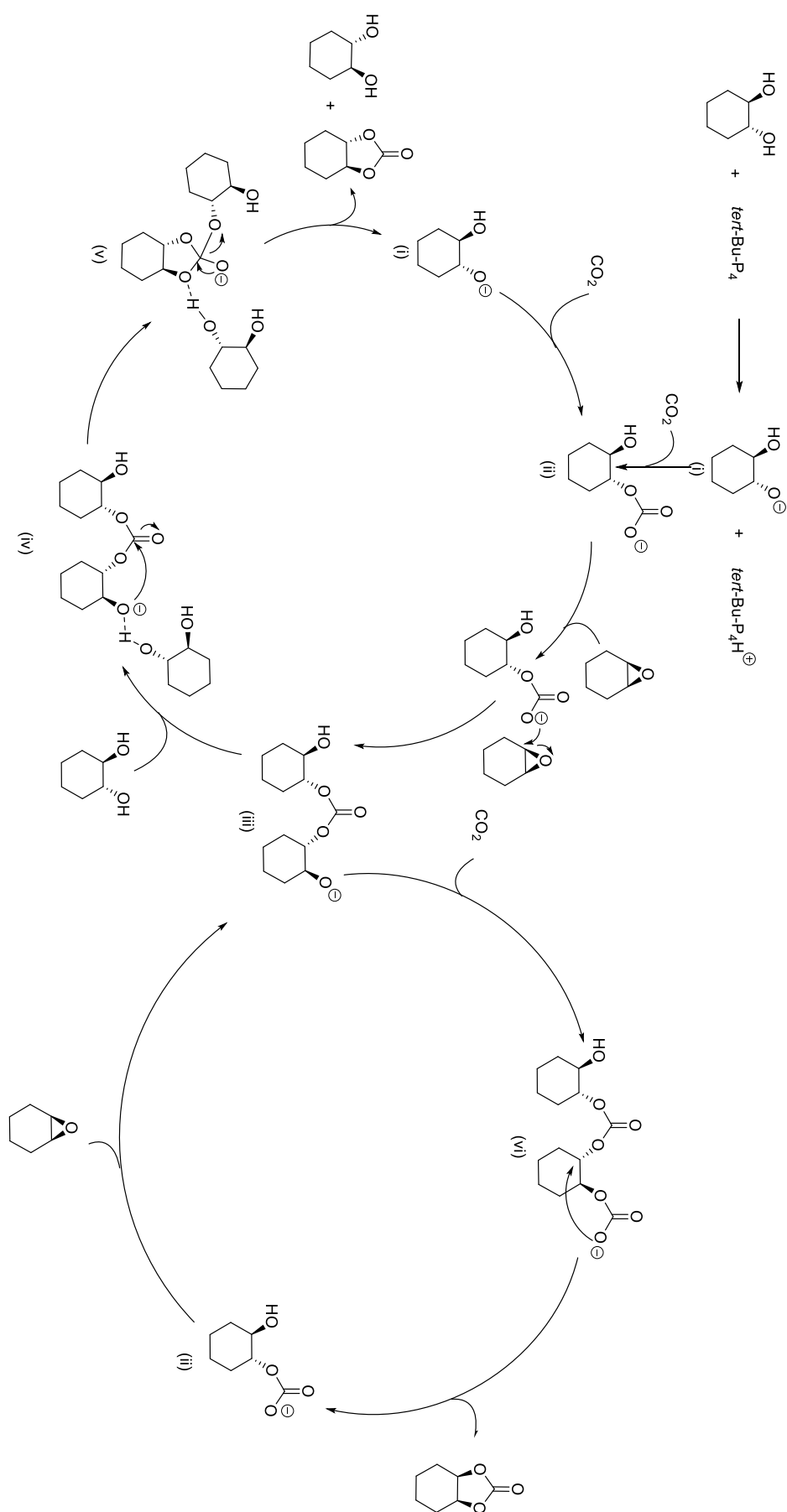
Figure 2.4. ¹H NMR spectrum (CDCl₃, 500 MHz) of the purified OCC from the precipitation of n-hexane (Table 2.4, entry 9). Conditions: 12.9 mmol of CHO, [tert-Bu-P₄]/[trans-CHD]/[CHO] = 1/8/400, T = 85 °C, t = 216 h, P_{CO2} = 0.1 MPa. The cyclohexane ring was marked as  while methyl group of tert-Bu-P₄ and grease were marked as  and , respectively.

Scheme 2.5 presents a tentative scheme of the mechanism involved during the coupling reaction of carbon dioxide and CHO. In the early steps, the phosphazene SB is suspected to deprotonate the *trans*-CHD by forming an alkoxide species (i). Such deprotonation reaction is well-known in the literature³³⁻³⁵. In the presence of CO₂, an intermediate species (ii) is formed by nucleophilic addition.^{28, 36-39} Note here that the alkoxide (i) will also attack free CHO leading to oligoethers. To light the scheme, such a reaction is not represented.

The presence of CHO in excess permits the intermediate (ii) to lead on it a nucleophilic attack resulting in an alkoxide (iii) stabilized by hydrogen-bonding with *trans*-CHD. To explain the presence of

the *trans*-CHC, the intermediate (iv) is suspected to undergo an alkoxide back-biting reaction which does not involve any carbon configuration inversion.³² As discussed in the “temperature and reaction time” section, the oligo-carbonates observed in the final product could be the result of a ring-opening oligomerization of the *in situ* generated *trans*-CHC under high temperature (85 °C), which is supported by Haba’s work²⁴ and Guillaume’s DFT calculations.²⁵

Unlikely the to synthesis of *trans*-CHC which follows an alkoxide back-biting mechanism, the generation of *cis*-CHC isomer could be the result of a carbonate back-biting process.⁴⁰ From the intermediate (iii) and in presence of CO₂, the as-induced carbonate dimer (vi) may undergo a carbonate back-biting reaction inescapably leading to the generation of the *cis*-CHC generation as a substitution product. Such process is supported by the reaction with a unique selectivity in *cis*-CHC (Table 2.4, entry 6). Note here that the complete deprotonation of *trans*-CHD in presence of 2 equivalents of *tert*-Bu-P₄ cannot afford the proton to the intermediate (iii) forming hydrogen bonding for its stabilization. As such, the subsequent carbonation of alkoxide allows the production of *cis*-CHC *via* a carbonate back-biting mechanism.



Scheme 2.5. The plausible mechanism involved in the synthesis of *trans*-CHC and *cis*-CHC from a CO₂ and CHO mixture in presence of both *trans*-CHD and *tert*-Bu-P₄.

2.3 Conclusion

The coupling of CO₂ and cyclohexane oxide provides an efficient approach to oligo-carbonate and its cyclic analogues sustainable, which has received a great deal of attention in the past decade. By tuning the catalyst content, the selectivity of each product such as *cis*-CHC, *trans*-CHC, and oligo-carbonate is manageable under mild conditions. With the addition of 2 equivalents of phosphazene (related to *trans*-CHD), the catalytic reaction allows delivering the unique product of *cis*-CHC. Such an efficient reaction would be interesting to prepare cyclic carbonate industrially, although the preparation of CO₂-based cyclic carbonate is not our main focus. The desired oligo-carbonate was obtained in presence of the excessive *trans*-CHD, which could be used as a chain extension agent for copolymers synthesis. Such results motivate us to continue on focussing on the CO₂-based polycarbonate preparation. As the progress of medical science stimulates the research of biomaterials in recent decades, poly (trimethylene carbonate), PTMC, that is an implantable biomaterial, has found broad study. To prepare PTMC exempt of all metal traces and devoted to biomaterials applications, the organocatalytic synthesis of PTMC is highly desirable by the advantage of CO₂ valorization greenly. In the next chapter, the research project will focus on the synthesis of PTMC from CO₂ and oxetane using organocatalysis.

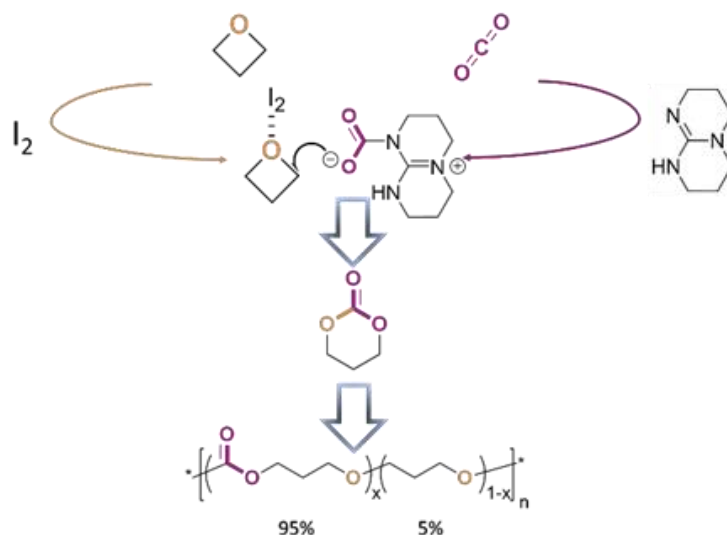
2.4 References

1. J. G. Jang, G. M. Kim, H. J. Kim and H. K. Lee, *Conster. Build. Mater.*, 2016, **127**, 762-773.
2. J. Nemirowsky, *J. Prakt. Chem.*, 1883, **28**, 439-440.
3. M. Taherimehr and P. P. Pescarmona, *J. Appl. Polym. Sci.*, 2014, **131**.
4. E. Alper and O. Yuksel Orhan, *Petroleum*, 2017, **3**, 109-126.
5. J. Ma, N. Sun, X. Zhang, N. Zhao, F. Xiao, W. Wei and Y. Sun, *Catal. Today*, 2009, **148**, 221-231.
6. Q.-W. Song, Z.-H. Zhou and L.-N. He, *Green Chem.*, 2017, **19**, 3707-3728.
7. H. K. Eigenmann, D. M. Golden and S. W. Benson, *J. Phys. Chem.*, 1973, **77**, 1687-1691.
8. S. Klaus, M. W. Lehenmeier, C. E. Anderson and B. Rieger, *Coord. Chem. Rev.*, 2011, **255**, 1460-1479.
9. M. North, S. C. Z. Quek, N. E. Pridmore, A. C. Whitwood and X. Wu, *ACS Catal.*, 2015, **5**, 3398-3402.
10. *USA Pat.*, US2773070A, 1956.
11. V. Caló, A. Nacci, A. Monopoli and A. Fanizzi, *Org. Lett.*, 2002, **4**, 2561-2563.
12. B. Chatelet, L. Joucla, J.-P. Dutasta, A. Martinez, K. C. Szeto and V. Dufaud, *J. Am. Chem. Soc.*, 2013, **135**, 5348-5351.
13. B. Chatelet, L. Joucla, J.-P. Dutasta, A. Martinez and V. Dufaud, *Chem. Eur. J.*, 2014, **20**, 8571-8574.
14. B. Chatelet, E. Jeanneau, J.-P. Dutasta, V. Robert, A. Martinez and V. Dufaud, *Catal. Commun.*, 2014, **52**, 26-30.
15. M. E. Wilhelm, M. H. Anthofer, R. M. Reich, V. D'Elia, J.-M. Basset, W. A. Herrmann, M. Cokoja and F. E. Kühn, *Catal. Sci. Technol.*, 2014, **4**, 1638-1643.
16. M. H. Anthofer, M. E. Wilhelm, M. Cokoja, M. Drees, W. A. Herrmann and F. E. Kühn, *ChemCatChem*, 2015, **7**, 94-98.

17. M. H. Anthofer, M. E. Wilhelm, M. Cokoja, I. I. E. Markovits, A. Pöthig, J. Mink, W. A. Herrmann and F. E. Kühn, *Catal. Sci. Technol.*, 2014, **4**, 1749-1758.
18. O. Coulembier, S. Moins, V. Lemaury, R. Lazzaroni and P. Dubois, *J. CO₂ Util.*, 2015, **10**, 7-11.
19. D. Zhang, S. K. Boopathi, N. Hadjichristidis, Y. Gnanou and X. Feng, *J. Am. Chem. Soc.*, 2016, **138**, 11117-11120.
20. M. C. Hacker and A. G. Mikos, in *Principles of Regenerative Medicine*, eds. A. Atala, R. Lanza, J. A. Thomson and R. M. Nerem, Academic Press, San Diego, 2008, DOI: <https://doi.org/10.1016/B978-012369410-2.50037-1>, 604-635.
21. A. Singh and M. M. Amiji, in *Biomedical Applications of Functionalized Nanomaterials*, eds. B. Sarmiento and J. das Neves, Elsevier, 2018, DOI: <https://doi.org/10.1016/B978-0-323-50878-0.00013-6>, 371-398.
22. H. Ma, A. K.-Y. Jen and L. R. Dalton, *Adv. Mater.*, 2002, **14**, 1339-1365.
23. A. R. Hollie, E. W. Celesta, R. Vikram, A. Sue Ann Bidstrup, L. H. Clifford and A. K. Paul, *J. Micromech. Microeng.*, 2001, **11**, 733.
24. K. Tezuka, K. Komatsu and O. Haba, *Polym J*, 2013, **45**, 1183.
25. W. Guerin, A. K. Diallo, E. Kirilov, M. Helou, M. Slawinski, J.-M. Brusson, J.-F. Carpentier and S. M. Guillaume, *Macromolecules*, 2014, **47**, 4230-4235.
26. S. E. Felder, M. J. Redding, A. Noel, S. M. Grayson and K. L. Wooley, *Macromolecules*, 2018, **51**, 1787-1797.
27. D. J. Darensbourg and S. J. Wilson, *Green Chem.*, 2012, **14**, 2665-2671.
28. L. Phan, D. Chiu, D. J. Heldebrant, H. Huttenhower, E. John, X. Li, P. Pollet, R. Wang, C. A. Eckert, C. L. Liotta and P. G. Jessop, *Ind. Eng. Chem. Res.*, 2008, **47**, 539-545.
29. K. J. Kolonko and H. J. Reich, *J. Am. Chem. Soc.*, 2008, **130**, 9668-9669.
30. Karl Kaupmees, Aleksander Trummel and a. I. Leitoa, *Croat. Chem. Acta*, 2014, **87**, 385-395.

31. V. Laserna, G. Fiorani, C. J. Whiteoak, E. Martin, E. Escudero-Adán and A. W. Kleij, *Angew. Chem. Int. Ed.*, 2014, **53**, 10416-10419.
32. D. J. Darensbourg and A. D. Yeung, *Macromolecules*, 2013, **46**, 83-95.
33. I. Weideman, R. Pfukwa and B. Klumperman, *Eur Polym J.*, 2017, **93**, 97-102.
34. H. Alamri, J. Zhao, D. Pahovnik and N. Hadjichristidis, *Polym. Chem*, 2014, **5**, 5471-5478.
35. H. Yang, Y. Zuo, J. Zhang, Y. Song, W. Huang, X. Xue, Q. Jiang, A. Sun and B. Jiang, *Polym. Chem*, 2018, **9**, 4716-4723.
36. M. Ding and H.-L. Jiang, *Chem. Commun.*, 2016, **52**, 12294-12297.
37. N. Aoyagi, Y. Furusho and T. Endo, *Tetrahedron Lett.*, 2013, **54**, 7031-7034.
38. W. Cheng, X. Chen, J. Sun, J. Wang and S. Zhang, *Catal. Today.*, 2013, **200**, 117-124.
39. M. Alves, B. Grignard, R. Mereau, C. Jerome, T. Tassaing and C. Detrembleur, *Catal. Sci. Technol*, 2017, **7**, 2651-2684.
40. D. J. Darensbourg and S.-H. Wei, *Macromolecules*, 2012, **45**, 5916-5922.

Organocatalytic synthesis of poly (trimethylene carbonate) from CO₂ and oxetane

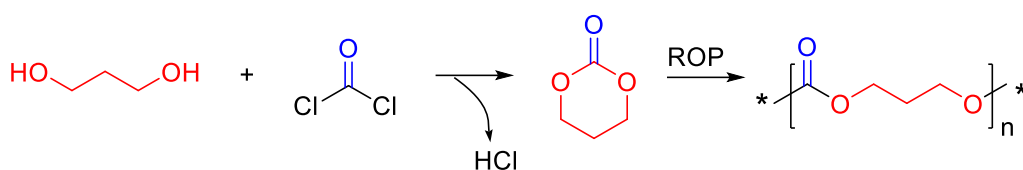


Keywords: Organocatalysts, carbon dioxide, polycarbonate, iodine, oxetane

In Chapter II, attempts of the copolymerization of CO₂ and CHO did not deliver the polycarbonate in success, it afforded some clues about the preparation of polycarbonate using organocatalysis. The desire for sustainability drives interest in the production of chemicals from carbon dioxide. The synthesis of poly (trimethylene carbonate), PTMC, by copolymerization of carbon dioxide and oxetane using organocatalysis affords a green route to this important polymer but has proven to be a very challenging process. Herein we report that the application of iodine, in combination with organic superbases provides a highly active system for the direct synthesis of PTMC from CO₂ with very high levels of carbonate linkage (95 % in selectivity). Mechanistic studies reveal the *in-situ* formation of trimethylene carbonate which eventually polymerizes through an active chain-end process from an I₂-oxetane adduct.

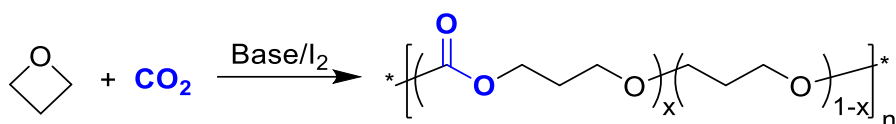
3.1 Introduction

Significant progress has been made towards using CO₂ in eco-friendly technologies for replacing conventional phosgene-based processes.¹⁻⁵ In this regard, the use of CO₂ has been extended beyond its initial applications for the preparation of synthon molecules such as linear and cyclic carbonates (cf Chapter II), ureas and isocyanates, and is now also being used to produce engineering plastics such as polycarbonates. While the copolymerization of epoxides (also referred to as oxiranes) and CO₂ has been the subject of extensive research,⁶ the polymers that result from them require the development of applications and markets for their exploitation. In contrast, poly(trimethylene carbonate), PTMC, has found broad study and commercial application as an implantable biomaterial and as a component in polyurethanes.⁷⁻¹¹ Currently PTMC is accessed via ring-opening polymerization of the 6-membered carbonate (Scheme 3.1),¹²⁻²⁶ trimethylene carbonate (TMC) which requires the use of phosgene-based CO sources for its synthesis as well as commonly being carried out under anhydrous conditions in toxic solvents using heavy metal catalysts, all of which increase the environmental impact of the process.²⁶⁻



Scheme 3.1. General procedure of poly(trimethylene carbonate) preparation.

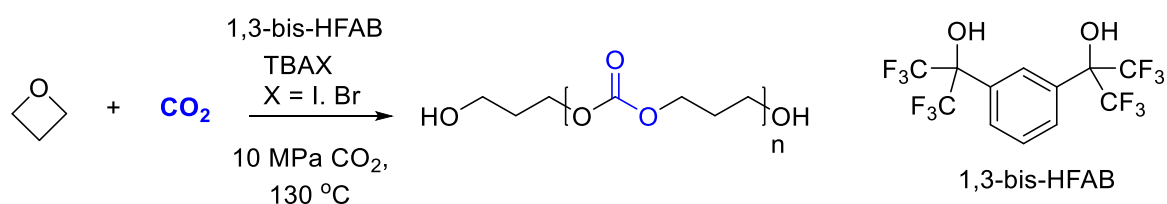
The derivation of a solvent-free process, using CO₂ as the carbonyl source in the absence of metals would provide a significant advance towards creating this polymer in a more sustainable manner. In an analogous manner to the copolymerization of epoxides and CO₂, PTMC can theoretically be produced by copolymerization of CO₂ with oxetane³⁰ (*i.e.* 1,3-epoxypropane, a four-membered cyclic ether, Scheme 3.2). Despite this promise, alongside the possibility of producing 6-membered cyclic carbonates,³ which can be readily polymerized by organic catalytic systems,^{31, 32} relatively few studies have focused on this potentially useful synthetic route, probably a consequence of a relative high price of raw materials and the inherent low reactivity of oxetanes that results from their low ring strain (112 vs 106 kJ.mol⁻¹ for oxirane vs oxetane)^{33, 34} and lower acidity^{35, 36}.



Scheme 3.2. Copolymerization of CO₂ and oxetane using a binary organocatalytic system.

Following the pioneering work of Baba *et al.*,^{37, 38} who produced PTMC by coupling CO₂ and oxetane under a vapor pressure method by using organotin halide complexes (100 °C, 5 MPa in CO₂, 4h, $M_{n,exp} \sim 4,250 \text{ g}\cdot\text{mol}^{-1}$), Darensbourg and coworkers developed a series of Cr,³⁹⁻⁴¹ Al⁴² and Co-based⁴³ catalytic systems to mediate the copolymerization of CO₂ and oxetane in solution. FTIR spectroscopic investigations allowed them to attest that the mechanism by which PTMC was produced involved either the polymerization of an *in-situ*-generated trimethylene carbonate (TMC) intermediate or a direct “chain up” of both oxetane and CO₂. The development of organocatalytic polymerization has

grown significantly over the past 20 years on account of both the green credentials and absence of metals from the resulting polymers.⁴⁴ In a seminal advance towards a metal-free catalytic system, Detrembleur and coworkers developed a binary system composed of 1,3-bis(2-hydroxyhexafluoroisopropyl)benzene and tetrabutylammonium iodide to copolymerize oxetane and CO₂ in bulk.⁴⁵ After 24 h at 130 °C under 10 MPa of CO₂ pressure, oligocarbonates of 2,000 g·mol⁻¹ were obtained (Scheme 3.3).



Scheme 3.3. Organocatalytic coupling of CO₂ with oxetane using 1,3-bis-HFAB.

Recently, some of us reported on the catalytic activity of an equimolar mixture of iodine and the 1,8-diazabicyclo-[5.4.0]-undec-7-ene (DBU) superbase to perform the cycloaddition of various epoxides and CO₂, in bulk, to yield 5-membered cyclic carbonates.⁴⁶ The efficiency of that binary catalyst system enabled a working pressure of CO₂ as low as 0.1 MPa, and was justified by the ability of DBU to properly activate CO₂ as part of a zwitterionic adduct⁴⁷ simultaneously with the formation of a carbon-oxonium bond interaction between I₂ and the oxirane through σ -hole (halogen) bonding.⁴⁸⁻⁵⁰ Very importantly, iodine is an inexpensive and environmentally friendly catalyst, which is currently applied in food,⁵¹ polymer,⁵² and pharmaceutical industries.⁵¹ The increased Lewis basicity of the oxetane monomers (compared to epoxides)⁵³, in combination with the high efficiency for the concomitant activation of both CO₂ and oxiranes of this catalytic system suggested that organocatalytic copolymerization of oxetane and CO₂ may be possible. In the presented chapter, we describe the use of various dual catalytic systems composed by iodine and different organic bases to promote the copolymerization of CO₂ and oxetane. We show that with 1,5,7-triazabicyclo[4.4.0]dec-5-ene (TBD), highly efficient copolymerization is possible under mild conditions with fast kinetics. Mechanistic

investigations reveal that TMC is formed and polymerized instantaneously to produce PTMC, initiated from an *in-situ* generated iodine/oxetane adduct in the system.

3.2 Results and Discussion

The previous work of the cycloaddition of epoxide and CO₂ catalyzed by I₂/DBU binary catalysts motivated us to examine the catalytic activity of such system toward CO₂/oxetane coupling reaction. Although I₂ in combination with DBU present the superior performance to yield 5-membered cyclic carbonates, it would be interesting to study other cocatalysts such as guanidine and phosphazene to examine the cocatalyst effect. As such, the cocatalyst screening experiments were performed and results were discussed.

3.2.1 Cocatalyst screening

Polymerizations of oxetane and CO₂ were first attempted with the I₂/DBU catalytic system. Reactions were performed in bulk, at 105 °C, under a 1 MPa CO₂ atmosphere. Arbitrarily, the catalytic loading content was fixed to 2.5 mol% of each I₂ and DBU with respect to the oxetane monomer. After 24 h, SEC analysis of the resulting material revealed the presence of oligomers, with a number-average molar mass (M_n) of 1,360 g·mol⁻¹ and a dispersity value ($M_w/M_n = \mathcal{D}_M$) of 1.71 (Table 3.1, entry 1).

¹H NMR spectroscopic analysis of the oligomers (Figure 3.1) revealed that 72% of the polymerized oxetane was selectively incorporated through carbonate linkages while 20% resulted in the production of ether bonds in the polymer. The remaining converted oxetane (8 mol% of total) was converted into the 6-membered cyclic carbonate, trimethylene carbonate (TMC).

Table 3.1. Copolymerization of oxetane and CO₂ catalyzed by I₂ and base in bulk. ^[a]

| Entry | Base | pK _a H ⁺ [e] | Time (h) | Oxetane Conversion (%) ^[b] | TOF (h ⁻¹) | Selectivity (%) ^[b] | | | M _n (SEC) ^[d] g·mol ⁻¹ | Đ _M ^[d] |
|-------|-------------------------|---------------------------------------|-------------|---|---------------------------|--------------------------------|-----------------------|-------------------|---|-------------------------------|
| | | | | | | TM C | Carbonate Linkages | Ether Linkages | | |
| 1 | DBU | 24.3 | 24 | 82 | 1.37 | 8 | 72 | 20 | 1,360 | 1.71 |
| 2 | MTBD | 25.5 | 24 | 46 | 0.77 | 11 | 71 | 18 | 5,240 | 1.35 |
| 3 | MTBD | 25.5 | 44 | 80 | 0.73 | 9 | 73 | 18 | 6,000 | 1.45 |
| 4 | TBD | 26.0 | 24 | 88 | 1.61 | <1 | 88 | 12 | 4,630 | 1.32 |
| 5 | P ₄ -tert-Bu | 42.7 | 24 | 15 | 0.25 | >99 | 0 | 0 | NA | NA |
| 6 | P ₄ -tert-Bu | 42.7 | 168 | 83 | 0.20 | 71 | 19 | 10 | 320 | 1.42 |

^[a] Copolymerization conditions: 7.88 mmol oxetane, 2.5 mol% I₂ and base cocatalyst, 1 MPa CO₂, 105 °C. ^[b]

Oxetane conversion and selectivity were determined from ¹H NMR spectroscopy of crude mixture; ^[c] Determined by SEC in tetrahydrofuran (THF) with polystyrene standard; ^[d] pK_a of bases conjugated acids in acetonitrile. ^[15]

We postulated that, similarly to the I₂-initiated ROP of tetrahydrofuran,⁵⁴ the self-oligomerization of oxetane in presence of iodine could explain the presence of ether bonds in the copolymer structure. This hypothesis was verified by addition of I₂ to oxetane ([oxetane]₀/[I₂]₀ = 40) in absence of CO₂ which resulted in production of oligomeric polyoxetane after 8 minutes at 105 °C (Figure 3.2), albeit in low yield (10 mol% of oxetane was converted).

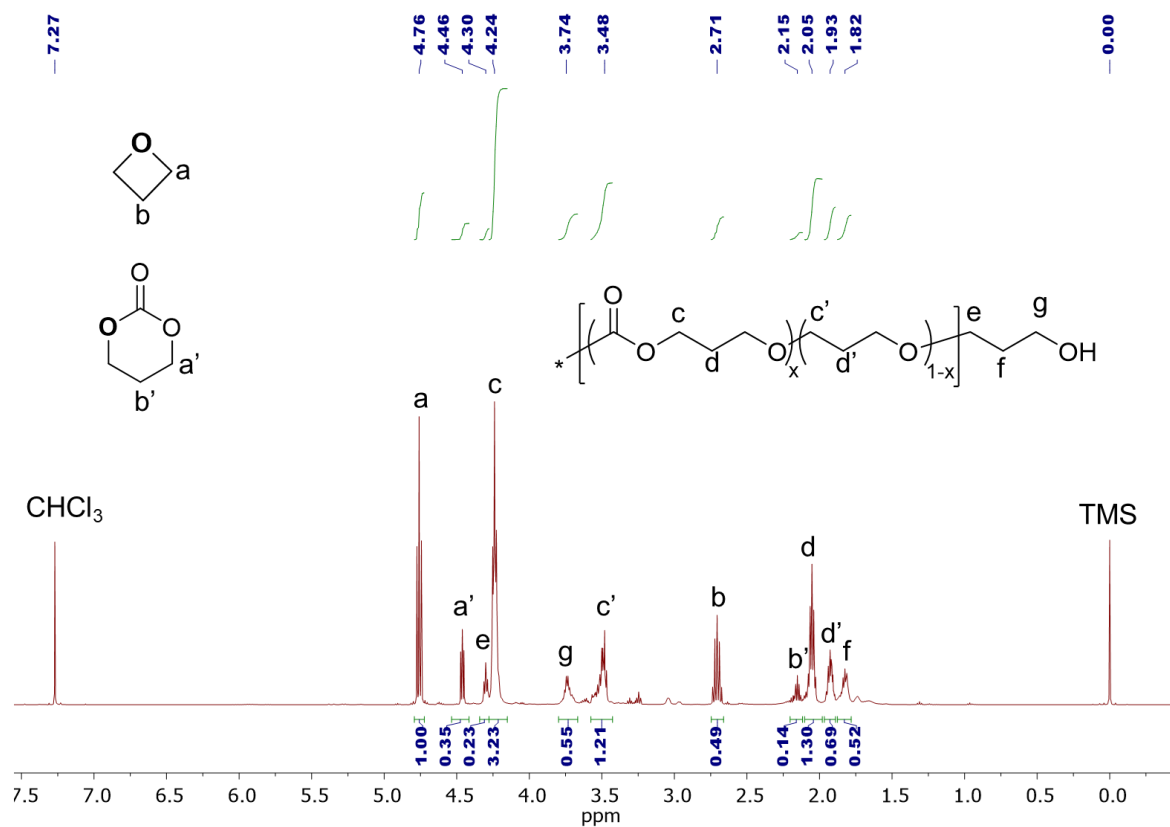


Figure 3.1. ^1H NMR spectrum (CDCl_3 , 500 MHz) of the resultant mixture of polymerization (Table 3.1, entry 1).

Conditions: 7.88 mmol oxetane, $[\text{I}_2]_0/[\text{DBU}]_0/[\text{EP}]_0 = 1/1/40$, 1 MPa CO_2 , 105 $^\circ\text{C}$, 24h.

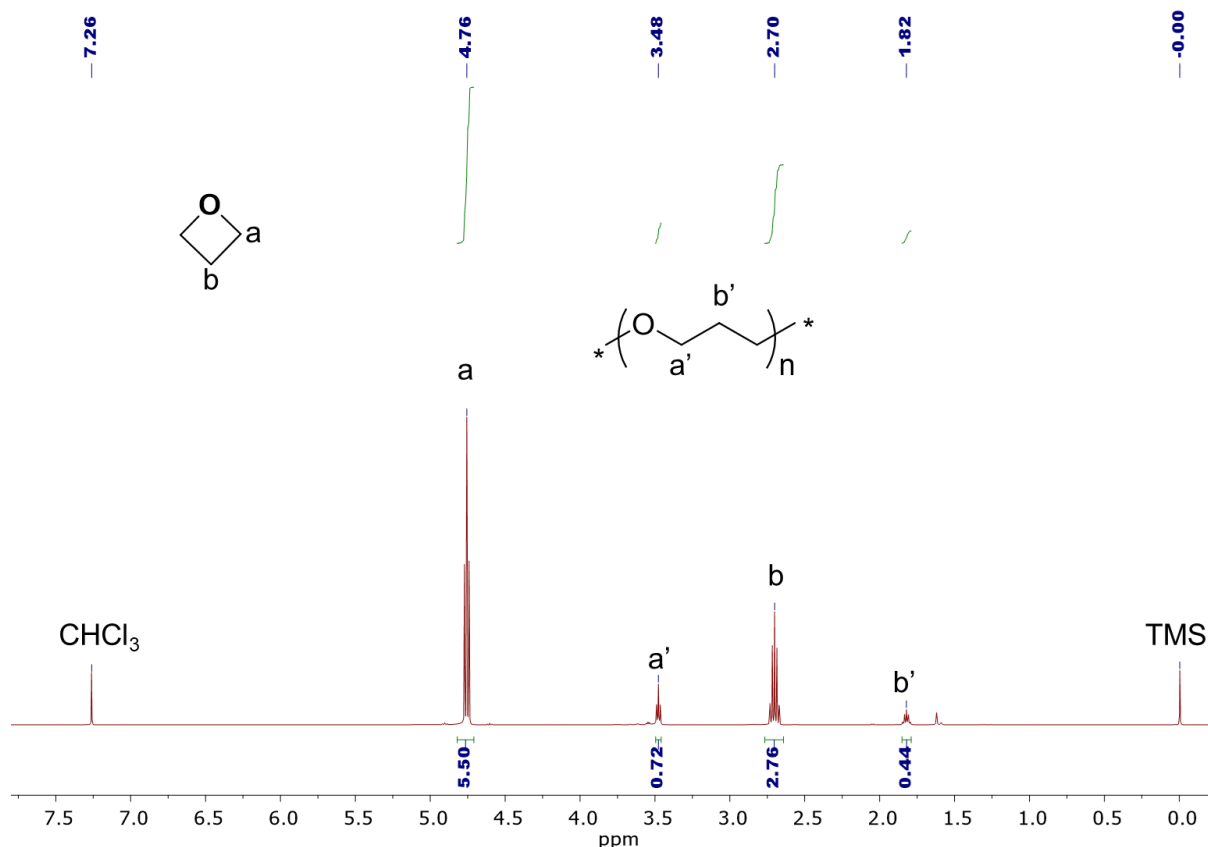


Figure 3.2. ¹H NMR spectrum (CDCl₃, 500 MHz) of the resultant mixture of oligomerization. Conditions: 7.88 mmol oxetane, [I₂]₀/[EP]₀ = 1/40, 0.1 MPa N₂, 105 °C, 8 minutes.

In order to limit the formation of ether linkages during the copolymerization, we sought to more efficiently activate the CO₂ towards incorporation into the resulting polymer. Guanidine-CO₂ complexes are known to be produced more easily as compared to amidine-CO₂ adducts, since the presence of adventitious water lead to the corresponding bicarbonate salt [BaseH]⁺[HCO₃]⁻⁵⁵ and no crystal structure of DBU-CO₂ adduct was reported in state-of-art. Hence bicyclic guanidines such as 7-methyl-1,5,7-triazabicyclo-[4.4.0]-dec-5-ene (MTBD) and 1,5,7-triazabicyclo[4.4.0]dec-5-ene (TBD) were chosen to examine their catalytic efficiencies for the copolymerization of CO₂ and oxetane as part of the binary catalyst system with I₂ (Table 1, entries 2 to 4).

Both guanidine bases were efficient for the copolymerization. After 24 h, MTBD allowed the production of a copolymer characterized by a *M_n* of 5,240 g·mol⁻¹ (*Đ_M* of 1.35) and a copolymer

composition similar to the one obtained by DBU. Attempts to further increase the molar mass of the polymer by prolonging the reaction time (from 24 to 44 h) led to a slightly broader dispersity ($\mathcal{D}_M \sim 1.45$) and enhancement of molar mass ($M_n = 6,000 \text{ g}\cdot\text{mol}^{-1}$), which is comparable with the highest M_n reported ($M_n = 7,100 \text{ g}\cdot\text{mol}^{-1}$) so far by using CO_2 .³⁹ Interestingly, calculated turn over frequencies (TOF) associated to that catalytic system (Table 3.2, entries 2 & 3) are double (TOF $\sim 0.7 - 0.8 \text{ h}^{-1}$, 1 MPa, 105 °C) that calculated from the 1,3-bis(2-hydroxyhexafluoroisopropyl)benzene /tetrabutylammonium iodide catalytic system reported previously (TOF = 0.35 h^{-1} , 2 MPa, 130°C) under comparable experimental conditions (Table 3.2, entry 10)⁴⁵ demonstrating the highly efficient nature of such I_2 -based catalytic systems.

Replacing MTBD by the more basic TBD resulted in a significant enhancement of the overall conversion after 24 h yielding a polymer with a comparable molar mass and dispersity ($M_n = 4,630 \text{ g}\cdot\text{mol}^{-1}$, $\mathcal{D}_M = 1.32$) but characterized by a further increase in TOF to 1.61 h^{-1} (Table 3.2, entry 4). Most notably however, the application of TBD as the basic cocatalyst, limited the ether linkages in the polymer to *ca.* 10 mol% thus resulting in a carbonate content of *ca.* 90 mol% (Table 3.1, entry 4). Note here that polymerization reactions were also performed from pristine I_2 and TBD for comparison (Table 3.5, entries 5-6), the inferior catalytic activity was observed on such reactions. Reasoning that the inherent basicity of the basic cocatalyst could explain the overall activity and selectivity of the process, we also applied 1-*tert*-butyl-4,4,4-tris(dimethylamino)-2,2-bis[tris(dimethyl amino)-phosphoranylideneamino]- $2\lambda^5,4\lambda^5$ -catenadi(phosphazene) (P_4 -*tert*-Bu) as a cocatalyst for this process (Table 3.1, entries 5 & 6). Unexpectedly, under the same experimental conditions, copolymerization failed, limiting the reaction to the *in-situ* production of TMC monomer in low yield ($\sim 15\%$). Interestingly, extending the reaction from 1 to 5 days allowed conversion of 30% of oxetane to TMC with no trace of polymerization (Table 3.3, entries 1 to 3). After 7 days (Table 3.1, entry 6 and Table 3.3, entry 4), traces of oligomers were detectable while maintaining a high selectivity in the production of TMC monomer.

Table 3.2. Copolymerization of oxetane and CO₂ with various catalysts. ^[a]

| Entry | Catalyst | Pressure (MPa) | Oxetane Conv. (%) ^[b] | Selectivity (%) ^[b] | | | TON _[g] | TOF (h ⁻¹) _[g] | <i>M_n</i> (SEC) ^[d] g·mol ⁻¹ | <i>Đ_M</i> ^[d] |
|-------------------------|----------------------------------|-------------------|-------------------------------------|--------------------------------|-----------------------|-------------------|--------------------|--|---|-------------------------------------|
| | | | | TMC | Carbonate Linkages | Ether Linkages | | | | |
| 1 | DBU | 1 | 82 | 8 | 72 | 20 | 32.8 | 1.37 | 1,360 | 1.71 |
| 2 | MTBD | 1 | 46 | 11 | 71 | 18 | 18.4 | 0.77 | 5,240 | 1.35 |
| 3^[e] | MTBD | 1 | 80 | 9 | 73 | 18 | 29.2 | 0.73 | 6,000 | 1.45 |
| 4 | TBD | 1 | 88 | <1 | 88 | 12 | 38.75 | 1.61 | 4,630 | 1.32 |
| 5 | P ₄ - <i>tert</i> -Bu | 1 | 15 | >99 | 0 | 0 | 6 | 0.25 | NA | NA |
| 6^[f] | P ₄ - <i>tert</i> -Bu | 1 | 83 | 71 | 19 | 10 | 33.2 | 0.20 | 320 | 1.42 |
| 7^[d] | 1.3-bis-HFAB | 10 | 39 | 2 | 98 | <1 | 13 | 0.54 | 1,000 | 1.15 |
| 8^[d] | 1.3-bis-HFAB | 10 | 92 | 2 | 98 | <1 | 30.6 | 1.27 | 2,000 | 1.30 |
| 9^[d] | 1.3-bis-HFAB | 5 | 72 | 5 | 95 | <1 | 23.9 | 0.99 | 1,500 | 1.33 |
| 10^[d] | 1.3-bis-HFAB | 2 | 25 | 4 | 96 | <1 | 8.32 | 0.35 | <1,000 | N.A |

[a] Copolymerization conditions: 7.88 mmol oxetane, 2.5 mol% I₂ and base cocatalyst, 1 MPa CO₂, 105 °C, t = 24 h. ^[b] Oxetane conversion and selectivity were determined from ¹H NMR spectroscopy of crude mixture; ^[c] Determined by SEC in tetrahydrofuran (THF) with polystyrene standard. ^[d] The results are based on the literature.⁴⁵ [e] t = 44 h. [f] = 168 h. [g] TON = [oxetane conv.]/[I₂]₀; TOF = TON/t.

Such lack of copolymerization activity and the unique selectivity towards TMC are probably the result of a strong complexation between the P₄-*tert*-Bu and the I₂ which suggests that the selective production of polycarbonates using such binary systems requires a balance of basicity to both enable polymer formation and reduce ether linkage formation.

Table 3.3. Coupling of CO₂ and oxetane using I₂/P₄-*tert*-Bu with various reaction time ^[a].

| Entry | Reaction time / days | Conv. % ^[b] | Selectivity % | | |
|-------|----------------------|------------------------|---------------|--------------------|----------------|
| | | | TMC | Carbonate Linkages | Ether Linkages |
| 1 | 1 | 15 | >99 | 0 | 0 |
| 2 | 3 | 20 | >99 | 0 | 0 |
| 3 | 5 | 30 | >99 | 0 | 0 |
| 4 | 7 | 83 | 71 | 19 | 10 |

[a] Coupling conditions: 7.88 mmol of oxetane, [M]₀/[I₂]₀/[P₄-*tert*-Bu] = 40/1/1, 3 MPa of CO₂, at 105 °C. [b]

Conversion and selectivity were determined from ¹H NMR spectroscopy of the product mixture.

3.2.2 Reaction conditions modification

Since the CO₂-based copolymers generated from the I₂/TBD catalytic system are produced with both high yield and selectivity for carbonate linkages, we selected to study this system with the aim of further enhancing molar mass control and carbonate selectivity. Studies of the influence of CO₂ pressure were conducted retaining equimolar ratios of I₂ and TBD in bulk oxetane at 105 °C (Table 3.4).

Table 3.4. Copolymerization of oxetane and CO₂ catalyzed by different loadings of I₂/TBD and CO₂ pressure at 105 °C. ^[a]

| Entry | catalysts loading / mol% | Time (day) | CO ₂ Pressure (MPa) | Con. ^[b] % | Selec. ^[b] % | M _n SEC ^[c] g·mol ⁻¹ | Đ _M SEC ^[c] |
|-------|--------------------------|------------|--------------------------------|-----------------------|-------------------------|---|-----------------------------------|
| 1 | 1.25 | 1 | 1.5 | 53 | 84 | 5,070 | 1.54 |
| 2 | 1.25 | 3 | 1.5 | 76 | 83 | 5,340 | 1.53 |
| 3 | 1.25 | 3 | 3 | 86 | 90 | 4,000 | 1.38 |
| 4 | 1 | 3 | 3 | 78 | 92 | 6,500 | 1.55 |
| 5 | 1 | 7 | 3 | 97 | 95 | 4,000 | 1.60 |

[a] Copolymerization conditions: 7.88 mmol of oxetane, 105 °C, [I₂]₀/[TBD]₀ = 1; [b] Conversion and selectivity of carbonate linkage were determined from ¹H NMR spectroscopy of product mixture; [c] Determined by SEC in tetrahydrofuran (THF) with polystyrene standard.

By performing reactions under a reduced catalyst loading of 1.25 mol% for 1 and 3 days with 1.5 MPa pressure of CO₂, 83 mol% of carbonate linkages were obtained (Table 3.4, entries 1 & 2). As may be expected, a further increase in both carbonate content (90 mol%) and overall conversion (86%) were observed when the CO₂ pressure was increased to 3 MPa (Table 3.4, entry 3). Notably, by further reducing catalyst loading to 1 mol%, 95% carbonate linkages resulted after 3 and 7 days (Table 3.4, entries 4 - 5). Notably, the M_n values of the resulting materials were slightly lower at higher oxetane conversions, *i.e.* for a higher pressure in CO₂.

3.3.3 MALDI-ToF spectrum analysis

To obtain more information on the polymer structure, MALDI-ToF mass spectrometry analyses of the resultant polymers were realized (Figure 3.3a). As a representative example the polymer produced with the highest carbonate linkages (Table 3.4, entry 3) displays a main population that corresponds to an almost perfectly alternating structure of carbon dioxide and oxetane, with signals spaced by $m/z = 102$ (Figure 3.3b, red-dotted distribution) corresponding to a sodium-charged α,ω -dihydroxyl PTMC presenting one more oxetane than CO₂ ($n = 1$, with n representing the number of pristine oxetane in the copolymer). It is worth to note that the Figure 3.3b reports both values of " n " and " m ". While " n " refers to the number of pristine oxetanes in the copolymer, " m " corresponds to the total polymerization degree (DP) of the copolymer [with $m = m'$ (number of carbonate repeating units) + n (number of ether repeating units)]. Additionally, other distributions are clearly visible which can be assigned to the same polymer unit but with 2, 3 and 4 molecules of CO₂ 'missing' from the polymer chain (Figure 3.3b, $n = 2$, $n = 3$ and $n = 4$). Notably, the absence of a population that has an equal number of oxetane and CO₂ units may indicate that oxetane is involved in the initiation step of the polymerization.

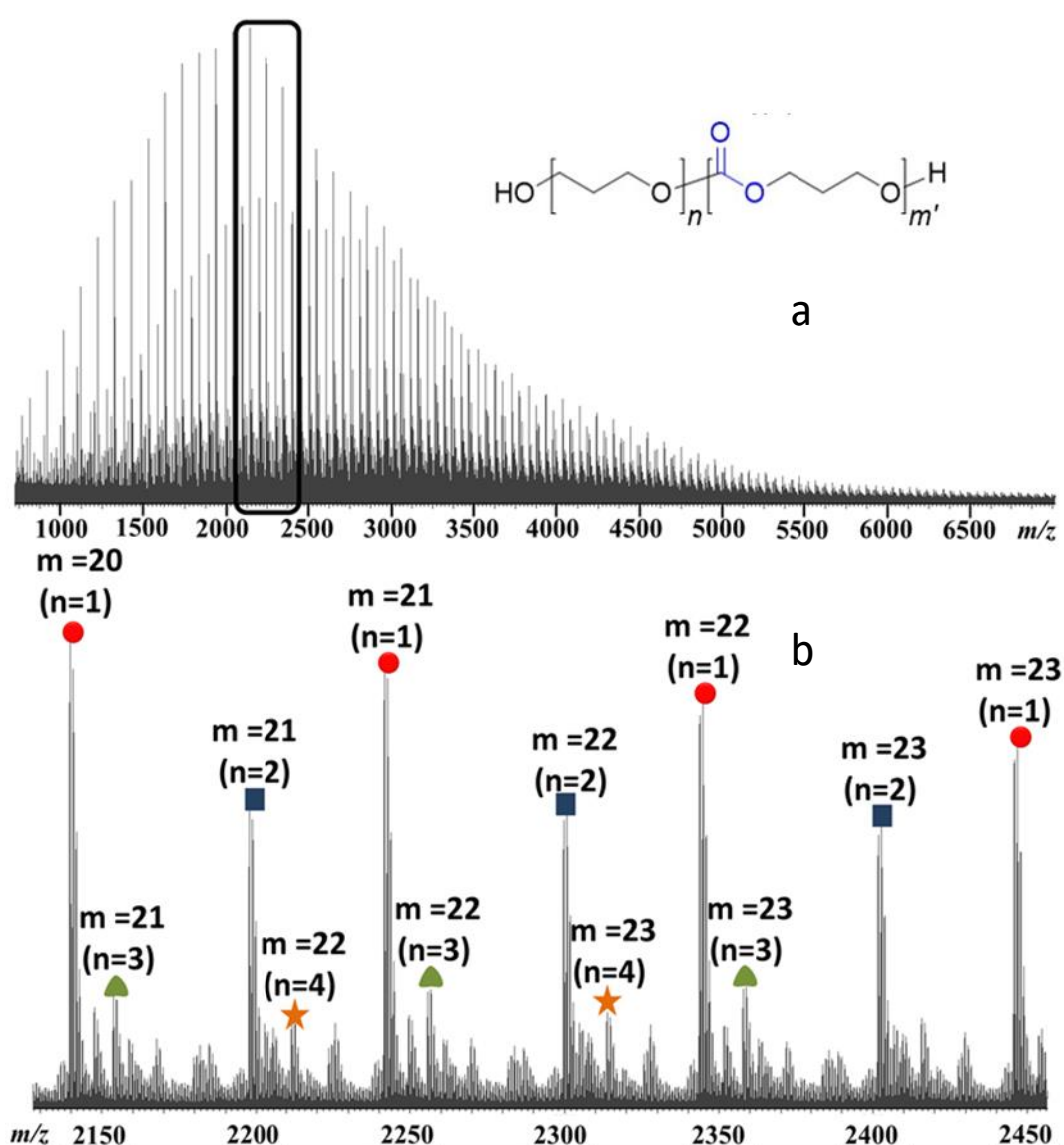


Figure 3.3. MALDI mass spectrum recorded for sample 3 (Table 3.4), global mass spectrum (a) and magnification between $m/z = 2130$ and $m/z = 2450$ (b). “ m ” represents the total polymerization degree and “ n ” the number of missing CO_2 molecule per structure (TMC unit).

3.3.4 Attempts of increase molar mass

Attempts to increase the molar mass of the resulting PTMC by modifying the initial I_2/TBD content or the relative ratio of I_2 -to-TBD did not lead to any significant change (Table 3.5). These observations reflect those from Darensbourg *et al.* in which the molar mass of the formed PTMC using a $(\text{salen})\text{CrCl}_2$ catalytic complex was limited to a few thousand as a consequence of the occurrence of rapid and reversible chain transfer reactions taking place with residual water.³⁹

Table 3.5. Optimization of coupling of CO₂ and oxetane using I₂/TBD under different catalysts ratio ^[a].

| Entry | TBD loading mol% | Catalyst ratio/ I ₂ :TBD | Selec. % | | | Con. % ^[b] | <i>M_n</i> ^[c] g·mol ⁻¹ | <i>D_M</i> ^[c] |
|-------------------------|------------------|--|----------|--------------------|----------------|-----------------------|--|-------------------------------------|
| | | | TMC | Carbonate Linkages | Ether Linkages | | | |
| 1 | 1.25 | 2:1 | 2 | 71 | 27 | 77 | 4,150 | 1.42 |
| 2 | 2.5 | 1:2 | <1 | 85 | 15 | 31 | 5,000 | 1.34 |
| 3 ^[d] | 2.5 | 1:2 | 2 | 94 | 4 | 51 | 4,280 | 1.47 |
| 4 | 5 | 1:1 | <1 | 57 | 43 | 97 | 4,970 | 1.32 |
| 5 | 2.5 | 0:1 | 0 | 0 | 0 | 0 | 0 | 0 |
| 6 ^[e] | 0 | 1:0 | 3 | 27 | 70 | 44 | 1,600 | 1.53 |

[a] Copolymerization conditions: 7.88 mmol of oxetane, 1 MPa of CO₂, at 105 °C for 24 h. [b] Conversion and selectivity were determined from ¹H NMR spectroscopy of product mixture. [c] Determined by size-exclusion chromatography (SEC) in tetrahydrofuran (THF) with polystyrene standard. [d] CO₂ pressure is 3 MPa for 3 days. [e] The yield of oligomer is extremely low (3%).

Reasoning that protic impurities could reasonably affect the polymerization with the present binary catalysts system during both propagation and initiating steps, polymerization was realized in the presence of benzyl alcohol (BnOH) and 1,4-butanediol (BuOH) as potential exogenous initiators. Reactions were performed at 105 °C for 24 h and for an initial oxetane-to-catalyst-to-initiator molar ratio of 100/2.5/1 (Table 3.6, entries 1-3). While a slight depression of molar mass of the resultant PTMC was indicated by SEC analysis (down to 3,100 g·mol⁻¹), no trace of incorporated alcohol was observed in the ¹H NMR spectra of the precipitated copolymers (Figure 3.4) where the expected chemical shift of benzyl group was not observed (7.40 to 7.19 ppm), suggesting that exogenous alcohols are only acting as protic sources. To further test this hypothesis, adding 1.25 mol% of exogenous water led to the isolation of oligomers with significantly lower molar mass (1,000 g·mol⁻¹, *D_M* = 1.79, Table 3.6, entry 4) which suggests that initiation of the polymerization does not involve a nucleophilic source and that exogenous alcohols as well as residual water (mainly present in the CO₂ gas) only limits the PTMC molar masses by proton transfer. Inefficiency of the nucleophilic alcohols to

end-cap PTMC chains may find origin in their deactivation when they are in presence of both CO₂ and superbase catalysts.⁵⁶

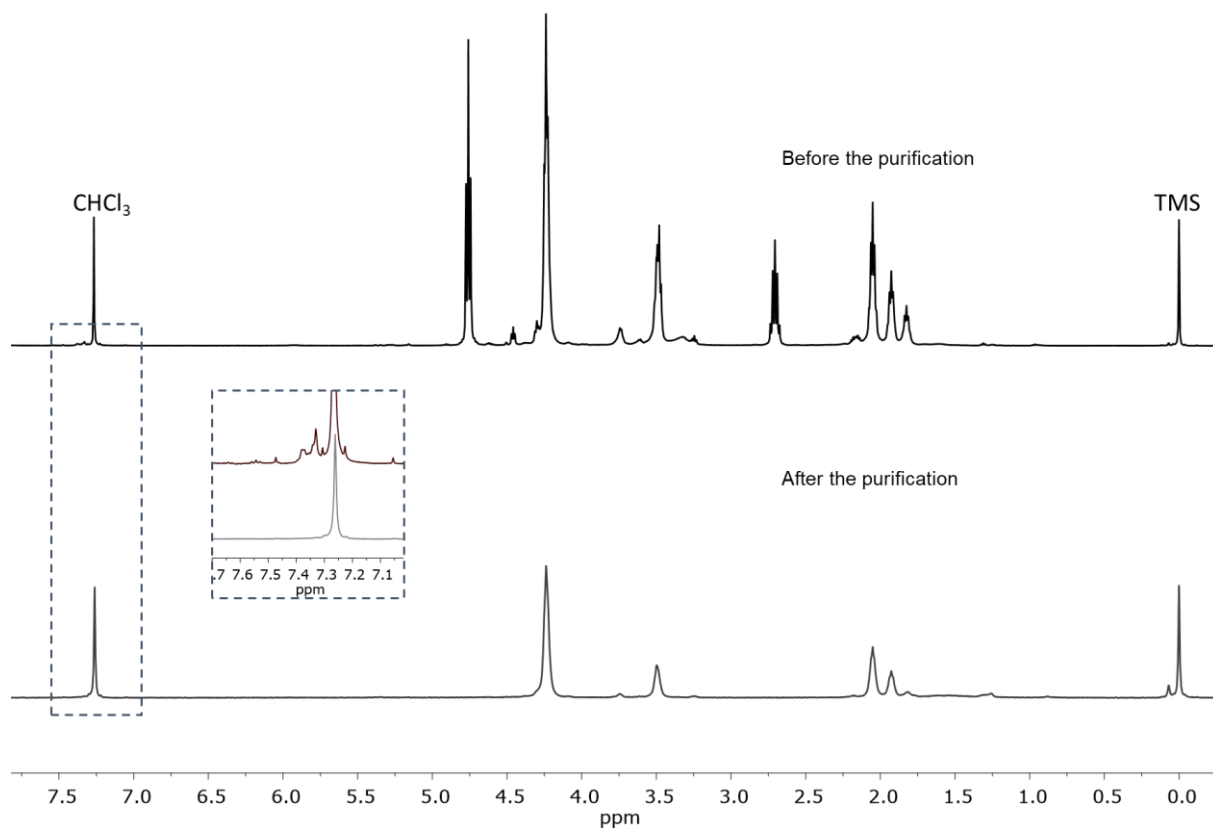


Figure 3.4. ¹H NMR spectrum (CDCl₃, 500 MHz) of copolymer before and after the precipitation from methanol (Table 3.5, entry 1). Conditions: 7.88 mmol of oxetane, [M]/[I₂]₀/[TBD]₀/[BnOH]₀ = 100/2.5/2.5/1, 1 MPa of CO₂, at 105 °C for 24 h.

Table 3.6. Copolymerization of CO₂ and oxetane using I₂/TBD with initiators ^[a].

| Entry | Initiator | Conv. % ^[b] | Selec. % | | | M_n^{SEC} ^[c] g·mol ⁻¹ | D_M^{SEC} ^[c] |
|------------------|------------------|------------------------|----------|--------------------|----------------|---|----------------------------|
| | | | TMC | Carbonate linkages | Ether linkages | | |
| 1 | BnOH | 72 | <1 | 78 | 22 | 3,100 | 1.56 |
| 2 | BuOH | 55 | 3 | 82 | 15 | 4,250 | 1.33 |
| 3 ^[d] | BnOH | 94 | 2 | 80 | 18 | 3,830 | 1.70 |
| 4 ^[e] | H ₂ O | 65 | 7 | 49 | 44 | 1,000 | 1.79 |

[a] Copolymerization conditions: 7.88 mmol of oxetane, [M]/[I₂]₀/[TBD]₀/[Initiator]₀ = 100/2.5/2.5/1, 1 MPa of CO₂, at 105 °C for 24 h. [b] Conversion and selectivity were determined from ¹H NMR spectroscopy of product mixture. [c] Determined by size-exclusion chromatography (SEC) in tetrahydrofuran (THF) with polystyrene standard. [d] 1 equivalent P₄-*tert*-Bu is used to deprotonate BnOH in first to obtain alkoxide ion. [e] [M]/[I₂]₀/[TBD]₀/[H₂O]₀ = 100/2.5/2.5/1.25.

3.3.5 Mechanism investigation

These observations, added to that of the formation of TMC in the process, led us to further investigate the mechanism by which the copolymerisation was occurring, with the aim to elucidate if the copolymers were mainly produced by ring-opening polymerization (ROP) of the TMC produced *in situ* or by a direct copolymerization by “chain up” process involving both oxetane and CO₂. To this end, the copolymerization was followed by ¹H NMR spectroscopy and selectivities in the production of TMC and carbonate/ether linkages and conversion were schematically reported in the Figure 3.5 and Figure 3.6, respectively.

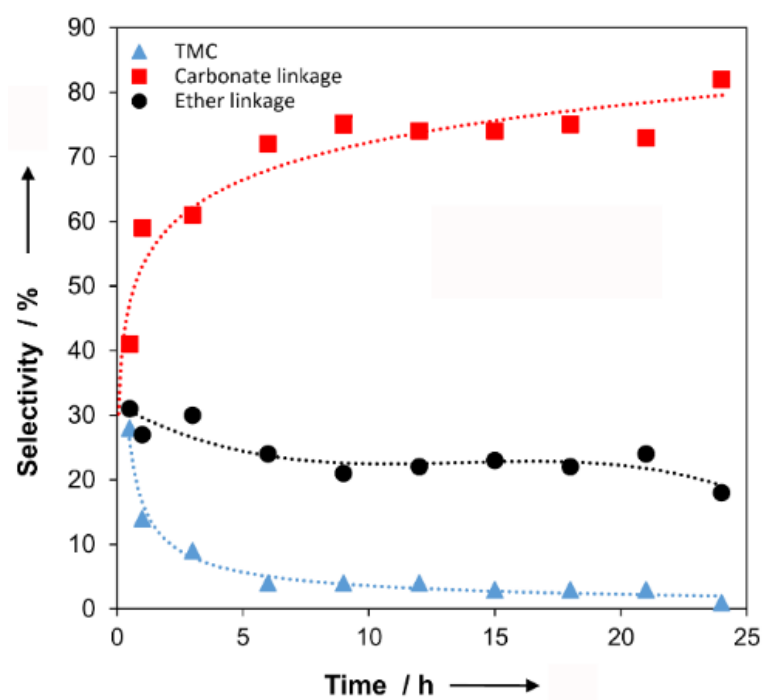


Figure 3.5. Chart of selectivity of product against time. Conditions of reaction: Copolymerization conditions: 197 μmol of I_2 (2.5 mol%), 7.88 mmol of oxetane, $[\text{M}]/[\text{I}_2]_0/[\text{TBD}]_0 = 40/1/1$, 1 MPa of CO_2 , at 105 °C.

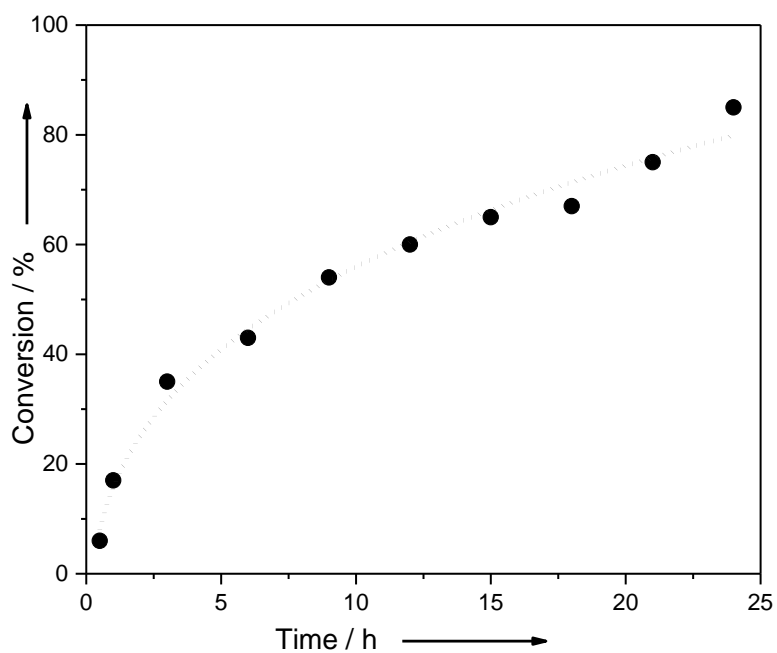
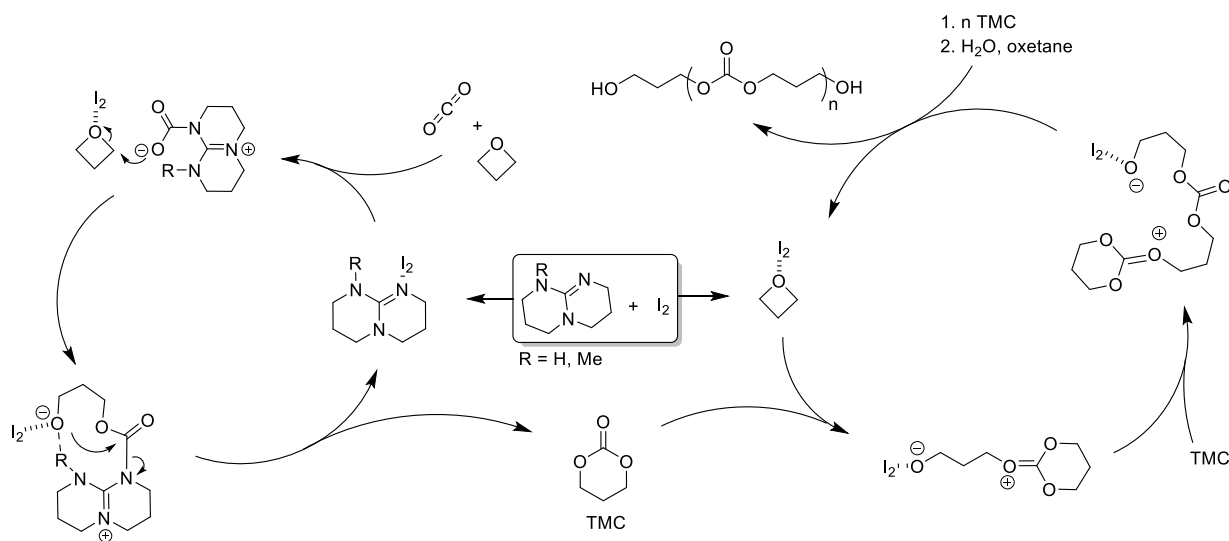


Figure 3.6. Chart of conversion of oxetane against time. Conditions of reaction: Copolymerization conditions: 197 μmol of I_2 (2.5 mol%), 7.88 mmol of oxetane, $[\text{M}]/[\text{I}_2]_0/[\text{TBD}]_0 = 40/1/1$, 1 MPa of CO_2 , at 105 °C.

After 30 minutes of reaction, both TMC monomer and copolymer coexist, before the relative quantity of TMC drops and copolymer increases. These observations are in agreement with Darensbourg's observations,⁴⁰ alongside the high selectivity to TMC with the P₄-*tert*-Bu cocatalyst, and suggest that TMC is formed before being polymerized through a secondary catalytic cycle to yield PTMC (Scheme 3.4). Notably, the high quantity of TMC monomer initially produced is accompanied by the presence of oligomers composed by ~ 40 mol% of carbonate that increase throughout the polymerization and ~ 30 mol% ether linkages that decrease throughout the reaction. These observations prompt us to propose a two-step process mechanism in which oxetane is activated by halogen bonding by I₂ while a zwitterionic species is created by activation of CO₂ by the TBD. The electrophilic activation of the oxetane allows it to undergo a nucleophilic attack from the CO₂-adduct zwitterion thus leading to an alkoxide intermediate that is stabilized by hydrogen bonding from the TBD N-H hydrogen. Finally, TMC is produced from an intramolecular nucleophilic substitution on the carbonyl group. As the CO₂ is in an excess, it is anticipated that free TBD will not be available to initiate ROP of the resulting TMC and instead, an active chain end (ACE) mechanism,⁵⁷ initiated by the I₂-oxetane adduct operates to produce PTMC, consistent with our observation of I₂-initiated oxetane ROP. The observation that exogenous alcohols do not act as initiators in the polymerization supports this mechanism.



Scheme 3.4. First step of copolymerization from CO₂/oxetane: generation of TMC and oligoetherification of oxetane. Second step of copolymerization from CO₂/oxetane: generation of copolymer by an “ACE” mechanism.

To support the postulated ACE ROP initiated from the I₂-oxetane adduct, the ROP of commercially available TMC monomer was undertaken in presence of a freshly prepared 1:1 I₂/oxetane adduct (Table 3.7, entry 1), under 1 MPa of nitrogen atmosphere at 105 °C and from an initial [TMC]₀/[I₂-oxetane adduct]₀ of 40.

Table 3.7. Polymerization of TMC initiated by the adduct of I₂/oxetane. ^[a]

| Entry | Conv. ^[b] % | | Selec. % ^[b] | | | M_n sec ^[c] g·mol ⁻¹ | \bar{D}_M sec ^[c] |
|----------|------------------------|----|-------------------------|--------------------|----------------|---|--------------------------------|
| | TMC | EP | TMC | Carbonate linkages | Ether linkages | | |
| 1 | >99 | 50 | <1 | 94 | 6 | 5,870 | 1.67 |
| 2 | >99 | 70 | <1 | 98 | 2 | 10,000 | 1.84 |

[a] Copolymerization conditions: 197 μmol of I₂/oxetane adduct (2.5mol%), [M]/[C] = 40/1, 1 MPa of N₂, at 105°C for 24 h. [b] Conversion and selectivity were determined from ¹HNMR spectroscopy of product mixture. [c] Determined by size-exclusion chromatography (SEC) in tetrahydrofuran (THF) with polystyrene standard.

Interestingly, after 24 h, quantitative conversion of the TMC monomer yielded a PTMC with M_n = 6,000 g·mol⁻¹, comparable to that observed from the CO₂-based polymerization procedure.

Interestingly a few percent of ether linkages were also observed in the polymer by ¹H NMR spectroscopic analysis which could indicate exchange to form an I₂-TMC adduct or partial decarboxylation of the TMC monomer under these conditions (Figure 3.7). Notably, only 50 mol% of the initially used adduct were consumed during the polymerization. Increasing the ratio of [TMC]₀/[I₂-oxetane adduct]₀ to 80 resulted in a PTMC with *M_n* = 10,000 g·mol⁻¹ suggesting the initiation capability of I₂/oxetane adduct in absence of water (Table 3.7, entry 2). Importantly, this polymerization proceeds efficiently in the absence of the TBD and hence demonstrates that the base is probably used during the first part of the process only, reinforcing then our hypothetical two-step mechanism.

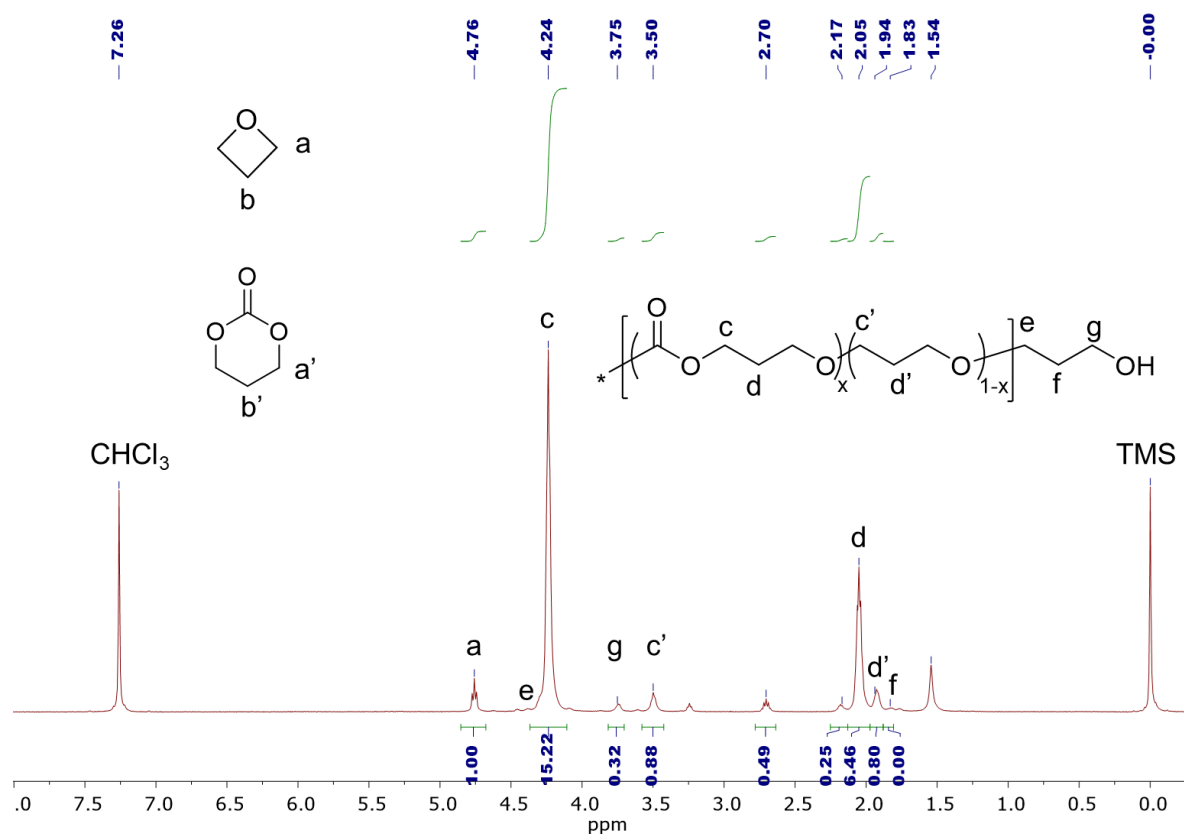


Figure 3.7. ¹H NMR spectrum (CDCl₃, 500 MHz) of the resultant mixture of polymerization (Table 3.6, entry 1). Copolymerization conditions: 197 μmol of I₂/oxetane adduct (2.5mol%), [TMC]₀/[Initiator] = 40/1, 1 MPa of N₂, at 105°C for 24 h.

3.3 Conclusions

The synthesis of poly (trimethylene carbonate) is reported through a green route using CO₂ and oxetane catalyzed by I₂ and guanidine with 1: 1 ratio under 105 °C, 3 MPa CO₂. The study reveals that the combination of iodine and the bicyclic guanidine, TBD, provides an efficient synthesis with high carbon dioxide incorporation (up to 95 mol%) in such mild conditions. Mechanistic studies revealed that polymerization most likely proceeds by formation of trimethylene carbonate monomer that is polymerized *in situ* via an activated chain end mechanism, initiated from an I₂/oxetane adduct. These advances afford a great opportunity to expand the scope of CO₂ utilization in polymer synthesis.

However, the *in situ* generated trimethylene carbonate cannot be maintained as the resultant under such conditions, which will limit the application of I₂-based catalyst system. To provide CO₂-based product in a controlled manner, developing a system that enable control the formation of product is necessary for our research. Inspired by the unique selectivity in TMC as catalyzed by I₂-phosphazene system, we were encouraged to investigate the synthesis of TMC from CO₂ and oxetane using other cocatalysts. In the next chapter, we focused on coupling CO₂ with oxetane to prepare TMC using I₂-based catalytic system that is promising to CO₂ valorization.

3.4 References

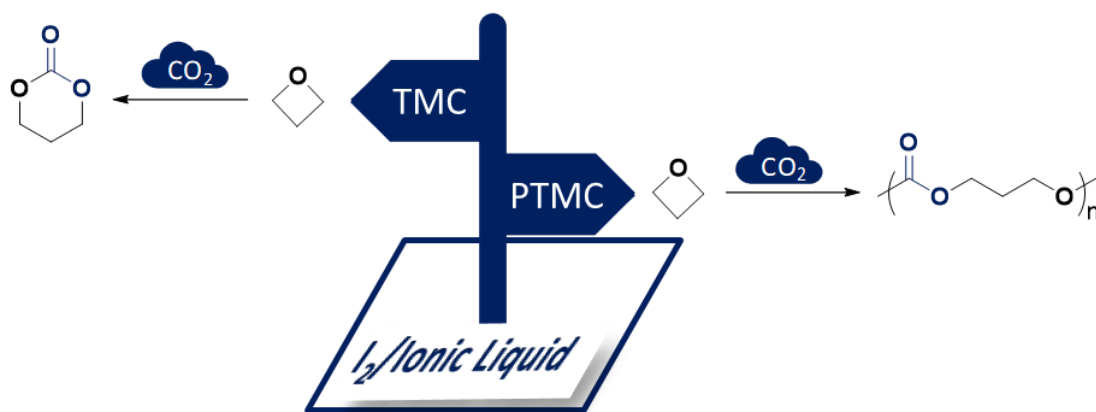
1. A.-H. L. Y.-N. L. L.-N. He, *Pure Appl. Chem.*, 2011, **84**, 581.
2. M. Honda, M. Tamura, K. Nakao, K. Suzuki, Y. Nakagawa and K. Tomishige, *ACS Catal.*, 2014, **4**, 1893-1896.
3. D. J. Darensbourg, A. Horn Jr and A. I. Moncada, *Green Chem.*, 2010, **12**, 1376-1379.
4. C. J. Whiteoak, N. Kielland, V. Laserna, E. C. Escudero-Adán, E. Martin and A. W. Kleij, *J. Am. Chem. Soc.*, 2013, **135**, 1228-1231.
5. G. L. Gregory, M. Ulmann and A. Buchard, *RSC Adv.*, 2015, **5**, 39404-39408.
6. G. Trott, P. K. Saini and C. K. Williams, *Philos. Trans. R. Soc. A Math. Phys. Eng. Sci. Sciences*, 2016, **374**.
7. B. Ghosh and M. W. Urban, *Science*, 2009, **323**, 1458-1460.
8. P. Kurt, L. J. Gamble and K. J. Wynne, *Langmuir*, 2008, **24**, 5816-5824.
9. P. Kurt and K. J. Wynne, *Macromolecules*, 2007, **40**, 9537-9543.
10. U. Makal, T. Fujiwara, R. S. Cooke and K. J. Wynne, *Langmuir*, 2005, **21**, 10749-10755.
11. S. S. Nair, E. J. McCullough, V. K. Yadavalli and K. J. Wynne, *Langmuir*, 2014, **30**, 12986-12995.
12. W. H. Carothers, G. L. Dorough and F. J. v. Natta, *J. Am. Chem. Soc.*, 1932, **54**, 761-772.
13. J. Matsuo, K. Aoki, F. Sanda and T. Endo, *Macromolecules*, 1998, **31**, 4432-4438.
14. H. Keul, R. Bächer and H. Höcker, *Makromol Chem J.*, 1986, **187**, 2579-2589.
15. S. Sarel and L. A. Pohoryles, *J. Am. Chem. Soc.*, 1958, **80**, 4596-4599.
16. T. Ariga, T. Takata and T. Endo, *Macromolecules*, 1997, **30**, 737-744.
17. H. R. Kricheldorf and J. Jenssen, *J. Macromol. Sci. A*, 1989, **26**, 631-644.
18. H. R. Kricheldorf, R. Dunsing and A. S. i. Albet, *Makromol. Chem. Macromol. Chem. Phys.*, 1987, **188**, 2453-2466.
19. A.-C. Albertson and M. Sjoling, *J. Macromol. Sci. A*, 1992, **29**, 43-54.

20. H. R. Kricheldorf, J. Jenssen and I. Kreiser-Saunders, *Makromol. Chem. Macromol. Chem. Phys.*, 1991, **192**, 2391-2399.
21. K. R. Carter, R. Richter, H. R. Kricheldorf and J. L. Hedrick, *Macromolecules*, 1997, **30**, 6074-6076.
22. P. Dobrzynski and J. Kasperczyk, *J. Polym. Sci. A - Polym. Chem.*, 2006, **44**, 3184-3201.
23. M. Helou, O. Miserque, J.-M. Brusson, J.-F. Carpentier and S. M. Guillaume, *Chemcatchem*, 2010, **2**, 306-313.
24. H. R. Kricheldorf and A. Stricker, *Macromol. Chem. Phys.*, 1999, **200**, 1726-1733.
25. T. F. Al-Azemi and K. S. Bisht, *Polymer*, 2002, **43**, 2161-2167.
26. W. H. Carothers and F. J. V. Natta, *J. Am. Chem. Soc.*, 1930, **52**, 314-326.
27. T. F. Al-Azemi, H. H. Dib, N. A. Al-Awadi and O. M. E. El-Dusouqui, *Tetrahedron*, 2008, **64**, 4126-4134.
28. M. R. Reithofer, Y. N. Sum and Y. Zhang, *Green Chem.*, 2013, **15**, 2086-2090.
29. S.-H. Pyo and R. Hatti-Kaul, *Adv. Synth. Catal.*, 2012, **354**, 797-802.
30. X. J. Li Siqi, *Prog. Chem.*, 2016, **28**, 1798-1810.
31. S. Tempelaar, L. Mespouille, O. Coulembier, P. Dubois and A. P. Dove, *Chem. Soc. Rev.*, 2013, **42**, 1312-1336.
32. L. Mespouille, O. Coulembier, M. Kawalec, A. P. Dove and P. Dubois, *Prog. Polym. Sci.*, 2014, **39**, 1144-1164.
33. H. K. Eigenmann, D. M. Golden and S. W. Benson, *J. Phys. Chem.*, 1973, **77**, 1687-1691.
34. S. S. Birgitta Ringner, Haruhiko Wantanabe, *Acta Chem. Scand*, 1971, **25**, 141-146.
35. S. Aoshima, T. Fujisawa and E. Kobayashi, *J. Polym. Sci. Part A Polym. Chem.*, 1994, **32**, 1719-1728.
36. J. A. Burkhard, G. Wuitschik, M. Rogers-Evans, K. Müller and E. M. Carreira, *Angew. Chemie Int. Ed.*, 2010, **49**, 9052-9067.

37. A. Baba, H. Kashiwagi and H. Matsuda, *Organometallics*, 1987, **6**, 137-140.
38. A. Baba, H. Meishou and H. Matsuda, *Die Makromol. Chemie, Rapid Commun.*, 1984, **5**, 665-668.
39. D. J. Darensbourg and A. I. Moncada, *Macromolecules*, 2010, **43**, 5996-6003.
40. D. J. Darensbourg, A. I. Moncada, W. Choi and J. H. Reibenspies, *J. Am. Chem. Soc.*, 2008, **130**, 6523-6533.
41. D. J. Darensbourg and A. I. Moncada, *Inorg. Chem.*, 2008, **47**, 10000-10008.
42. D. J. Darensbourg, P. Ganguly and W. Choi, *Inorg. Chem.*, 2006, **45**, 3831-3833.
43. D. J. Darensbourg and A. I. Moncada, *Macromolecules*, 2009, **42**, 4063-4070.
44. T. Satoh, in *Encyclopedia of Polymeric Nanomaterials*, eds. S. Kobayashi and K. Müllen, Springer Berlin Heidelberg, Berlin, Heidelberg, 2014, DOI: 10.1007/978-3-642-36199-9_194-1, pp. 1-14.
45. M. Alves, B. Grignard, A. Boyaval, R. Méreau, J. De Winter, P. Gerbaux, C. Detrembleur, T. Tassaing and C. Jérôme, *ChemSusChem*, 2017, **10**, 1128-1138.
46. O. Coulembier, S. Moins, V. Lemaury, R. Lazzaroni and P. Dubois, *J. CO₂ Util.*, 2015, **10**, 7-11.
47. D. J. Heldebrant, P. G. Jessop, C. A. Thomas, C. A. Eckert and C. L. Liotta, *J. Org. Chem.*, 2005, **70**, 5335-5338.
48. M. I. Konaklieva, M. L. Dahl and E. Turos, *Tetrahedron Lett.*, 1992, **33**, 7093-7096.
49. T. Clark, M. Hennemann, J. S. Murray and P. Politzer, *J. Mol. Model.*, 2007, **13**, 291-296.
50. M. H. Kolář and P. Hobza, *Chem. Rev.*, 2016, **116**, 5155-5187.
51. T. Kaiho, in *Iodine Chemistry and Applications*, 2014, DOI: doi:10.1002/9781118909911.ch23, pp. 433-437.
52. M. Sawamoto, in *Iodine Chemistry and Applications*, ed. T. Kaiho, 2014, DOI: doi:10.1002/9781118909911.ch27, ch. 27, pp. 489-500.
53. S. Searles, M. Tamres and E. R. Lippincott, *J. Am. Chem. Soc.*, 1953, **75**, 2775-2777.

54. F. Cataldo, *Eur. Polym. J.*, 1996, **32**, 1297-1302.
55. C. Villiers, J.-P. Dognon, R. Pollet, P. Thuéry and M. Ephritikhine, *Angew. Chemie Int. Ed.* , 2010, **49**, 3465-3468.
56. C. Das Neves Gomes, O. Jacquet, C. Villiers, P. Thuéry, M. Ephritikhine and T. Cantat, *Angew. Chemie Int. Ed.* , 2012, **51**, 187-190.
57. D. Delcroix, B. Martín-Vaca, D. Bourissou and C. Navarro, *Macromolecules*, 2010, **43**, 8828-8835.

From selective formation of trimethylene carbonate to its “on-demand” polymerization: Impact of the iodine/ionic liquid cooperative catalytic system



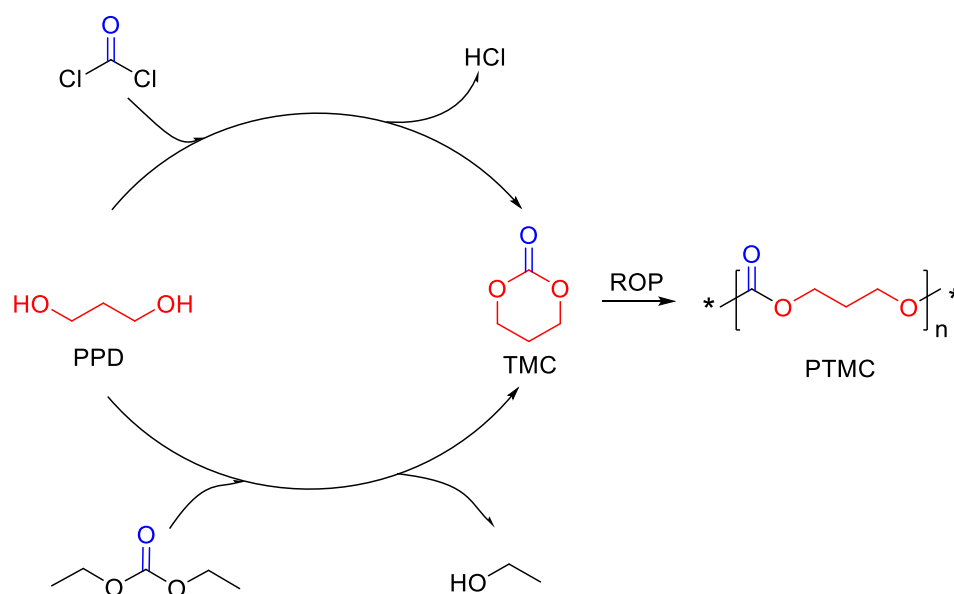
Keywords: Organocatalysts, carbon dioxide, trimethylene carbonate, ionic liquid.

As detailed in the Chapter III, the combination of iodine and TBD provides an efficient synthesis strategy with high carbon dioxide incorporation (up to 95 mol%) in mild conditions (105 °C, 3 MPa CO₂). Mechanistic studies revealed that the polymerization most likely proceeds by formation of the trimethylene carbonate (TMC) monomer and its subsequent polymerization *in situ* via an activated chain end mechanism. In our work, we also demonstrated that an equimolar combination of I₂ and *tert*-Bu-P₄ phosphazene as catalytic complex represents an innovative approach to carbon dioxide valorization by generating pure TMC monomer. Such result, alongside with reported works of TMC preparation using CO₂ and oxetane reagents,¹⁻⁴ provides a green alternative to the synthesis of TMC using I₂-based catalysts that can be used for the preparation of controlled polymers.

Herein, a novel procedure for the preparation of TMC from oxetane and CO₂ in a controllable pathway and as catalyzed by I₂-based binary system under mild conditions [with a high level of TMC selectivity (up to 93%)] is reported. Temperature-dependent studies revealed that both TMC monomer and its corresponding PTMC polymer can be produced “on-demand” by adequately adapting the experimental conditions.

4.1 Introduction

Environmental and economic concerns have intensively promoted research on CO₂ valorization to replace toxic and environmentally poisoning phosgene.^{5, 6} Conventionally, syntheses applied to the TMC production involve the use of 1,3-propanediol (PPD) with either phosgene or linear dialkylcarbonate (Scheme 4.1).⁷ To the best of our knowledge, only few studies have been treated to the development of green routes to valorize CO₂ and oxetane for the production of TMC, probably owing to their relatively low ring strain reactivity (E_r) compared to the 3-membered analogues, i.e. oxiranes (106 vs 112 kJ·mol⁻¹ for E_r oxetane vs E_r oxirane).^{8, 9}



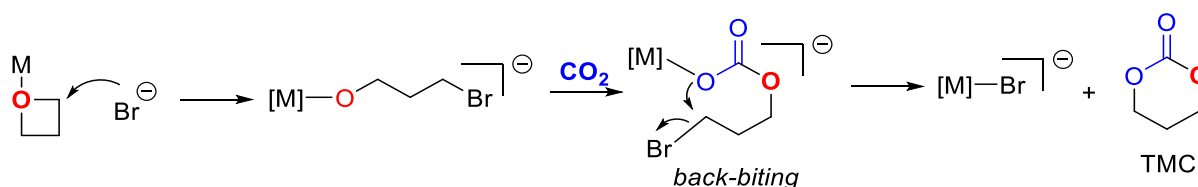
Scheme 4.1. Conventional methods used for the TMC preparation and its polymerization into PTMC.

After Baba pioneered the controllable coupling of CO_2 and oxetane using organotin halide,¹⁰ most of the work was focused on the preparation of TMC monomer by using metal-based chemical routes. As a few examples, Darensbourg developed oxovanadium derivatives⁴ to prepare TMC with 99 mol% in selectivity under a 3.5 MPa CO_2 , 60 °C for 8 h, while Kleij reported the use of aluminium-based³ catalysts to yield 95 mol% TMC after 18 h under a 1 MPa CO_2 , 70 °C. Very interestingly, Buckley and Wijayantha contributed to the coupling of CO_2 and oxetane to synthesize TMC *via* an electrochemical process under a 0.1 MPa CO_2 .¹

As TMC is an important polymer precursor to fabricate biomaterials, a metal-based catalytic preparation of TMC limits the applications of such useful monomer owing to the presence of cytotoxic metal traces in the final material. Moreover, environmental pollution, high costs, and the inherent oxygen and moisture sensitivity of metal-based catalysts are stimulating the development of organo-based catalysts pronouncedly with the benefits of green credentials and absence of metal-associated toxicity.

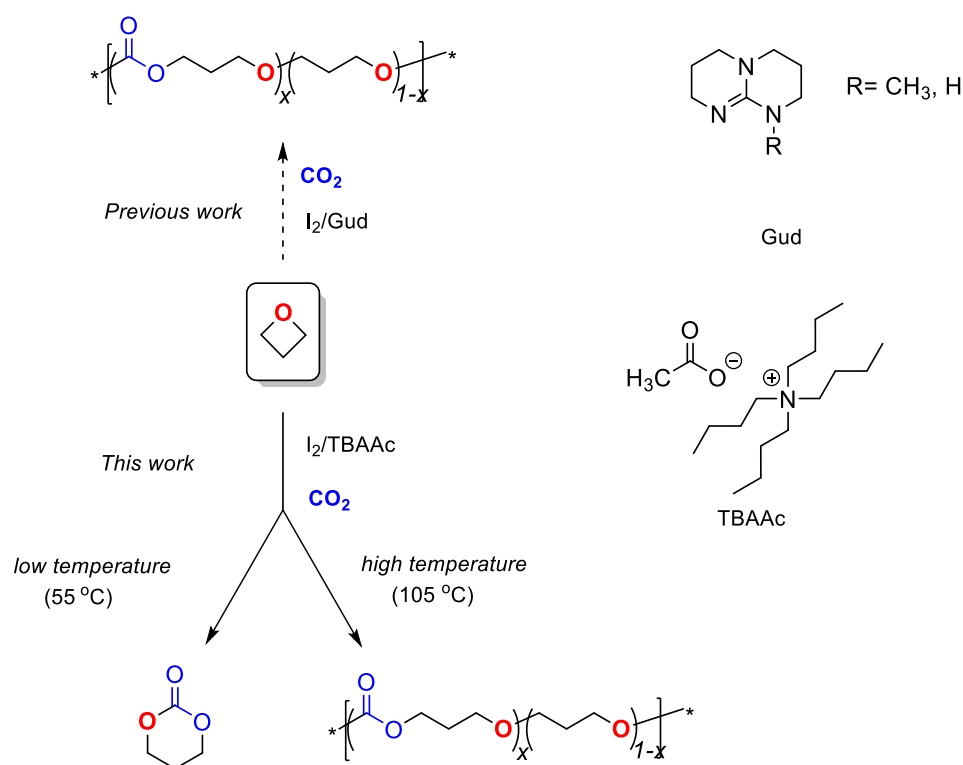
Our recent work on the cycloaddition of epoxide and CO_2 using an iodine-based binary catalytic

system, demonstrated that an equimolar mixture of I_2 and a superbase such as phosphazene would lead to the preparation of pure TMC (see Chapter III).¹¹ Although the yield associated to the production of TMC was relatively low (30 % after 5 days), this method reveals that the product formation from CO_2 depends on the nature of the co-catalyst. Inspired by the cycloaddition of CO_2 and epoxide in presence of ionic liquid (tetrabutylammonium chloride),¹² alongside with the Darensbourg's work⁴ described earlier (Scheme 4.2), it is promising to develop a I_2 -based binary catalytic system involving an ionic liquid as co-partner to promote the exclusive production of TMC. As acetate has been used for the opening of oxetane ring successfully in presence of Lewis acid to apply such anion to our research for the purpose of ring-opening oxetane under mild conditions.



Scheme 4.2. Preparation of TMC from CO_2 and oxetane using metal-based catalysis (Counter-cation omitted for clarity).

In this chapter, and as compared to the Chapter III, we will demonstrate that a temperature-dependent synthesis of both TMC and PTMC from a CO_2 and oxetane mixture is possible by the use of an iodine/tetrabutylammonium acetate (TBAAC) binary system (Scheme 4.3). Kinetics and calculated activation energy suggested that the formation of PTMC derives from *in situ* generated TMC.



Scheme 4.3. Schematic comparison between both Chapter III and Chapter IV results (Gud = guanidine, TBD when R = H, MTBD when R = methyl).

4.2 Results and discussion

Inspired by the Darensbourg's and Detrembleur's work on developing binary systems based on the use of a tetrabutylammonium salts (TAS) co-catalysts,^{4, 13} this work will present the results obtained from a CO_2 /oxetane reaction in presence of a mixture of iodine and various TAS. As an initiating point of investigation, tetrabutylammonium acetate (TBAAc) was selected as co-catalyst, under a CO_2 pressure of 1 MPa in bulk. The reaction temperature was the first parameter to be tuned to selectively produce TMC or PTMC.

4.2.1 Temperature effect

The effect of the temperature was first evaluated in bulk, under a 1 MPa CO_2 pressure, at 105 °C and in presence of an equimolar mixture of I_2 and TBAAc ($[\text{I}_2]_0/[\text{TBAAc}]_0 = 1$) used at 2 mol% (relative to the 1,3-epoxypropane used as representative oxetane monomer). Initial study on the temperature

effect was carried on by using TBAAc as received and for a reaction time of 6 h. Results are summarized in Table 4.1.

Table 4.1. Temperature effect of coupling CO₂ with oxetane using I₂/TBAAc as catalysis ^[a]

| Entry | Catalyst ratio I ₂ :TBAAc | T (°C) | Oxetane Conv. % ^[b] | Selectivity % ^[b] | | |
|------------------|---|---------|-----------------------------------|------------------------------|---------|----------------|
| | | | | TMC | polyTMC | ether linkages |
| 1 | 1:1 | 105 | 4 | 75 | 25 | <1 |
| 2 | 2:1 | 105 | 95 | 2 | 51 | 47 |
| 3 | 2:1 | 85 | 70 | 30 | 30 | 40 |
| 4 | 2:1 | 75 | 68 | 64 | 18 | 18 |
| 5 | 2:1 | 65 | 50 | 72 | 11 | 17 |
| 6 | 2:1 | 55 | 27 | 82 | 4 | 14 |
| 7 ^[c] | 2:1 | 65 | 60 | 30 | 28 | 42 |

[a] Copolymerization conditions: 7.88 mmol of oxetane, 1MPa CO₂, 6 h; [b] Conversion and selectivity were determined from ¹H NMR spectroscopy of product mixture; [c] TBAAc replaced by TBD.

After 6 h, despite an elevated selectivity in the production of TMC, as determined by ¹H NMR analysis with the representing signal $\delta = 4.46$ ppm (75 mol%), the overall very low conversion (4 mol%) suggest co-catalysts were necessary to catalyze this reaction (Table 4.1, entry 1, Figure 4.1).

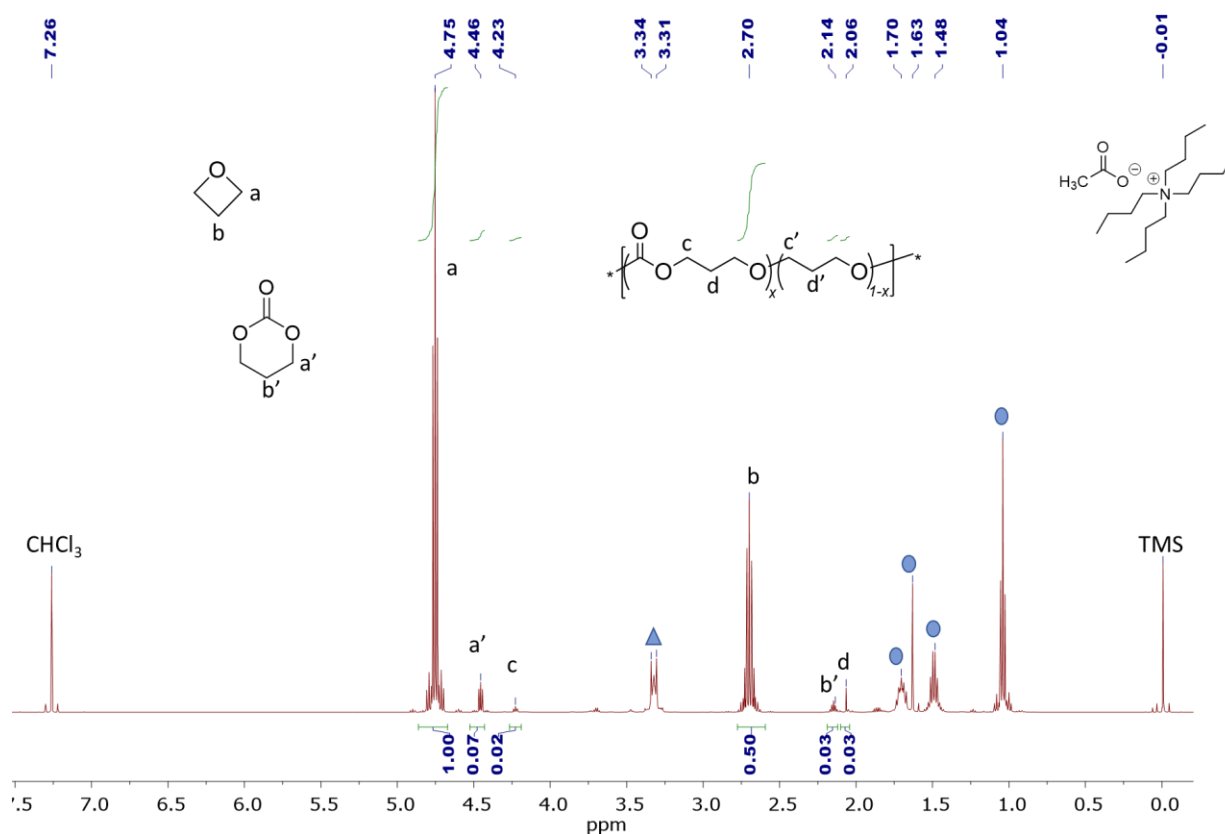


Figure 4.1. ^1H NMR spectrum (CDCl_3 , 500 MHz) of the resultant mixture of coupling reaction (Table 4.1, entry 1). Conditions: 7.88 mmol oxetane, $[\text{I}_2]_0/[\text{TBAAC}]_0/[\text{oxetane}]_0 = 1/1/50$, 1 MPa CO_2 , 105 $^\circ\text{C}$, 6h. TBAAC alkyl groups (●); methyl groups of acetate (▲).

To speed up the reaction, 2 equivalents of I_2 relative to TBAAC ($[\text{I}_2]_0/[\text{TBAAC}]_0 = 2$) were used to exam the overall catalytic activity. After 6 h, the catalytic complex did not lead to the selective synthesis of the desired TMC but impressively afforded 95 mol% of oxetane conversion in polymer structure (Table 4.1, entry 2). While SEC analysis was not used to characterize it, ^1H NMR analysis concluded on the presence of a poly(carbonate-co-ether) composed by 51 mol% of carbonate repeating units with the representing signals at $\delta = 4.23$ ppm for carbonate linkages and $\delta = 3.50$ ppm for ether linkages. As mainly presented in the state-of-the-art and also demonstrated in Chapter III of this thesis, the TMC polymerization rate was dramatically affected by the reaction temperature when a cationic mechanism is involved for its polymerization.¹⁴ Moreover, cationic polymerization of TMC under high temperature resulted in low molecular weight polycarbonate ($M_n < 6,000 \text{ g}\cdot\text{mol}^{-1}$) and a

small proportion of ether linkages, which is the consequence of the degradation and decarboxylation of polymer chain.^{15, 16} As such, the polymerization of an *in-situ* generated TMC from CO₂/oxetane could be tuned by lowering the reaction temperature to limit the reaction to an exclusive production of TMC. To support this hypothesis, a series of temperature-dependent experiments was then performed ([I₂]₀/[TBAAc]₀ = 2) under a 1 MPa CO₂ pressure and for 6 h. Aliquots were withdrawn and analyzed by ¹H NMR spectroscopy (Table 4.1, entries 3 – 6).

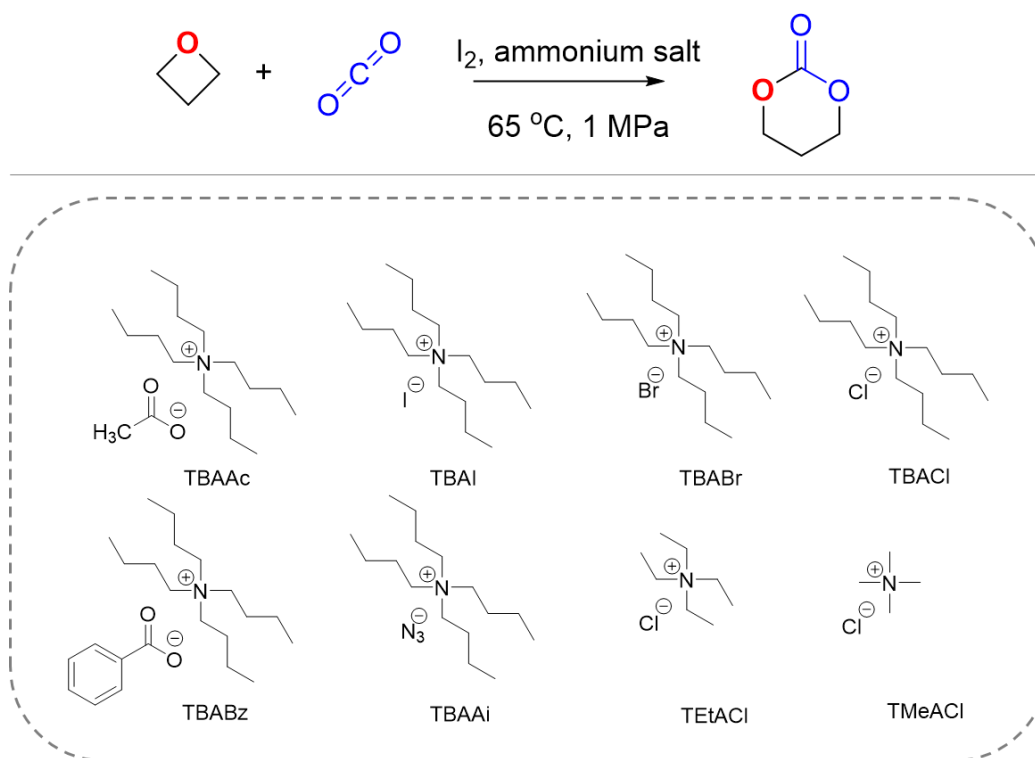
Decreasing the temperature of the reaction by 20 °C (from 105 to 85 °C) already allowed the selectivity toward TMC to be enhanced (Table 4.1, entry 3). Such increased selectivity in TMC formation (and then the diminished production of oligomers) motivated us to drop down the temperature to 55 °C. The overall oxetane conversion was decreased (~ 70 to ~30 mol%) with lowering temperature, the TMC formation was impressively enhanced to ~ 80 mol% in selectivity at 55°C (Table 4.1, entry 6). Replacing TBAAc by a TBD superbase resulted in an uncontrollable reaction (Table 4.1, entry 7) yielding, after 6 h, only 30 mol% of TMC and significant amount oligoethers (42 mol% in selectivity).

Such result, alongside the unique selectivity in TMC production when a I₂/*tert*-Bu-P₄ catalytic complex is used under a 3 MPa CO₂ pressure,¹¹ suggests that the nature of the cocatalyst is of great importance and should be investigated in details. Furthermore, the level of dryness of the co-catalyst has a tremendous impact on the selectivity of the process. By using dry TBAAc (cf. Experimental Section) at 65°C, a selectivity towards TMC of 86 mol% was obtained while contents in *poly*TMC and ether linkages are limited to 2 and 12 mol%, respectively (Table 4.2, entry 1). More impressively, decreasing the temperature to 55°C importantly improves the selectivity in TMC production by reaching 94 mol% (overall oxetane conversion ~ 20%, Table 4.3, entry 1).

4.2.2 Cocatalyst screening

In this study, TBAAc activity was compared to the tetramethyl-, tetraethyl- and tetrabutyl ammonium salts (Scheme 4.4). Experimental conditions were similar to the ones already presented, i.e. a $[I_2]_0/[cocatalysts]_0/[oxetane]_0$ ratio of 2/1/50, a reaction time of 6 h, a temperature of 65 °C and a P_{CO_2} of 1 MPa.

At a first glance, all studied co-catalysts presented a lower selectivity for TMC production as compared to TBAAc. Among these, tetrabutylammonium benzoate (TBABz) induced a relatively high TMC selectivity (60 mol%) for a moderated overall yield of 36 mol% (Table 4.2, entry 5). Unfortunately, 37 mol% of ether bonds were also produced which limits the interest of that co-catalyst.



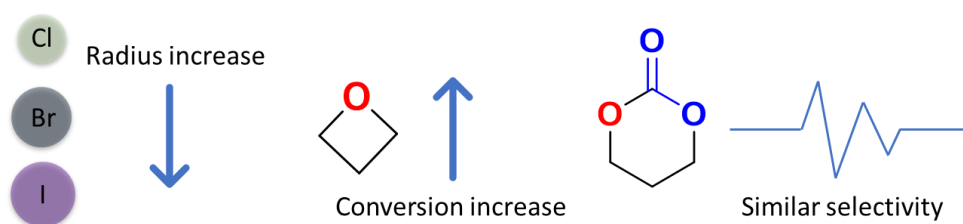
Scheme 4.4. I_2 -based binary catalytic system for CO_2 /oxetane coupling reaction (co-catalysts were all dried before use).

Table 4.2. Coupling of CO₂/oxetane in presence of various ammonium salts co-catalysts. ^[a]

| Entry | Co-catalysts | Conversion/ % ^[b] | Selectivity / % ^[b] | | |
|-------|--------------|---------------------------------|--------------------------------|---------|-------|
| | | | TMC | polyTMC | ether |
| 1 | TBAAc | 45 | 86 | 2 | 12 |
| 2 | TBAI | 43 | 35 | 24 | 41 |
| 3 | TBABr | 56 | 24 | 20 | 56 |
| 4 | TBACl | 60 | 31 | 22 | 47 |
| 5 | TBABz | 36 | 60 | 3 | 37 |
| 6 | TEtACl | 42 | 3 | 11 | 86 |
| 7 | TMeACl | 5 | <1 | <1 | >99 |
| 8 | TBAAi | <1 | <1 | <1 | <1 |

[a] Conditions: [I₂]₀/[cocatalysts]₀/[oxetane]₀ = 2/1/50, t = 6 h, T = 65 °C, P_{CO2} = 1 MPa. [b] The selectivity and conversion of oxetane were calculated by ¹H NMR.

Since halide-based ionic liquids are known to be used as efficient co-catalysts for CO₂/1,3-epoxypropane cycloaddition,¹⁷⁻¹⁹ tetrabutylammonium chloride (TBACl), tetrabutylammonium bromide (TBABr) and tetrabutylammonium iodide (TBAI) were selected to examine their catalytic activity when used together with I₂ (Table 4.2, entries 2 - 4). Although comparable to superior overall conversions, halide-contained catalysts provided a 2 to 3 times lower selectivity in TMC (24 – 35 mol%, Table 4.2, entries 2 - 4) as compared to TBAAc. Interestingly, by increasing the halide atom radius of the ammonium salt (Cl < Br < I), the oxetane conversion increased from 43 to 60 mol% with a more or less comparable selectivity in TMC (around 30 mol%), suggesting that the halide counter-anion does not affect the CO₂-involved coupling reaction but only contributes to the activation of the oxetane co-monomer (Scheme 4.5).



Scheme 4.5. Effect of using halogen-based as co-catalyst

Since the length of alkyl chains on the ammonium cation affects the solubility of ionic liquid and hence influence the activity of homogenous catalysis,^{20, 21} tetraethylammonium chloride (TEtACl) and tetramethylammonium chloride (TMeACl) were also compared in terms of catalytic efficiency and selectivity. Unfortunately, TEtACl involved an inferior activity towards coupling reaction between carbon dioxide and the oxetane that limit the selectivity for TMC to 3 mol% (Table 4.2, entry 6). As expected, since its methyl analogue presents a very low solubility in bulk at 65°C, an inferior catalytic activity was observed and only 5 % conversion was obtained (Table 4.2, entry 7). Finally, tetrabutylammonium azide (TBAAi) was examined as potent co-catalyst since it has been successfully applied to CO₂/oxetane copolymerization along with a metal salen based catalyst.²² The coupling reaction also failed probably due to a catalyst deactivation. Such hypothesis is supported by the work of Haight & Jones who demonstrated that the reaction between I₂ and azide anion inevitably leads to the production of nitrogen gas and iodide.²³

4.2.3 Reaction conditions modification

In the previous paragraph, a I₂/TBAAc binary system (used at a 2-for-1 ratio at 65°C) has been used to efficiently convert oxetane in TMC. As also presented in Section 4.2.1, lowering the temperature to 55°C improves even more the overall selectivity of TMC by pushing it to 94 mol% when a pressure in CO₂ of 1 MPa is applied. Unfortunately, such elevated selectivity was observed from a relatively low overall conversion of the as-used oxetane.

The experimental results obtained for two initial ratios ($[I_2]_0/[TBAAC]_0/[oxetane]_0 = 2/1/50$ and $2/1/100$) performed at 55°C, under two different pressures in CO₂ (1 and 3 MPa) and for two reaction times (6 and 24 h) (Table 4.3). It is important to note that the pressure in CO₂ was limited to 3 MPa for some practical issues.

Table 4.3. Coupling of oxetane and CO₂ catalyzed by different loadings of I₂/TBAAC and CO₂ pressure at 55°C^[a]

| Entry | Catalyst ratio (I ₂ /TBAAC/oxetane) | t / h | Pressure /MPa | Conversion / % ^[b] | Selectivity / % ^[b] | | |
|-------|---|-------|------------------|----------------------------------|--------------------------------|---------|-------|
| | | | | | TMC | polyTMC | ether |
| 1 | 2/1/50 | 6 | 1 | 20 | 94 | 2 | 4 |
| 2 | 2/1/50 | 24 | 1 | 94 | 73 | 12 | 15 |
| 3 | 2/1/100 | 6 | 1 | 6 | 95 | 2 | 3 |
| 4 | 2/1/100 | 24 | 1 | 20 | 91 | 4 | 5 |
| 5 | 2/1/100 | 24 | 3 | 23 | 99 | 0 | 1 |
| 6 | 2/1/100 | 48 | 3 | 40 | 94 | 1 | 5 |

[a] Coupling conditions: 9.85 mmol of oxetane, 55 °C; [b] Conversion of oxetane and selectivity were determined from ¹H NMR spectroscopy of product mixture.

Very interestingly, keeping constant the amount of TBAAC to 2 mol% and increasing the reaction time to 24 h under 1 MPa in carbon dioxide (Table 4.3, entry 2) did not allow to achieve a high selectivity toward the TMC product but provide oligomers with *ca.* 27 mol%. Because all three parameters including catalytic loading, reaction time and CO₂ pressure could influence the overall selectivity of the process, the modification of these parameters one-by-one was studied to select the best experimental conditions allowing TMC to be selectively produced in a high yield.

By reducing the initial TBAAC content to 1 mol% (Table 4.3, entries 3-4), we could achieve a selectivity of 90 mol% for TMC. Very interestingly, the increase in CO₂ pressure renders possible a high selectivity in TMC for an overall conversion of 40 mol% after 48 h while an impressive selectivity of 99 mol% TMC after 24 h for an overall yield of 23% (Table 4.3, entries 5 – 6).

Since simple optimizations of the reaction conditions allowed the production of TMC with an appreciable selectivity, the influence of iodine to TBAAc ratio was also investigated to further increase the yield of TMC. At the exception of one reaction realized without TBAAc (Table 4.4, entry 1), all other experiments were carried out with 1 mol% of the ammonium salt (rel. to oxetane), under 3 MPa CO₂ at 55 °C in bulk for 24 h (Table 4.4).

The reaction performed with 1 mol% of iodine only allowed 60 mol% of TMC to be produced while a massive amount of polyTMC and ether linkages were also produced. The high amount of ether linkages (27 mol%) could result from the reaction between I₂ and oxetane, yielding a charge transfer complex (CTC), a triiodide and a pentaiodide.²⁴ Such phenomenon will be presented and explained later on in this chapter (UV-vis spectroscopy analysis). These results suggest that the presence of a TBAAc co-catalyst is necessary and iodine is essential for an efficient CO₂ and oxetane coupling.

Table 4.4. Different catalyst ratios of I₂ and TBAAc for CO₂ and oxetane coupling reaction at 55 °C. ^[a]

| Entry | Catalyst ratio (I ₂ /TBAAc/oxetane) | Conversion/ % ^[b] | Selectivity / % ^[b] | | |
|-------|---|---------------------------------|--------------------------------|---------|-------|
| | | | TMC | polyTMC | ether |
| 1 | 1/0/100 | 13 | 60 | 13 | 27 |
| 2 | 0/1/100 | 0 | 0 | 0 | 0 |
| 3 | 1/1/100 | <1 | <1 | <1 | <1 |
| 4 | 1.25/1/100 | <1 | <1 | <1 | <1 |
| 5 | 1.50/1/100 | <1 | <1 | <1 | <1 |
| 6 | 1.75/1/100 | 7 | 95 | 5 | 0 |
| 7 | 2/1/100 | 23 | 99 | 0 | 1 |

[a] Coupling conditions: 9.85 mmol of oxetane, 55 °C, 3 MPa CO₂ for 24 h; [b] Conversion of oxetane and selectivity were determined from ¹H NMR spectroscopy of product mixture.

The result of TBAAc-dependent reaction supported this conclusion since no catalytic activity was observed in presence of pristine TBAAc (Table 4.4, entry 2). Notably, attempts to adjust I₂/TBAAc ratios (for [I₂]₀/[TBAAc]₀ < 2) in order to increase the TMC selectivity were unsuccessful limiting the

production of TMC to 95 mol% in selectivity for a conversion 7 mol% when a $[I_2]_0/[TBAAC]_0$ ratio of 1.75 was applied (Table 4.4, entries 3 - 6). The inferior activity of these co-catalysts mixtures suggests a possible interaction between I_2 and TBAAC that could somehow lead to a catalyst annealing.

To understand the interaction between I_2 and TBAAC, UV-Vis spectroscopy was applied with the titration of I_2 and TBAAC into THF to mimic the scenario of I_2 /TBAAC in oxetane solution (Figure 4.2). The spectra were recorded at room temperature with the addition of I_2 /TBAAC in nanomole-scale in the 225 to 550 nm wavelengths range. With the addition of I_2 alone, the interaction between I_2 and THF can be observed by the formation of a complex (CTC) presenting an absorption band at $\lambda = 290$ nm with the concomitant presence of triiodide ($\lambda = 366$ nm) and pentaiodide species ($\lambda = 442$ nm) (Figure 4.2).^{9,24}

Right after reaction with I_2 only ($10 \text{ nmol}\cdot\text{L}^{-1}$), an equimolar amount of TBAAC was added to the mixture. In presence of a $[I_2]_0/[TBAAC]_0 = 1$, a considerable enhancement of both CTC and triiodide absorbances is clearly observed while the contribution of the pentaiodide structure disappears. Further addition of I_2 allowed the absorptions of both CTC and triiodide species to increase gradually to a maximum absorbance obtained for a $[I_2]_0/[TBAAC]_0$ ratio of 2. Alongside with the results presented in Table 4.4, these titration results suggest that the activation of oxetane using I_2 /TBAAC (2:1) catalysts could be realized *via* CTC and triiodide species.

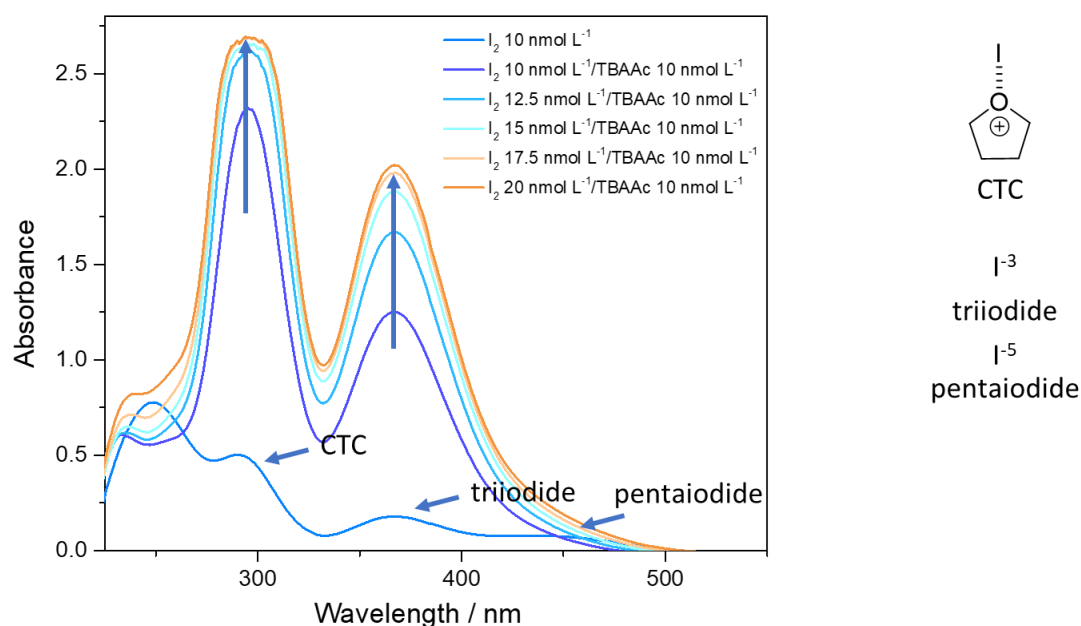


Figure 4.2. Titration of I_2 and TBAAc in THF solution under room temperature from 225 nm to 550 nm.

4.2.4 Solvent effect

On the basis of results discussed in section 4.2.3 (1 mol% in TBAAc and 2 mol% of I_2 , 3 MPa CO_2), a great selectivity in TMC (> 95 mol%) was yielded. These experimental conditions were applied to study and further increase the oxetane conversion while maintaining a unique TMC selectivity by using different solvents. Indeed, it has been reported that using an appropriate solvent (acetonitrile and toluene) for the coupling of CO_2 and oxetane could allow the reaction to be controlled both thermodynamically and kinetically.^{1, 4, 25}

Reactions were carried out under the above-mentioned experimental conditions (55 °C, 3 MPa CO_2 , I_2 : TBAAc = 2:1, 1 mol% TBAAc) while using an initial oxetane monomer concentration of 7.5 mol·L⁻¹ (Table 4.5).

Table 4.5. Solvent effects for CO₂ and oxetane coupling catalyzed by I₂ and TBAAC^[a]

| Entry | Solvent | Polarity Index (PI) | Conversion/ % [b] | Selectivity / % [b] | | |
|------------------|---------------------------------|---------------------|----------------------|---------------------|---------|-------|
| | | | | TMC | polyTMC | ether |
| 1 | n-Hexane | 0.10 | 85 | 70 | 16 | 14 |
| 2 | Toluene | 2.40 | 22 | 78 | 7 | 15 |
| 3 | CHCl ₃ | 2.70 | 20 | 93 | 0 | 7 |
| 4 | CH ₂ Cl ₂ | 3.10 | 30 | 93 | 4.5 | 2.5 |
| 5 | 1,4-dioxane | 5.27 | 80 | 85 | 7 | 8 |
| 6 | DMF | 6.40 | 36 | 99 | <1 | <1 |
| 7 ^[c] | DMF | 6.40 | 57 | 97 | 3 | 0 |
| 8 ^[d] | DMF | 6.40 | 93 | 93 | 4 | 3 |
| 9 | DMAc | 6.50 | 15 | 67 | 13 | 20 |
| 10 | NMP | 6.70 | 10 | 90 | 10 | 0 |

[a] Coupling conditions: 4.92 mmol of oxetane, [I₂]₀: [TBAAC]₀: [oxetane]₀ = 2:1:50, [oxetane]₀ = 7.5 mol·L⁻¹, 55 °C, 3 MPa CO₂ for 48 h; [b] Conversion of oxetane and selectivity were determined from ¹H NMR spectroscopy of product mixture. [c] 72 h; [d] 96 h.

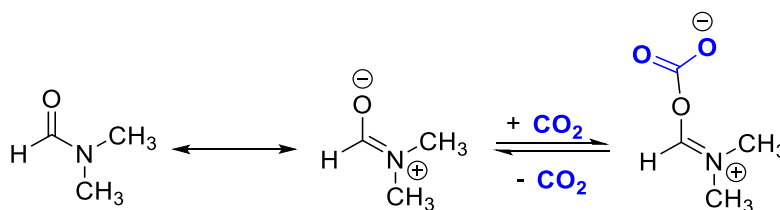
By performing the reaction in presence of *n*-hexane, 70 mol% TMC with the concomitant of ~ 15 mol% of carbonate and ether linkages was obtained, respectively, while 85 mol% of oxetane was converted to the products after 48 h (Table 4.5, entry 1). A similar selectivity for TMC (78 mol%) was observed when toluene was used (Table 4.5, entry 2). Such low selectivity toward the desired product could be ascribed to the low polarity solvent used, which promotes the polymerization of TMC to PTMC. The detail is discussed as the following. As the ceiling temperature (T_c) of the polymerization depends on the polymerization enthalpy (ΔH_p), entropy change (ΔS_p), and equilibrium monomer concentration ($[M]_{eq}$) (equation 4.1). It describes that T_c is decreased with an initial concentration of monomer ($[M]$) is decreased.²⁶ However, the influence of solvent on ΔH_p and ΔS_p is omitted in this equation.

$$T_c = \frac{\Delta H_p}{\Delta S_p + R \ln([M]_{eq})} \quad \text{equation 4.1}$$

On the basis of Albertsson's research,²⁷ it is likely that the conformation of cyclic carbonate monomer is forced to change into a more or less favored conformation when solvents with different polarity (different dielectric constants) used, determining the ring strain and ΔH_p . The high difference in polarity between monomer and solvent would result in promoting monomer's ring strain and hence increasing the absolute value for ΔH_p . Moreover, with the addition of solvent, ΔS_p increases, consequently changing the system thermodynamics. However, such ΔS_p value increase could be mitigated by adding a solvent with similar polarity to the reaction, since the favored interaction between monomer and solvent with similar polarity provides an ordered network and hence prevents a pronouncedly increase in entropy.²⁷ As such, solvent intermedia affect the T_c remarkably owing to the considerable change in absolute value of ΔH_p and ΔS_p . For example, the polymerization of 2-allyloxymethyl-2-ethyl-trimethylene carbonate in toluene ($2 \text{ mol}\cdot\text{L}^{-1}$), ΔH_p is $-11.1 \pm 0.026 \text{ kJ}\cdot\text{mol}^{-1}$ and the entropy change (ΔS_p) is $-21.9 \pm 1.5 \text{ J}\cdot\text{mol}^{-1}\cdot\text{K}^{-1}$, while in acetonitrile ($2 \text{ mol}\cdot\text{L}^{-1}$) these values change to $\Delta H_p = -7.6 \pm 0.072 \text{ kJ}\cdot\text{mol}^{-1}$ and $\Delta S_p = -18.3 \pm 1.0 \text{ J}\cdot\text{mol}^{-1}\cdot\text{K}^{-1}$.²⁷

In order to obtain TMC and reduce the polymerization induced from CO_2 and oxetane coupling, decreasing T_c turns to be a feasible approach. Since the inherent carbonate group renders the high dielectric constant to TMC monomer, adding the solvent with high polarity would decrease ΔH_p and maintain ΔS_p leading to a low T_c . As might be expected, an enhancement in the TMC selectivity (93 mol%) was observed with a low oxetane conversion (20 - 30 mol%) with the use of high polarity solvents, such as chloroform (CHCl_3) and dichloromethane (CH_2Cl_2), while only traces of polyTMC and ether linkages have been observed (Table 4.5, entries 3-4). Notably, the use of 1,4-dioxane involves a reaction providing a comparable TMC selectivity (85 mol%) with a minor by-product (carbonate, 7 mol%, and ether 8 mol%) after 80 mol% of oxetane was incorporated (Table 4.5, entry 5), suggesting that the polarity of the reaction medium indeed affected the polymerization of *in situ* generated TMC.

With the exception of dimethylacetamide (DMAc), all highly polar solvents including N-methyl-2-pyrrolidone (NMP) and dimethyl formamide (DMF) considerably reduce the propensity of the oxetane and the as-formed TMC to be polymerized, limiting the reaction to the production of TMC monomer. Very interestingly, after 48 hours of reaction, performing the reaction in DMF allows an oxetane conversion of 36 mol% to be obtained with a TMC selectivity of 99 mol%. By extending the reaction time to 72 h, a slight drop of TMC selectivity (97 mol%) with minor byproducts (carbonate linkages, 3 mol%) was observed through improving the conversion to a reasonable 57 mol% (Table 4.5, entry 7). Notably, as observed by ^1H NMR analysis (Figure 4.3), after 96 h of reaction to an overall conversion of 93 mol% and a selectivity in TMC of 93 mol% was obtained (Table 4.5, entry 8). Such a unique conversion to cyclic carbonate could be the result of an improved activation of the CO_2 by DMF (Scheme 4.6).²⁸⁻³⁰



Scheme 4.6. The possible activation of CO_2 by DMF.

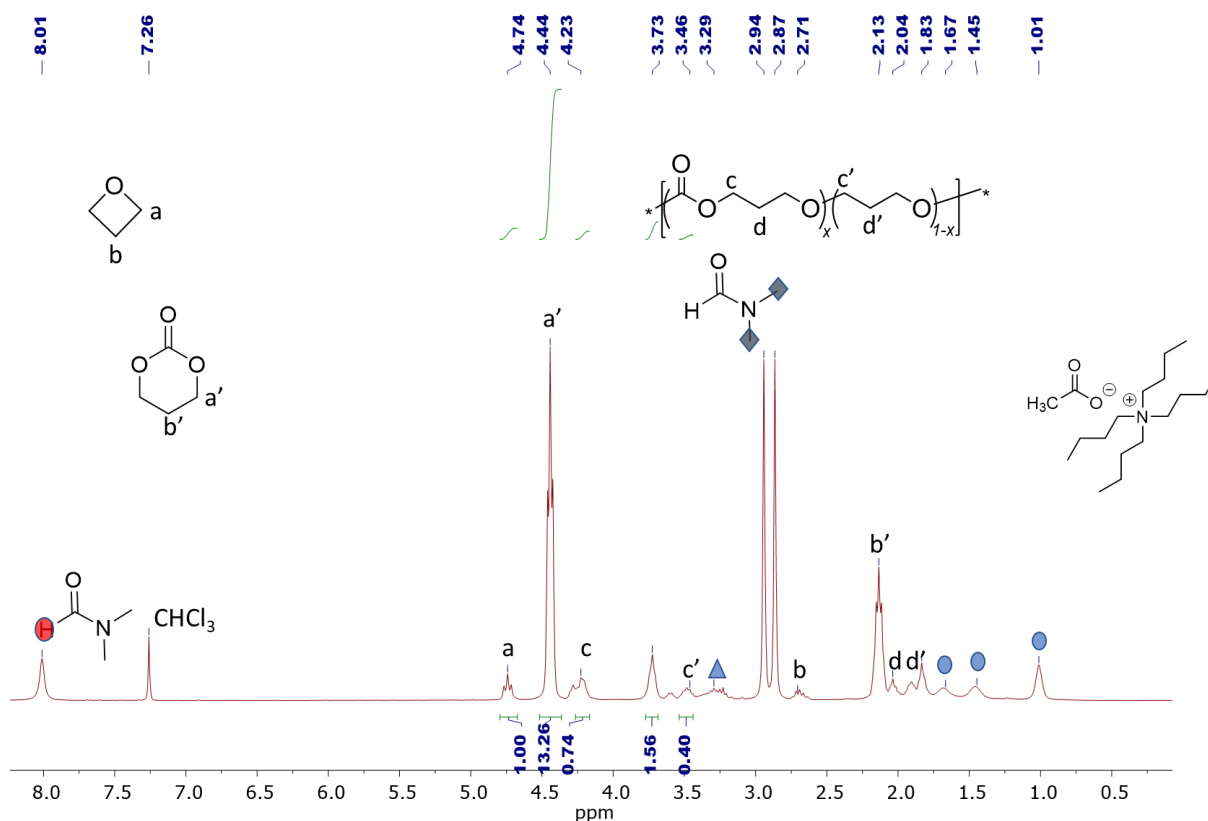


Figure 4.3. ^1H NMR spectrum (CDCl_3 , 300 MHz) of the resultant mixture of coupling reaction (Table 4.5, entry 8).

Conditions: 4.92 mmol oxetane, $[\text{I}_2]_0/[\text{TBAAc}]_0/[\text{oxetane}]_0 = 2/1/50$, $[\text{oxetane}]_0 = 7.5 \text{ M}$, 3 MPa CO_2 , 55 $^\circ\text{C}$, 96h.

TBAAc alkyl group (●), methyl group of acetate (▲).

4.2.5 Copolymer synthesis

On the basis of our previous results (Section 4.2.1) that the possibility to selectively limit the reaction between carbon dioxide and oxetane to TMC monomer at low temperature, attempts to directly prepare PMTC chains by applying a I_2/TBAAc catalytic complex at high temperature were realized. Reactions were initially carried out in bulk at 105 $^\circ\text{C}$, under 3 MPa CO_2 , with an initial ratio of $[\text{I}_2]_0: [\text{TBAAc}]_0: [\text{oxetane}]_0$ equal to 2:1:50 and for 24 h. SEC analysis of the crude mixture revealed the presence of a polymer characterized by a number-average molar mass (M_n) of 2,300 $\text{g}\cdot\text{mol}^{-1}$ and a dispersity value ($M_w/M_n = \mathcal{D}_M$) of 1.57. ^1H NMR analysis of the product revealed that 71.2 mol% of oxetane were incorporated to the polymer chains as carbonate repeating units while 27.1 mol%

served as ether bonds suggesting the formation of a poly(carbonate-co-ether) structure (Table 4.6, entry 1). On the basis of the catalytic loading effect, reducing the co-catalyst molar amounts by half (i.e. for a $[I_2]_0:[TBAAC]_0:[\text{oxetane}]_0 = 2:1:100$) allows a higher molar mass copolymer to be produced ($M_n = 4,400 \text{ g}\cdot\text{mol}^{-1}$; $\bar{D}_M = 1.69$) containing 78 mol% of carbonate linkages (Table 4.6, entry 2). These results are in agreement with the results presented in Chapter III where a reduced catalyst loading retaining CO_2 pressure at 3 MPa benefits the selectivity towards carbonate linkages.¹¹

Table 4.6. Copolymerization of oxetane and CO_2 catalyzed by I_2 and TBAAC at 105 °C ^[a]

| Entry | $[I_2]_0/[TBAAC]_0$ / $[\text{oxetane}]_0$ | t / h | Conversion / % ^[b] | Selectivity / % ^[b] | | | M_n (SEC) ^[c] g·mol ⁻¹ | \bar{D}_M ^[c] |
|-------|---|-------|----------------------------------|--------------------------------|---------|-------|---|----------------------------|
| | | | | TMC | polyTMC | ether | | |
| 1 | 2:1:50 | 24 | 99 | 1.7 | 71.2 | 27.1 | 2,300 | 1.57 |
| 2 | 2:1:100 | 24 | 97 | 3 | 78 | 19 | 4,400 | 1.69 |
| 3 | 2:1:200 | 48 | 98 | 5 | 82 | 13 | 5,400 | 1.46 |
| 4 | 2:1:400 | 96 | 89 | 9 | 84 | 7 | 6,400 | 1.63 |

[a] Coupling conditions: 0.039 mmol of TBAAC, 105 °C, 3 MPa CO_2 ; [b] Conversion of oxetane and selectivity were determined from ^1H NMR spectroscopy of product mixture. [c] Determined by SEC in tetrahydrofuran (THF) with polystyrene standards.

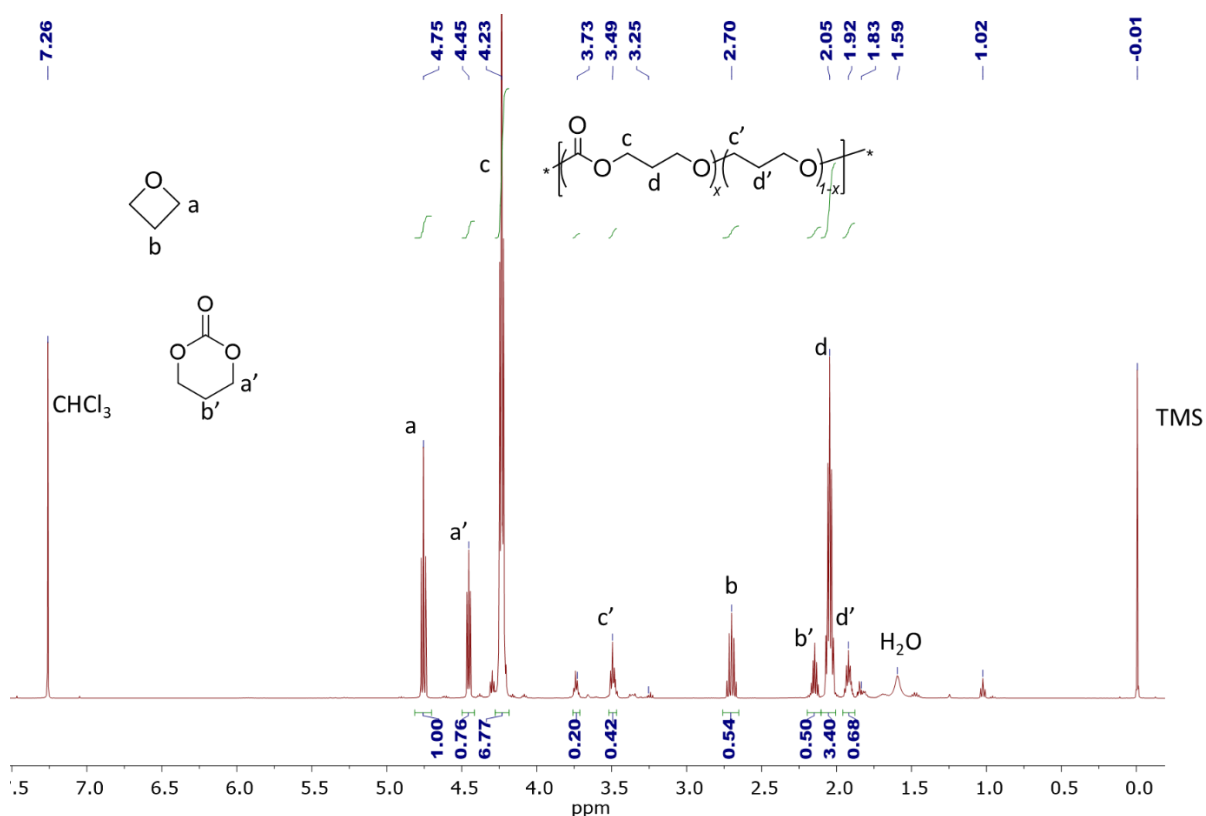


Figure 4.4. ^1H NMR spectrum (CDCl_3 , 500 MHz) of the resultant mixture of copolymerization (Table 4.6, entry 4).

Conditions: 15.76 mmol oxetane, $[\text{I}_2]_0/[\text{TBAAC}]_0/[\text{oxetane}]_0 = 2/1/400$, 3 MPa CO_2 , 105 $^\circ\text{C}$, 96h.

Notably, by further decreasing the catalyst loading to 0.5 mol% in TBAAC ($[\text{I}_2]_0/[\text{TBAAC}]_0/[\text{oxetane}]_0 = 2/1/200$), and after 48 h, a slight enhancement of the copolymer carbonate content was observed (82 mol%) yielding a copolymer characterized by a M_n of 5,400 $\text{g}\cdot\text{mol}^{-1}$ and a \bar{D}_M of 1.49 (Table 4.6, entry 3). A further reduced catalyst loading of 0.25 mol% in TBAAC (relative to the oxetane content) kinetically required 96 h to reach an overall conversion of 89 mol% (Table 4.6, entry 4). Such experimental condition yielded a copolymer characterized by a molar mass slightly higher than the one previously obtained ($M_n = 6,400 \text{ g}\cdot\text{mol}^{-1}$, $\bar{D}_M = 1.63$) but interestingly composed by a reduced amount of ether linkages as determined by ^1H NMR analysis (Figure 4.4).

To verify the composition of the resulted copolymer, the precipitation of the crude mixture (Table 4.6, entry 4) from methanol was characterized by ^1H NMR spectroscopy (Figure 4.5). The copolymer is characterized by 96 mol% of carbonate content and a minor ether-linkages of 4 mol% (Figure 4.6).

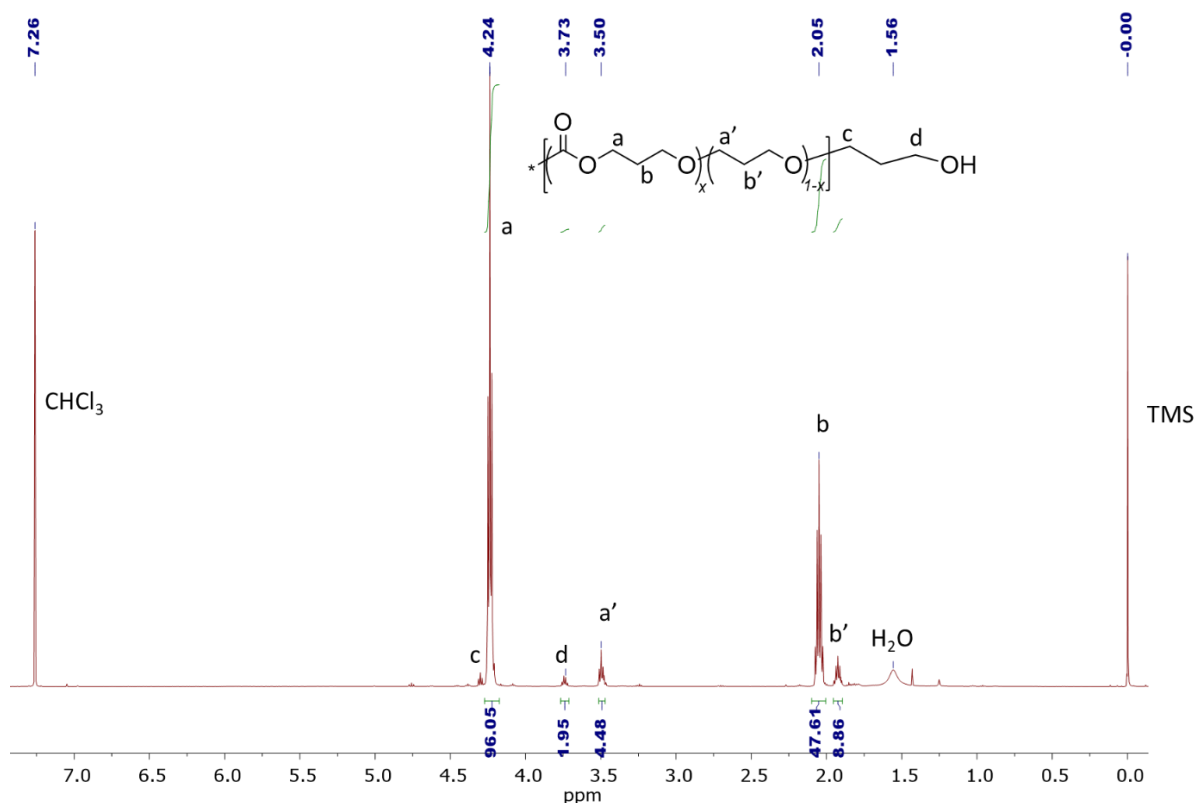


Figure 4.5. ^1H NMR spectrum (CDCl_3 , 500 MHz) of the copolymer purified from the precipitation in methanol (Table 4.6, entry 4). Conditions: 15.76 mmol oxetane, $[\text{I}_2]_0/[\text{TBAAC}]_0/[\text{oxetane}]_0 = 2/1/400$, 3 MPa CO_2 , 105 $^\circ\text{C}$, 96h.

As a representative example, the polymer containing the highest carbonate linkages (Table 4.6, entry 4) displays a signal spaced by $m/z = 102$ (Figure 4.6) corresponding to a sodium-charged α,ω -dihydroxyl PTMC presenting two more oxetane than CO_2 (the signal at $m/z = 1585.47$). It is worth to note that Figure 4.6 reports both values of “ n ” and “ m ”. While “ n ” refers to the number of pristine oxetanes in the copolymer, “ m ” corresponds to the polymerization degree (DP) of TMC. Additionally, the signal at $m/z = 1527.43$ is assigned to the same polymer unit, misses 3 CO_2 on the polymer chain.

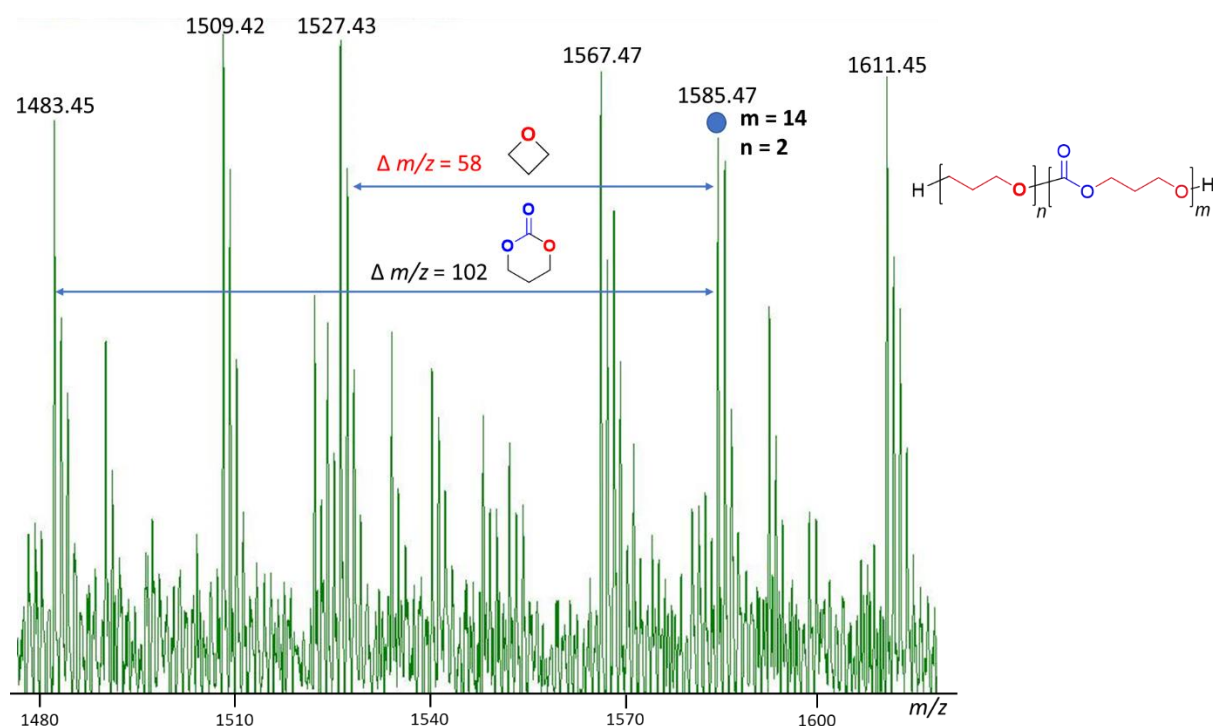


Figure 4.6. MALDI mass spectrum recorded for the sample of entry 4 (Table 4.6) after the precipitation from methanol, magnification between $m/z = 1480$ and $m/z = 1610$ (b). “ m ” represents the TMC unit and “ n ” the number of oxetane unit.

4.2.6 Kinetics of coupling reaction

- *Rate law of coupling reaction*

To understand the kinetic behavior of such coupling reaction and to provide information for the further mechanism study, the reaction rates associated to different concentrations in individual reagents (oxetane and CO_2) and catalysts were studied by a series of experiments.

As a very general expression, the overall rate law of the reaction can be simply expressed by equation 4.2.

$$r = k_{\text{obs}}[\text{oxetane}]^x[\text{Cat.}]^y[\text{CO}_2]^z \quad (\text{equation 4.2})$$

Where r is the reaction rate;

k_{obs} is the observed rate constant;

[oxetane] is the oxetane concentration;

[Cat.] is the I_2 /TBAAC binary catalyst with a fixed ratio of 2:1;

$[\text{CO}_2]$ is the CO_2 concentration;

and exponents x , y , and z the partial orders in oxetane, catalyst and carbon dioxide, respectively.

The kinetic experiments were performed at 55 °C since the selectivity of TMC is superior with minor by-product (Table 4.1, entry 6), and the aliquot of resultant was analyzed by ^1H NMR spectroscopy to determine the conversion of oxetane.

Reaction order in [oxetane]: The reaction order in oxetane was determined by independent experiments with respect to varying concentrations of oxetane (5.84, 6.48, 7.68 and 10.09 $\text{mol}\cdot\text{L}^{-1}$), in CH_2Cl_2 . Considering its chemical inertness and comparable physical properties (boiling point) and controllability in the initial period (Table 4.5, entry 4), CH_2Cl_2 should be comparable to solvent-free conditions. Experiments were conducted in a total volume of 0.64 mL with 0.306 $\text{mol}\cdot\text{L}^{-1}$ of I_2 , 0.5 equivalent of TBAAC, at 55 °C, under 3 MPa of CO_2 (conditions in which the maximum yield of TMC was obtained).

^1H NMR spectroscopic was used to monitor the reaction at the initial stage of the process (low conversion, 5 – 20 %) that was assumed as “steady-state”.³¹ A plot of the initial rate of coupling reaction vs the initial oxetane concentration evidently revealed a linear dependence confirming a first order kinetics suggesting that the ring-opening process of the oxetane is the rate-limiting step (Figure 4.7).

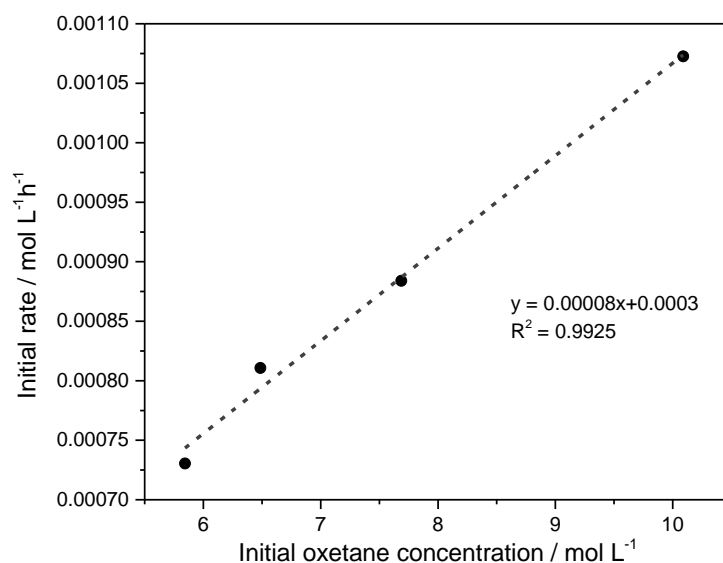


Figure 4.7. Linear fitting to the initial rate of coupling reaction ($\text{mol}\cdot\text{L}^{-1}\cdot\text{h}^{-1}$) vs the initial concentration of oxetane ($\text{mol}\cdot\text{L}^{-1}$). Experimental conditions: $0.306\text{ mol}\cdot\text{L}^{-1}\text{I}_2$ with 0.5 equivalent TBAAc, 3 MPa CO_2 , 55 °C .

Reaction order in [Cat]: The reaction order in catalyst was determined by performing the reaction with $7.68\text{ mol}\cdot\text{L}^{-1}$ oxetane in CH_2Cl_2 under 3 MPa CO_2 at 55 °C and over the range of $[\text{Cat.}] = 0.184, 0.246, 0.306, 0.492\text{ mol}\cdot\text{L}^{-1}$. ^1H NMR spectroscopic analyses revealed a linear relationship between the initial rate and the initial catalyst concentration that indicated a first order with respect to $[\text{Cat.}]$ (Figure 4.8). Such result revealed that only one CTC complex was involved in the catalytic circle.

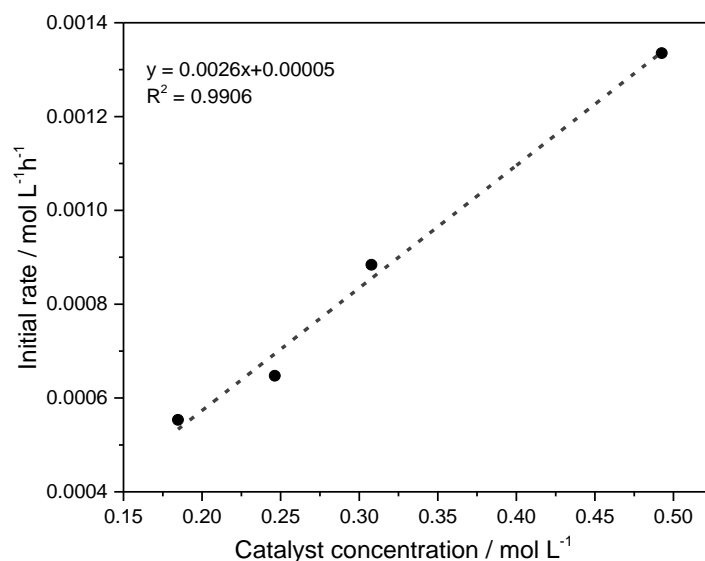


Figure 4.8. Plot of the initial rate of coupling reaction vs catalyst concentration presenting a linear fit as determined by ¹H NMR spectroscopy. Experimental conditions: initial [oxetane] = 7.68 mol·L⁻¹, in CH₂Cl₂, at 55 °C, 3 MPa CO₂.

Reaction order in [CO₂]: The reaction order in CO₂ was studied by varying the initial CO₂ pressure applied to the medium. Owing to the fact that a reaction temperature of 55 °C is slightly higher than the oxetane boiling point (50 °C), a pressurized atmosphere in CO₂ of 0.1 MPa cannot be applied to perform the reaction which could lead to mass transfer and provide inaccurate results. As such, the pressure-dependent reactions, alongside with the pressure limitation of autoclave (0 - 5 MPa), were carried out over the range 0.5 – 3 MPa at 55 °C, with 0.306 mol·L⁻¹ I₂ and 0.5 equivalent TBAAc in presence of 7.68 mol·L⁻¹ oxetane. The ¹H NMR spectroscopic analysis revealed a linear dependence on CO₂ pressure in the range of 0.5 – 2 MPa CO₂ suggesting a first order in [CO₂]. When a relatively high pressure was applied (2 – 3.5 MPa), the order of [CO₂] was shifted to zero suggesting that CO₂ insertion in the catalytic circle was rapid under high pressure range (2 – 3.5 MPa CO₂) (Figure 4.9). Such conclusion is in agreement with Rieger’s observation that a first order in CO₂ is obtained at low pressure (0.5 – 2.5 MPa) while a zero order is observed for higher pressure (2.5 – 4.5 MPa).³²

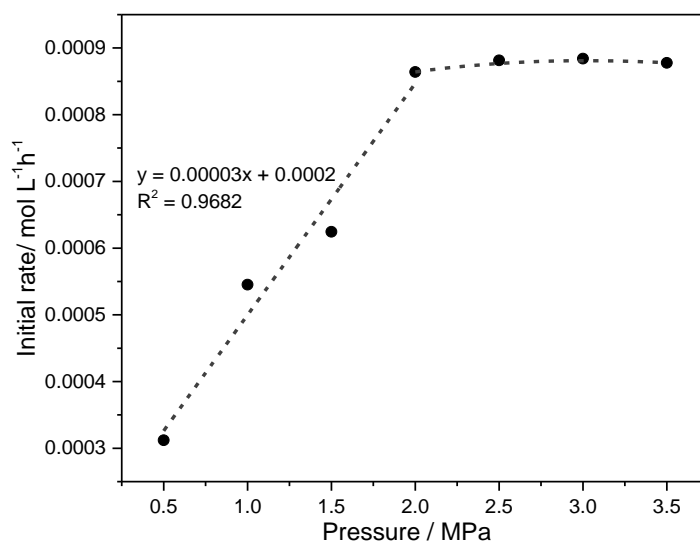


Figure 4.9. Plot of the initial rate of coupling reaction vs the initial CO₂ pressure. A linear relationship between the initial rate (mol·L⁻¹·h⁻¹) and CO₂ pressure (MPa) under low pressure range (0.5 – 2 MPa) while an independent relationship was observed under high pressure (2 – 3.5 MPa). Experimental conditions: [oxetane] = 7.68 mol·L⁻¹, [Cat.] = 0.306 mol·L⁻¹ at 55 °C in CH₂Cl₂.

On the basis of that partial orders determination, the rate law of the coupling reaction can be expressed by the equation 4.2 for a pressure range of 2 – 3.5 MPa.

$$r = k_{\text{obs}}[\text{oxetane}]^1[\text{Cat.}]^1[\text{CO}_2]^0 \quad (\text{equation 4.2})$$

- *Activation energy*

The rate law determination allows the activation energies for both coupling and copolymerization to be determined. The activation energies determination was conducted by performing coupling reactions under various temperatures. Aliquots of the mixtures were monitored by ¹H NMR spectroscopy to get access to the oxetane conversion and the selectivity of the resultant products.

Experiments were performed under an initial concentration of 7.68 mol·L⁻¹ of oxetane in CH₂Cl₂, a 0.306 mol·L⁻¹ of I₂ with 0.5 equivalent TBAAc and 3 MPa CO₂. The CO₂ was chosen in the relatively high pressure since zero-order with respect to [CO₂] (Figure 4.9) was observed suggesting that under a high CO₂ pressure the initial rate (*r*) is related to the initial concentration of catalyst ([Cat.]) and oxetane

([oxetane]) only. The initial rates for the formations of both TMC and PTMC vs temperature are illustrated in Figure 4.10.

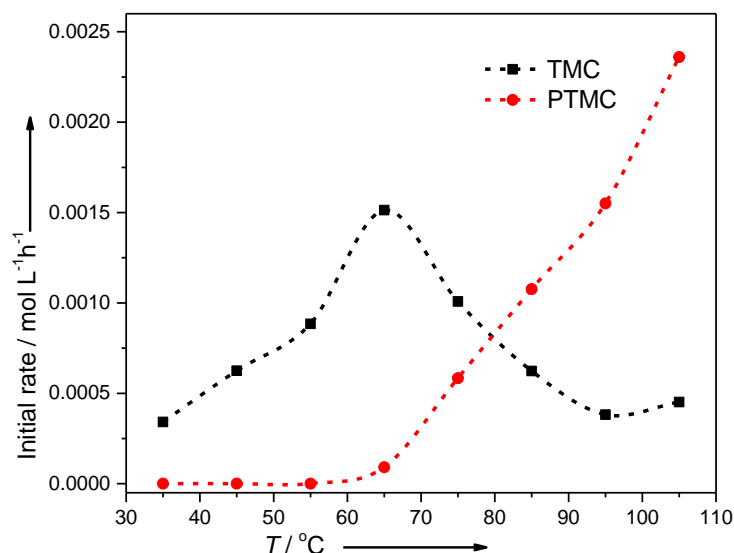


Figure 4.10. The initial rates of formation of TMC (black square) and PTMC (red circle) versus reaction temperature. Experimental conditions: [oxetane] = 7.68 mol·L⁻¹, [Cat.] = 0.306 mol·L⁻¹, 3 MPa CO₂ in CH₂Cl₂.

Evolutions of both initial rates of TMC and PTMC formations clearly revealed that the initial rate of TMC reaches a maximum ($\sim 0.0015 \text{ mol}\cdot\text{L}^{-1}\cdot\text{h}^{-1}$) at 65 °C. At such temperature, the process is accompanied by the presence of a slow PTMC production that increases exponentially with the reaction temperature. Alongside with the proposed mechanism of CO₂ and oxetane copolymerization as catalyzed by I₂ and guanidine (cf. Chapter III),¹¹ it suggested that the *in situ* generated TMC is incorporated to the polymer chain rapidly under relatively high temperatures (95 – 105 °C). To provide the relative activation energies of both TMC and PTMC formation, the energy barrier determination of TMC was studied in a low temperature range going from 35 to 65 °C while the one of the PTMC production was calculated between 75 and 105 °C. As such, the rates under the corresponding temperature were applied to the calculation of rate constant (k) for the further activation energy (E_a) determination via Arrhenius plots (Figure 4.11).

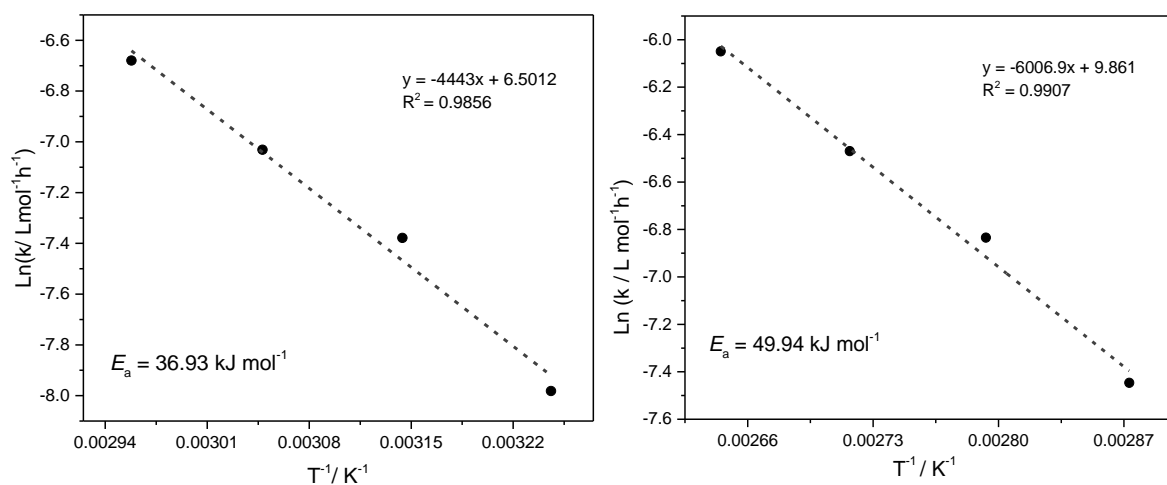


Figure 4.11. Arrhenius plots for TMC (left) and PTMC (right). The equations for the linear fit were provided on the top right while the activation energies for both formations were given in the bottom left corners as insets. Experimental conditions: [oxetane] = $7.68 \text{ mol} \cdot \text{L}^{-1}$, [Cat.] = $0.306 \text{ mol} \cdot \text{L}^{-1}$, 3 MPa CO_2 in CH_2Cl_2 .

The schematic energetic reaction pathway for both TMC ($36.93 \text{ kJ} \cdot \text{mol}^{-1}$) and PTMC ($49.94 \text{ kJ} \cdot \text{mol}^{-1}$) production is shown in Figure 4.12. Such small energetic difference between E_{as} ($\Delta E_a = 13 \text{ kJ} \cdot \text{mol}^{-1}$) allows the explanation of low controllability of TMC formation in bulk suggesting that the presence of solvent is necessary to the unique preparation of TMC. As comparison, the required energy to produce PTMC is only slightly higher than the one calculated by Darensbourg when applying the very efficient chromium salen catalytic complexes ($E_a = 45.6 \pm 3 \text{ kJ} \cdot \text{mol}^{-1}$).³³

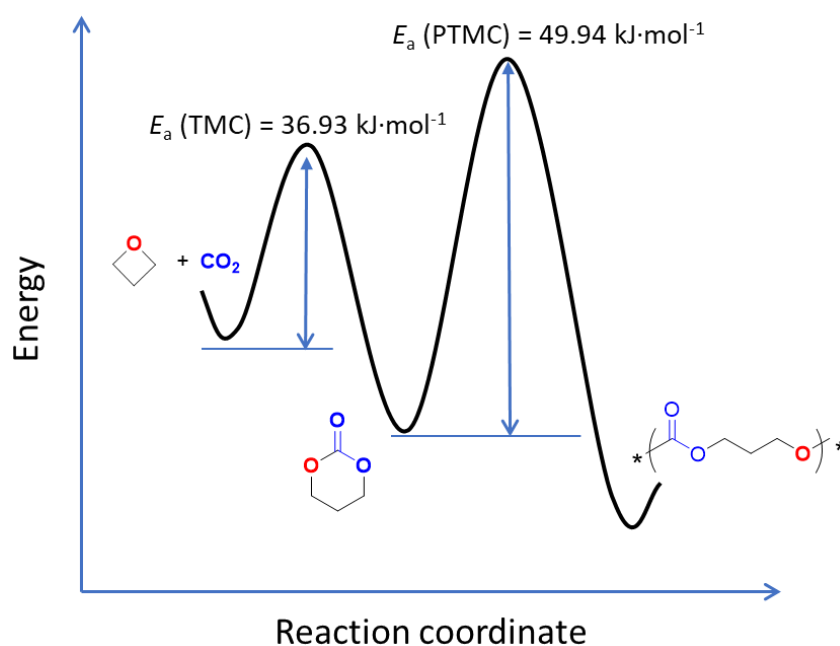


Figure 4.12. The schematically representation of reaction pathway for the formation of TMC and PTMC with experimentally determined activation energies, $E_a(\text{TMC}) = 36.93 \text{ kJ}\cdot\text{mol}^{-1}$, $E_a(\text{PTMC}) = 49.94 \text{ kJ}\cdot\text{mol}^{-1}$.

4.3 Conclusion

A novel green procedure for trimethylene carbonate syntheses and its polymer formation is reported using commercially available organocatalysts. A high level of TMC selectivity was achieved from CO_2 and oxetane using iodine in combination with ionic liquid (tetrabutylammonium acetate) as catalysts under mild conditions either in bulk or in DMF. Kinetic study and calculated activation energy reveal that the *in-situ* generated trimethylene carbonate can be polymerized “on-demand” by an adequate change in the temperature of reaction. Such green and temperature-dependent procedure provides a useful route to CO_2 utilization in both small molecule and polymer synthesis.

4.4 References

1. B. R. Buckley, A. P. Patel and K. G. U. Wijayantha, *Eur. J. Org. Chem.*, 2015, **2015**, 474-478.
2. D. J. Darensbourg and A. I. Moncada, *Macromolecules*, 2009, **42**, 4063-4070.
3. C. J. Whiteoak, N. Kielland, V. Laserna, E. C. Escudero-Adán, E. Martin and A. W. Kleij, *J. Am. Chem. Soc.*, 2013, **135**, 1228-1231.
4. D. J. Darensbourg, A. Horn Jr and A. I. Moncada, *Green Chem.*, 2010, **12**, 1376-1379.
5. F. Shi, Y. Deng, T. SiMa, J. Peng, Y. Gu and B. Qiao, *Angew. Chem. Int. Ed.*, 2003, **42**, 3257-3260.
6. D. Ballivet-Tkatchenko, S. Camy and J. S. Condoret, in *Environmental Chemistry: Green Chemistry and Pollutants in Ecosystems*, eds. E. Lichtfouse, J. Schwarzbauer and D. Robert, Springer Berlin Heidelberg, Berlin, Heidelberg, 2005, DOI: 10.1007/3-540-26531-7_49, pp. 541-552.
7. W. H. Carothers and F. J. V. Natta, *J. Am. Chem. Soc.*, 1930, **52**, 314-326.
8. H. K. Eigenmann, D. M. Golden and S. W. Benson, *J. Phys. Chem.*, 1973, **77**, 1687-1691.
9. J. Grundnes, M. Tamres and S. N. Bhat, *J. Phys. Chem.*, 1971, **75**, 3682-3687.
10. A. Baba, H. Kashiwagi and H. Matsuda, *Organometallics*, 1987, **6**, 137-140.
11. J. Huang, J. D. Winter, A. P. Dove and O. Coulembier, *Green Chem.*, 2019, DOI: DOI: 10.1039/c8gc03607a.
12. Q. He, J. W. O'Brien, K. A. Kitselman, L. E. Tompkins, G. C. T. Curtis and F. M. Kerton, *Catal. Sci. Technol.*, 2014, **4**, 1513-1528.
13. M. Alves, B. Grignard, A. Boyaval, R. Méreau, J. De Winter, P. Gerbaux, C. Detrembleur, T. Tassaing and C. Jérôme, *ChemSusChem*, 2017, **10**, 1128-1138.
14. H. R. Kricheldorf and B. Weegen-Schulz, *J. Polym. Sci. A Polym. Chem.*, 1995, **33**, 2193-2201.
15. H. R. Kricheldorf, J. Jenssen and I. Kreiser-Saunders, *Makromol. Chem.*, 1991, **192**, 2391-2399.
16. H. R. Kricheldorf and J. Jenssen, *J. Macromol. Sci. A*, 1989, **26**, 631-644.

17. C. Martín, G. Fiorani and A. W. Kleij, *ACS Catal.*, 2015, **5**, 1353-1370.
18. Y. Kumatabara, M. Okada and S. Shirakawa, *ACS Sustainable Chem. Eng.*, 2017, **5**, 7295-7301.
19. V. Caló, A. Nacci, A. Monopoli and A. Fanizzi, *Org. Lett.*, 2002, **4**, 2561-2563.
20. M. Gervais, A. Forens, E. Ibarboure and S. Carlotti, *Polym. Chem.*, 2018, **9**, 2660-2668.
21. V. Rejsek, D. Sauvanier, C. Billouard, P. Desbois, A. Deffieux and S. Carlotti, *Macromolecules*, 2007, **40**, 6510-6514.
22. D. J. Darensbourg, P. Ganguly and W. Choi, *Inorg. Chem*, 2006, **45**, 3831-3833.
23. G. P. Haight and L. L. Jones, *J. Chem. Educ.*, 1987, **64**, 271.
24. F. Cataldo, *Eur. Polym. J.*, 1996, **32**, 1297-1302.
25. T. W. Christian Reichardt, in *Solvents and Solvent Effects in Organic Chemistry*, Wiley, 2010, DOI: doi:10.1002/9783527632220.ch5, ch. 5.
26. F. S. Dainton and K. J. Ivin, *Q. Rev. Chem. Soc.*, 1958, **12**, 61-92.
27. P. Olsén, J. Undin, K. Odelius, H. Keul and A.-C. Albertsson, *Biomacromolecules*, 2016, **17**, 3995-4002.
28. L. Wang, L. Lin, G. Zhang, K. Kodama, M. Yasutake and T. Hirose, *Chem. Commun.*, 2014, **50**, 14813-14816.
29. J. A. Kozak, J. Wu, X. Su, F. Simeon, T. A. Hatton and T. F. Jamison, *J. Am. Chem. Soc.*, 2013, **135**, 18497-18501.
30. M. Aresta, A. Dibenedetto, L. Gianfrate and C. Pastore, *J. Mol. Catal. A: Chem.*, 2003, **204-205**, 245-252.
31. C. Martín and A. W. Kleij, *Beilstein J. Org. Chem.*, 2014, **10**, 1817-1825.
32. M. W. Lehenmeier, S. Kissling, P. T. Altenbuchner, C. Bruckmeier, P. Deglmann, A.-K. Brym and B. Rieger, *Angew. Chem. Int. Ed.*, 2013, **52**, 9821-9826.
33. D. J. Darensbourg, A. I. Moncada, W. Choi and J. H. Reibenspies, *J. Am. Chem. Soc.*, 2008, **130**, 6523-6533.

Conclusion and outlooks

Environmental protection and depletion of fossil fuels have stimulated the research of CO₂ valorization. The transformation of CO₂ into fine chemicals has received a great deal of attention since such abundant and non-toxic C1 feedstock is promising to replace highly toxic phosgene. Due to its fully oxidized state and symmetric molecular structure, CO₂ is characterized by an inert activity requiring the development of catalytic tools to valorize it. Thanks to the progress of catalytic chemistry, varying catalysis has been applied to transform CO₂ into fine chemicals such as carboxylic acid, urethane, cyclic carbonates, and CO₂-based copolymers. With replacing fossil-fuel plastics as a future perspective, the copolymerization of CO₂ with other monomers such as oxygen-based heterocycles have been researched on a sophisticated level using metal-based catalysis. However, the drawbacks of environmental pollution, high costs and the inherent oxygen and moisture lability restrict the applicability of metal-based catalysis, especially in the fields of biomaterials and microelectronics. To overcome these drawbacks, organo-based catalysis is being developed with the benefits of green credentials and absence of metal-associated toxicity.

In this thesis, the copolymerization of CO₂ with cyclohexane oxide (CHO) and oxetane using organo-based catalysis is studied, respectively. The first project (Chapter II) focused on the preparation of poly(cyclohexane carbonate) from CHO and CO₂ in presence of *trans*-cyclohexane diol and phosphazene superbase. The results reveal that the selectivity of oligocarbonate and its cyclic analogues (*trans*-cyclohexane carbonate and *cis*-cyclohexane carbonate) can be tuned by changing the catalysis content. The unique product of *cis*-cyclohexane carbonate (98 mol% in selectivity) was obtained with 2 equivalents of phosphazene (related to *trans*-cyclohexane diol) under a 0.1 MPa CO₂, at 85 °C, after 24 h, which opens perspectives for industrial fabrication. The desired oligocarbonate ($M_n = 1,040 \text{ g}\cdot\text{mol}^{-1}$) was produced in presence of 8 equivalents of *trans*-cyclohexane diol (related to phosphazene), which can be used as the agent for chain extension.

The second project of preparing CO₂-based polycarbonate focused on the copolymerization of CO₂ with oxetane using I₂-based organocatalysis (Chapter III). After screening the co-catalyst and modifying experimental conditions (catalyst content and pressure), a poly (trimethylene carbonate) (PTMC) ($M_n = 4,000 \text{ g}\cdot\text{mol}^{-1}$) with high carbonate content (up to 95 mol%) was produced in presence of I₂ and guanidine superbases with a ratio of 1:1 under a 3 MPa CO₂, at 105 °C, for 7 days. The mechanism study suggests that the *in situ* generated trimethylene carbonate is polymerized to yield PTMC following an active chain end mechanism. Such catalytic method provides a novel approach to prepare PTMC without metal trace in the product, which is interesting to the application of biomaterials.

Inspired by the insight of Chapter III that unique selectivity of trimethylene carbonate was produced using I₂ and phosphazene as catalysis, the continuing work of the project was to study the synthesis of TMC from CO₂ and oxetane using I₂ and ionic liquid as catalysis. Up to 93 mol% selectivity of TMC with 93 mol% conversion of oxetane was observed in presence of I₂ and tetrabutylammonium acetate as catalysis in dimethylformamide solution under a 3 MPa CO₂, at 55 °C, for 96 h. Kinetic study and activation energy provide useful information for the further mechanism study and theoretical calculation.

The fact that organocatalytic copolymerization of CO₂ with oxygen-based heterocycles can deliver the final product without metal trace, is interesting to the chemical community. Because of its green valorization potential compared to its polluting metal counterpart, further investigations will be stimulated. In terms of coupling CO₂ with oxetane to obtain TMC and corresponding polymer formation, the mechanism of such reaction is still unclear. Theoretical calculations would bring useful clues in combination with bench work to reveal it. Moreover, the pathway of polymerization of *in situ* generated TMC under high temperature should be explored in future. It will be interesting to introduce the trifluoroacetate as co-catalyst for the copolymerization process to figure out the exact initial step and fine structure of copolymer chain. The further investigation of preparing PTMC with high molar mass should focus on decreasing the moisture in reactions since the high purity of CO₂ resource still

contains some moisture that promotes the chain transfer reaction and hence results in polycarbonates with the comparable low molar mass ($< 10,000 \text{ g}\cdot\text{mol}^{-1}$). The gas purifying system could be applied to the reaction to handle such issue. Interestingly, the oxetane substrates such as 3,3-dimethyloxetane, 3-phenyloxetane and 2-phenyloxetane, are capable to couple with CO_2 yielding the corresponding cyclic carbonates using iodine/ionic liquid catalytic system. The preparation of polycarbonate from CO_2 and various oxetanes could be of high interest to develop polycarbonates with the high performance of mechanical properties. As iodine, a typical Lewis acid, has been applied as catalysis to oxetane activation, it would be interesting to introduce other metal-free Lewis acids such as boron-based compounds for the coupling of CO_2 and oxetane. Recently, anionic polymerization of oxetane was reported recently using aluminium-based catalysis, it would be interesting to introduce CO_2 as the building block to prepare PTMC under ambient CO_2 pressure.

Experimental Section

5.1 General comments

5.1.1 Materials and methods

All reagents and solvents were purchased from Sigma-Aldrich, TCI, Alfa aesar, Air Liquide and used as received, unless otherwise noted. 1,8-Diazabicyclo[5.4.0]-undec-7-ene (DBU, Sigma Aldrich, 98%), 7-methyl-1,5,7-triazabicyclo[4.4.0]dec-5-ene (MTBD, Sigma-Aldrich, 98%), cyclohexane oxide (CHO, Sigma-Aldrich, 98%) and oxetane (TCI, 98%) were distilled from CaH_2 (Alfa aesar, 92%) and stored in a glove-box and glove-box freezer ($-35\text{ }^\circ\text{C}$), respectively. 1,5,7-Triazabicyclo[4.4.0]dec-5-ene (TBD, 98%), *trans*-1,2-cyclohexanediol (*trans*-CHD, Sigma-Aldrich, 98%), and *cis*-1,2-cyclohexanediol (*cis*-CHD, Sigma-Aldrich, 99%) were dried by anhydrous tetrahydrofuran (THF) three times before the storage in glove-box. The white crystal of 1-*tert*-butyl-4,4,4-tris(dimethylamino)-2,2-bis[tris(dimethylamino)-phosphoranylideneamino]- $2\lambda^5,4\lambda^5$ -catenadi(phosphazene) (*tert*-Bu- P_4) was obtained and storage in glove-box from *tert*-Bu- P_4 hexane solution (Sigma-Aldrich, $\sim 0.8\text{ M}$ in hexane) by removing the solvent under vacuum. Tetrabutylammonium acetate (TBAAC, Sigma-Aldrich, 97%), tetrabutylammonium chloride (TBACl, Sigma-Aldrich, 97%), tetrabutylammonium bromide (TBABr, Sigma-Aldrich, $\geq 98\%$), tetrabutylammonium iodide (TBAI, Sigma-Aldrich, 98%), tetrabutylammonium benzoate (TBABz, Sigma-Aldrich, $\geq 99\%$), tetraethylammonium chloride (TEtACl) and tetramethylammonium chloride (TMeACl) were dried under vacuum at $120\text{ }^\circ\text{C}$ for 3 h. Anhydrous solvents such as dimethylformamide (DMF), *n*-hexane and 1,4-dioxane was used as received from Sigma-Aldrich. Tetrahydrofuran (THF), dichloromethane (DCM), chloroform (CHCl_3), dimethylacetamide (DMAc) and methylpyrrolidone (NMP) were distilled from CaH_2 and stored in the glove-box. Toluene was distilled from sodium and storage in glove-box. All solvents, CHO and oxetane were thoroughly degassed, by performing several freeze-thaw cycles under vacuum, before use with reactions. High pressure reactions were carried out in an autoclave Suurmond BV, steel type 3/10 mL, 10 MPa. N50 grade CO_2 (99.999%, $\text{H}_2\text{O} < 0.5\text{ ppm}$) was used as received.

5.1.2 Measurements

^1H NMR spectra were measured at 298 K using 300 and 500 MHz advance Bruker spectrometer with tetramethylsilane (TMS) as an internal standard ($\delta = 0.00$ ppm) in chloroform-d (CDCl_3). Positive-ion MALDI-Mass Spectrometry (MALDI-MS) experiments were recorded using a Waters QToF Premier mass spectrometer equipped with a Nd:YAG (third harmonic) operating at 355 nm with a maximum output of 65 μJ delivered to the sample in 2.2 ns pulses at 50 Hz repeating rate. Time-of-flight mass analyses were performed in the reflectron mode at a resolution of about 10,000. All the samples were analyzed using trans-2-[3-(4-tert-butylphenyl)-2-methylprop-2-enylidene]malononitrile (DCTB) as matrix. That matrix was prepared as 40 $\text{mg}\cdot\text{ml}^{-1}$ solution in CHCl_3 . The matrix solution (1 μL) was applied to a stainless-steel target and air-dried. Polymer samples were dissolved in THF to obtain 1 $\text{mg}\cdot\text{ml}^{-1}$ solution and 50 μL of 2 $\text{mg}\cdot\text{ml}^{-1}$ NaI solution in acetonitrile has been added to the polymer solution. Therefore, 1 μL of this solution was applied onto the target area already bearing the matrix crystals, and air-dried. For the recording of the single-stage MS spectra, the quadrupole (rf-only mode) was set to pass all the ions of the distribution, and they were transmitted into the pusher region of the time-of-flight analyzer where they were mass analyzed with 1s integration time. Data were acquired in continuum mode until acceptable averaged data were obtained. Size exclusion chromatography (SEC) was performed in THF at 308 K using a Polymer Laboratories liquid chromatograph equipped with a PL-DG802 degasser, an isocratic HPLC pump LC 1120 (flow rate = 1 mL min^{-1}), a triple detector: refractive index (ERMA 7517), capillary viscometry and light scattering RALS (Viscotek T-60) (Polymer Laboratories GPC - RI/UV) and four columns: a PL gel 10 μm guard column and three PL gel Mixed - B 10 μm columns. Polystyrene (PS) standards were used for calibration. UV-Vis spectroscopic measurements were taken using a Perkin Elmer Lambda 25 instrument.

5.2 General procedure for the synthesis of carbonates

5.2.1 General procedure for the synthesis of carbonates from CHO and CO₂ as catalyzed by *trans*-CHD and *tert*-Bu-P₄

Synthesis of oligo-carbonates from CHO and CO₂. The CO₂-based carbonates were synthesized following the general procedure. In brief, a 10 mL Schlenk flask with magnetic stirrer was flame dried 3 times before immediately being taken into a N₂-filled glove-box. After the reactor had cooled to ambient temperature, the reagents, *trans*-CHD (40 mg, 0.344 mmol), *tert*-Bu-P₄ (27.28 mg, 0.043 mmol, 0.25 equivalent) and CHO (17.22 mmol, 1.74 mL) were charged to the flask. The flask was sealed, removed from the glove-box, placed in liquid nitrogen to be cooled down and degassed by nitrogen. CO₂ was filled into the reactor after the flask was warmed up to room temperature *via* a Schlenk-line. The flask was heated to the desired temperature under CO₂ atmosphere. After the allotted reaction time, the flask was again cooled by liquid nitrogen before the CO₂ gas was released slowly. Aliquots of the coupling mixture were withdrawn for ¹H NMR spectroscopic characterization to determine both overall conversion and selectivity. The residue of the mixture was dissolved in a small volume of THF (2 mL) and precipitated from n-hexane for oligo-carbonate purification. The resultant oligomer was dried under vacuum at 40 °C overnight (Yield = 0.04 g, 0.04 mmol, 8%).

Synthesis of *cis*-cyclohexane carbonates from CHO and CO₂. The experimental procedure followed the protocol of oligo-carbonate synthesis with 5.17 mmol CHO, 5 mol% catalyst loading (0.172 mmol *trans*-CHD with 2 equivalents of *tert*-Bu-P₄). The pure *cis*-CHC was obtained as pale yellow needles after recrystallization from ethyl acetate-petroleum ether. (Yield = 454 mg, 3.2 mmol, 93%)

¹H NMR (500 MHz, CDCl₃): δ 4.68 (m, 2 H, -CH), 1.91 (m, 4 H, -CH₂-), 1.63-1.42 (m, 4H, -CH₂-). ¹³C NMR (125 MHz, CDCl₃): δ 155.4 (C=O), 75.7 (CH), 26.5 (-CH₂-), 18.9 (-CH₂-).

5.2.2 General procedure for the synthesis of carbonates from CO₂ and oxetane using iodine-based catalysis.

Synthesis of poly (trimethylene carbonate) from CO₂ and oxetane using iodine and guanidine catalytic system. The CO₂-based copolymers were synthesized following the general procedure. In brief, a 10 mL pressure reactor (Autoclave Suurmond BV, steel type 3/10 mL, 10 MPa) with magnetic stirrer was dried in an oven at 70 °C overnight before immediately being taken into a N₂-filled glove-box. After the reactor had cooled to ambient temperature, the reagents, I₂ (50 mg, 0.197 mmol), co-catalysts (see text) and oxetane (7.88 mmol, 0.512 mL) were charged to the vessel. The vessel was sealed, removed from the glove-box and placed in liquid nitrogen to be cooled down. CO₂ was condensed into the reactor while cold *via* a Schlenk-line until the appropriate pressure was achieved. The reactor was sealed again and heated to the desired temperature. After the allotted reaction time, the reactor was again cooled by liquid nitrogen before the CO₂ gas was released slowly. Aliquots of the polymerization mixture were withdrawn for ¹H NMR spectroscopic characterization to determine both overall conversion and selectivity. The residue of the mixture was dissolved in a small volume of THF (5 mL) and precipitated from methanol. The resultant copolymer was dried under vacuum at 40 °C overnight (Yield = 0.58 g, 0.125 mmol, 86%). When catalyst = TBD (0.197 mmol, 0.0274 g): ¹H NMR (500 MHz, CDCl₃, 298K): δ 4.29 (t, 2H, ³J_{HH} = 6.0 Hz, -CH₂), 4.23 (t, 4H, ³J_{HH} = 6.0 Hz, -OCH₂), 3.73 (t, 2H, ³J_{HH} = 6.0 Hz, -CH₂), 3.49 (t, 4H, ³J_{HH} = 6.3 Hz, -OCH₂), 2.04 (quint, 2H, ³J_{HH} = 6.3 Hz, -CH₂), 1.92 (quint, 2H, ³J_{HH} = 6.3 Hz, -CH₂), 1.82 (quint, 2H, ³J_{HH} = 6.3 Hz, -CH₂). ¹³C NMR (125 MHz, CDCl₃) δ 155.07 (C=O), 64.45 (-O-CO₂-CH₂-), 67.18 (-O-CH₂-CH₂-), 29.21 (-O-CH₂-CH₂-), 28.23 (-CO₂-CH₂-CH₂-). SEC (THF): M_n = 4630 g·mol⁻¹, Đ_M = 1.32.

Synthesis of trimethylene carbonate from CO₂ and oxetane using iodine and ionic liquid catalytic system. The experimental procedure followed the protocol of poly (trimethylene carbonate) synthesis.

In brief, a 10 mL pressure reactor (Autoclave Suurmond BV, steel type 3/10 mL, 10 MPa) with magnetic stirrer was dried in an oven at 70 °C overnight before immediately being taken into a N₂-filled glove-box. After the reactor had cooled to ambient temperature, the reagents, I₂ (50 mg, 0.197 mmol), co-catalysts (TBAAc, 29.7 mg, 0.098 mmol, for example), oxetane (4.92 mmol, 0.320 mL) and solvent (DMF, 0.320 mL, for example) were charged to the vessel. The vessel was sealed, removed from the glove-box and before being placed in liquid nitrogen to be cooled down. CO₂ was condensed into the reactor while cold *via* a Schlenk-line until the appropriate pressure was achieved. The reactor was sealed again and heated to the desired temperature. After the allotted reaction time, the reactor was again cooled by liquid nitrogen before the CO₂ gas was released slowly. Aliquots of the polymerization mixture were withdrawn for ¹H NMR spectroscopic characterization to determine overall conversion and selectivity. The residue of the mixture was dissolved in a small volume of CH₂Cl₂ (5 mL) and passed through silica gel. After the evaporation of under vacuum, the residue was recrystallized two times from concentrated THF solution to cold diethyl ether. (Yield = 0.47 g, 4.6 mmol, 81%). ¹H NMR (500 MHz, CDCl₃) δ 4.46 – 4.44 (t, 4H, ³J_{HH} = 5.7 Hz, -O-CH₂-CH₂-), 2.27 – 2.08 (quintet, 2H, ³J_{HH} = 5.7 Hz -CH₂-CH₂-CH₂-). ¹³C NMR (125 MHz, CDCl₃) δ 148.25 (C=O), 67.72 (-O-CH₂-CH₂-), 21.51 (-CH₂-CH₂-CH₂-).

Publications

1. The following publications arise as a result of the work in this thesis:

Metal-free synthesis of poly(trimethylene carbonate) by efficient valorization of carbon dioxide

Jin HUANG, Julien De WINTER, Andrew P DOVE, Olivier COULEMBIER.

Green chemistry, DOI: [10.1039/C8GC03607A](https://doi.org/10.1039/C8GC03607A) (Chapter III)

2. From selective formation of trimethylene carbonate to its “on-demand” polymerization: Impact of the iodine/ionic liquid cooperative catalytic system (Forthcoming) (Chapter IV)
3. Update and challenges in CO₂-based polycarbonate synthesis (review) (Forthcoming, Chem. Soc. Rev.) (Chapter I)

Jin HUANG, Joshua C. WORCH, Andrew P. DOVE, and Olivier COULEMBIER